

# OPTIMIZED DESIGN OF WIND TURBINE JACKET FOUNDATIONS

IMPROVED EFFICIENCY AND ACCURACY  
IN THE SEQUENTIAL INTEGRATED APPROACH

DAWID AUGUSTYN

MASTER THESIS

RAMBOLL



AALBORG UNIVERSITY  
DENMARK





AALBORG UNIVERSITET

## Master Thesis

---

**Title:**

Optimized Design of Wind Turbine Jacket Foundations  
*Improved efficiency and accuracy in the sequential integrated approach*

**Author:**

Dawid Augustyn

**Supervisors:**

Lars Damkilde Aalborg University  
Ronnie Refstrup Pedersen Rambøll and Aalborg University  
Martin Bjerre Nielsen Rambøll

---

**Major:**

Structural and Civil Engineering

**Project Period:**

February– June 2016

**University:**

Aalborg University Esbjerg  
The Faculties of Engineering and Science

**Company collaboration:**

Rambøll Offshore Wind

**Date of Completion:**

June 9, 2016

**Keywords:**

Offshore wind, Reduced models, Superelement, Augmented Craig-Bampton, Force-Controlled, Direct Expansion, Soil, Winkler, Coupled, Sequential Integrated



# Abstract

Modern-day offshore wind turbine foundations are designed by using the so-called *Sequential Integrated* approach, where two parties are involved: a Wind Turbine Manufacturer and a Foundation Designer. The information exchange between the parties is realized by means of reduced and linearized systems. The accuracy of the final design strongly depends on the quality of these reduced models and their ability to describe the physical structure, i.e the internal dynamics, wave loading and soil modelling. This thesis investigates the quality of the currently used approach and strives for improving the accuracy and efficiency, by implementing new methods.

The first part of the thesis describes the theoretical background for the reduction methods, including the common methods i.e Guyan and Craig-Bampton, but also the relatively new Augmented Craig-Bampton. Furthermore, the soil modelling approaches are described, including the non-linear methods, e.g Winkler spring method. The theoretical basis points out the limitation of the methods and serves as a starting point for further investigations.

The second part investigates the main scope of work i.e the reduced foundation models, the modal representation of the tower and the non-linear soil modelling.

In order to assess the quality of the reduced foundation models, three methods are compared with the non-reduced reference system. The standard load calculation procedure is performed by using a high fidelity jacket, modelled in Rambøll's in-house Offshore Structural Analysis Program ROSAP combined with the reference 5 MW NREL turbine that is implemented in the Rambøll's in-house aero-elastic code. The results demonstrate that the Guyan method cannot properly describe the internal brace dynamics while the Craig-Bampton in some cases cannot efficiently describe the influence of the internal wave loading. Therefore, the robust Augmented Craig-Bampton method is proposed, which delivers the same accuracy as the reference solution. Moreover, the Augmented Craig-Bampton reduction method combined with the efficient Direct Expansion recovery-run procedure significantly increases both, the efficiency and accuracy of the analysis.

Secondly, the modal tower representation in an aero-elastic code– FLEX5 is investigated. The approach implemented in the code, which includes only two tower bending modes, is compared with the reference, non-reduced tower model. A significant error has been found. Therefore, it was concluded that the number of internal modes is not sufficient. A sensitivity study has been performed, which demonstrated that ten modes should be implemented in order to properly describe the tower stiffness.

Finally, the linearized soil representation for an offshore wind turbine has been investigated. The model based on linear soil is compared to a model with non-linear soil representation. The results significantly differ, especially when a high displacement level has been introduced in the soil. Therefore, two solutions have been proposed for mitigating the problem. The most precise and robust solution is to exclude piles from the linear jacket reduced model and implement the non-linear soil representation externally. This approach delivers the same results as the non-reduced jacket with non-linear soil, but demands an additional implementation in the aero-elastic code. In order to overcome this problem, a so-called *user-defined* linearized soil approach is proposed, which can properly estimate the ultimate pile displacement, but requires geotechnical expertise.



# Foreword

The following thesis is a culmination point of my Master's programme in Structural and Civil Engineering completed at Aalborg University, Esbjerg. In the second semester we had an opportunity to make our project in collaboration with the company, Rambøll. Under these circumstances I met Ronnie Refstrup Pedersen, who was our supervisor and works there. The focus of the project was the foundation for offshore wind turbines. The offshore engineering field seems very appealing for me, both from the academical and the practical point of view. Therefore, I decided to dedicate the third semester to an internship at Rambøll Offshore Wind, where I had the opportunity to get an insight into the industrial approach on how to design wind turbines.

A glimpse into the load calculation procedures, especially for the complicated, multi-member jacket foundations, confirmed my conviction that this specific field of engineering is the one I would like to contribute to and make a difference. From that point on, it was just one step to initialize the master project, which investigates the reduced foundation modelling in the offshore wind turbine design. The presented thesis is an outcome of the work performed during the period from February to June 2016 in collaboration between the Aalborg University, Esbjerg and Rambøll Offshore Wind, Esbjerg. Even though I am listed as the only author, I would like to mention a few people without whom this thesis would not be accomplished.

I would like to express my greatest gratitude to Professor Lars Damkilde, not only for supervising this thesis, but also for the whole two years, when he was like a mentor to me. Eye-opening discussions with him are challenging, but as it always turns out, very helpful and developing. Additionally, I would like to thank Ronnie, who introduced me to Rambøll and created a bridge between the academia and the industrial world. As a supervisor, he always had time for a discussion and good advices on current problems, but also knows all the *right* people in the company. One of these people is Martin Bjerre Nielsen, who was my *every-day* company supervisor. A special thanks to him for answering my countless questions and supporting me in the process of creating the thesis.

Moreover, I would like to mention the whole Rambøll Offshore Wind office in Esbjerg, who helped me to solve many technical software problems. These people created the atmosphere in the office, which turned it into a place where I wanted to be, rather only have to be. A special thanks to my girlfriend, who helped me to make the thesis reader-friendly. Finally, I would like to thank my parents, whose support let me be in the place, where I am now.

Esbjerg, Denmark,  
June 9, 2016

---

Dawid Augustyn  
augustyn.dawid@gmail.com



# Contents

<b>Abstract</b>	<b>i</b>
<b>Foreword</b>	<b>iii</b>
<b>1 Introduction</b>	<b>1</b>
1.1 Statement of the physical problem . . . . .	2
1.2 Industrial implementation . . . . .	3
1.3 Aims of the thesis . . . . .	4
1.4 Thesis outline . . . . .	5
<b>I THEORETICAL BASIS FOR LOAD CALCULATIONS</b>	<b>7</b>
<b>2 Dynamic substructuring and model reduction</b>	<b>11</b>
2.1 Assembly . . . . .	12
2.2 Model Reduction . . . . .	14
2.3 Summary of the Dynamic Substructuring concept . . . . .	19
<b>3 Soil-structure interaction</b>	<b>21</b>
3.1 Modelling approaches . . . . .	21
3.2 Non-linear Winkler Springs . . . . .	25
<b>4 State-of-the-art procedures</b>	<b>29</b>
4.1 Reduced foundation models . . . . .	31
4.2 Aero-elastic calculations . . . . .	34
4.3 Recovery-run procedures . . . . .	35
<b>II REFINED REDUCED FOUNDATION MODELS</b>	<b>37</b>
<b>5 Foundation modelling and recovery-run procedures</b>	<b>41</b>
5.1 Methodology . . . . .	43
5.2 Foundation reduction and Recovery-Run . . . . .	46
5.3 Results . . . . .	48
5.4 Discussion . . . . .	52
<b>6 Tower modelling</b>	<b>55</b>
6.1 Methodology . . . . .	57
6.2 Numerical model . . . . .	57
6.3 Results . . . . .	59
6.4 Discussion . . . . .	62

<b>7 Non-linear soil modelling</b>	<b>65</b>
7.1 Methodology . . . . .	66
7.2 Numerical model . . . . .	67
7.3 Results . . . . .	69
7.4 User-definer linearization . . . . .	74
7.5 Discussion . . . . .	76
<b>III CLOSING REMARKS</b>	<b>79</b>
<b>8 Conclusion</b>	<b>83</b>
<b>9 Recommendation for Further Research</b>	<b>85</b>
<b>Bibliography</b>	<b>86</b>
<b>IV APPENDICES</b>	<b>91</b>
<b>A Boolean matrices</b>	<b>93</b>
<b>B Derivation of Augmented Craig-Bampton reduction method</b>	<b>95</b>
<b>C Proper Orthogonal Decomposition</b>	<b>97</b>
<b>D Jacket geometry</b>	<b>99</b>

# Chapter 1

## Introduction

The energy policy of many countries is based on renewable sources. The European Commission's target for 2020 is to have at least 20% of the energy produced by using renewable sources. Denmark has the plan to be fully dependent on renewable sources by 2050, Germany aims to be dependent in 80% by that time. Not only the European countries follow that pattern, e.g. the United States and China want to achieve 54 GW and 30 GW offshore wind capacity by 2030 and 2020, respectively [1].

**Table 1.1:** Prediction of the European capacity and cost of the offshore wind energy [2].

	2015	2020	2030
LCoE <sup>1</sup> [EUR/MWh]	130	110	90
Capacity [GW]	12	30	65

The European cumulative offshore wind capacity is expected to grow from 12 GW today to at least 65 GW by 2030 [2]. In order to achieve that ambitious plan, the cost of offshore energy has to be decreased from the initial 130 EUR/MWh to 90 EUR/MWh in 2030, see Tab. 1.1.

The potential for a cost reduction lays in the foundation design, production and commissioning procedures. The rapid development in the offshore industry resulted in a strong expectation on delivering turbines in a reasonably short period of time. As a result, some of the design procedures are based on the adopted methods from the oil and gas industry. However, an offshore turbine is a highly dynamic structure, while an oil rig, responds in a rather quasi-static manner. In order to ensure the target reliability of the structure, a significant level of conservatism is introduced.

Investigation by DNV [3] demonstrated that by improving the design methods, the cost of offshore energy can be decreased by 15%. An internal Rambøll study shows that by introducing a refined design method, the mass of the supporting structure can be optimized by 10-20%, compared to the conservative preliminary design, depending on how precise the initial starting parameters were.

The above-mentioned argumentation serves as a basis for the reason of this thesis. The goal is to strive for more accurate, therefore cost-effective design methods for the offshore wind turbine design. The focus is given to modelling of the complex, coupled and multi-member support structure, i.e. the jacket foundation.

---

<sup>1</sup>Levelized Cost of Electricity- total cost of designing, commissioning and operating the turbine related to the expected power output over the lifetime.

## 1.1 Statement of the physical problem

An offshore wind turbine is a complicated structure in terms of geometry, modelling and installation. It consists of three main parts: wind turbine (blades, nacelle and tower), foundation (monopile, jacket, tripod, gravity base) and a structure assembling it in the ground (piles, suction buckets). An exemplary offshore wind turbine is depicted in Fig. 1.1.

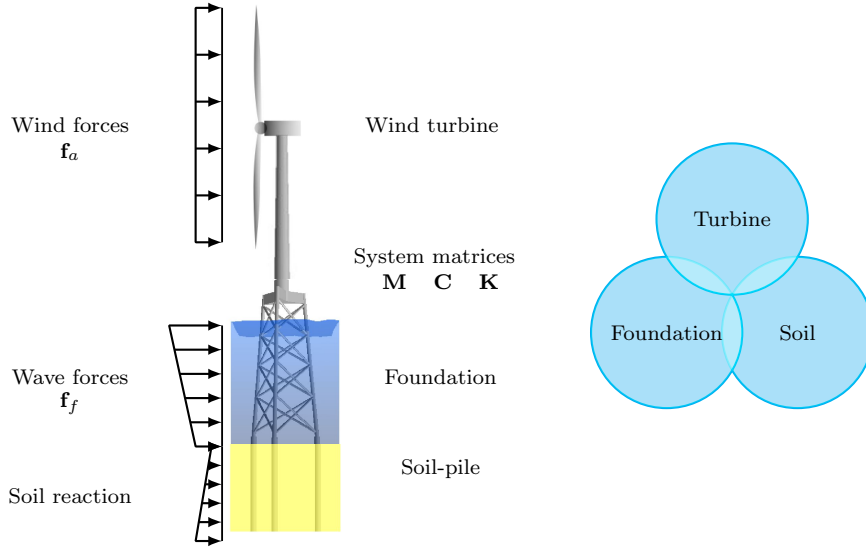


**Figure 1.1:** Coupled wind turbine model.

The structure is exposed to demanding environmental excitation i.e wind, wave and current. The interaction between the excitation and a structure itself leads to a highly non-linear, coupled problem which has to be properly modelled and solved.

One of the aspects that requires a special treatment is the modelling of aerodynamic forces caused by the wind acting on the blades and tower. The aerodynamic forces  $\mathbf{f}_a(\mathbf{K})$  depend on the stiffness  $\mathbf{K}$  of the blades and the underlying system, i.e. the tower, the substructure and the foundation. Additionally, the wave forces  $\mathbf{f}_f(\dot{\mathbf{u}})$  acting on the foundation structure might depend on the relative velocities  $\dot{\mathbf{u}}$  between the fluid particle and the structure. On top of that the pile stiffness  $\mathbf{K}(\mathbf{u})$  depends on the displacement level  $\mathbf{u}$  introduced in the soil due to the combined wind  $\mathbf{f}_a(\mathbf{K})$  and wave  $\mathbf{f}_f(\dot{\mathbf{u}})$  forces.

Moreover, the dynamic analysis strongly depends on the damping of the system. Again, in the case of the wind turbine the modelling of that phenomena is a complicated problem. A fully operational turbine can experience damping from many sources. The aerodynamic damping is introduced when wind reacts with the blades. The tower top displacements lead to the difference in the relative velocity between the blades and wind. The velocity is increased when blades are moving in the wind direction and decreased when the opposite occurs. The same reasoning is valid for the water motion due to the wave. When the supporting structure leans towards the wave, the force is increased and the opposite happens when the movement of the structure is off the wave. Therefore, the damping of the system is dependent on the velocity  $\mathbf{C}(\dot{\mathbf{u}})$ .

The standard equation of motion that combines all the above-mentioned physical phenomena can be introduced as:

$$\mathbf{M}\ddot{\mathbf{u}} + \mathbf{C}(\dot{\mathbf{u}})\dot{\mathbf{u}} + \mathbf{K}(\mathbf{u})\mathbf{u} = \mathbf{f}_a(\mathbf{K}) + \mathbf{f}_f(\dot{\mathbf{u}}), \quad (1.1)$$

where  $\mathbf{M}$ ,  $\mathbf{C}$ ,  $\mathbf{K}$  are the system mass, damping and stiffness matrices respectively,  $\mathbf{u}$  is the displacement vector,  $\mathbf{f}_a$ ,  $\mathbf{f}_f$  are wind and wave forces, respectively. The time dependency is omitted for simplicity. The force and soil non-linearities are included by the state dependent

stiffness matrix. Moreover, the coupling of the problem is included explicitly by modelling the whole system in one equation and solving it by using the one time integration method.

The application of Eq. 1.1 guarantees that the physical coupling and interaction between the system parts is inherently performed. The coupling can be symbolized as in Fig. 1.1b, where all of the parts are connected and share the influence between each other coherently.

Equation 1.1 is one of the methods regarding how to model an offshore wind turbine. However, the way the industry is organized does not allow to use that method. A wind turbine is in most cases designed by two main parties: a Foundation Designer and a Wind Turbine Manufacturer. A foundation designer is responsible for delivering the detailed design of the foundation including piles. The latter models and designs the wind turbine including the tower. As a result of that approach the described method cannot be implemented due to:

- **confidential reason** – each of the parties use the information that are sensitive and cannot be public i.e (blade geometry, controller parameters, soil parameters). That makes it impossible to set up one software shared by both parties.
- **practical reason** – each party prepares an extensive model, where the level of detail is too high in order to perform the general dynamic analysis. The application of that model would significantly decrease the efficiency of the analyses.
- **legal reason** – each party is responsible only for the design of a specific part of a total turbine. Therefore, a clear division of responsibility needs to be reached, which cannot be guaranteed by using the given approach.

Due to the mentioned reasons, the state-of-the-art approach to design an offshore wind turbine is not realized by means of Eq. 1.1, even though it is the most optimal method solely from the engineering point of view. Instead, the so-called *Sequential Integrated* approach is adopted.

## 1.2 Industrial implementation

To accommodate the non-engineering requirements of the parties, the new approach has been developed. It is called *Sequential Integrated* because, unlike the previous approach, the analyses are integrated sequentially in two separate software. An outlook of the method is presented in Fig. 1.2. More details on the method are given in Ch. 4 herein, or in [4].

A Wind Turbine Manufacturer developed a refined aero-elastic code, schematically represented in Fig. 1.2a, with the highly accurate models. However, the foundation model is required to account for flexibility and dynamic of the underlying structure. The model, which is applied by a Wind Turbine Manufacturer, does not have to be very refined and detailed, but it should resemble the general dynamic of the foundation. Therefore, a so-called reduced *superelement SE* is provided by a Foundation Designer.

As output of the analyses a Wind Turbine Manufacturer delivers interface forces  $\mathbf{g}_j$  between the tower and a foundation. These forces are applied by a Foundation Manufacturer into a detailed foundation model and based on that information the detailed foundation design can be performed (Fig. 1.2b).

The fully coupled Eq. 1.1 needs to be adopted into the *Sequential integrated* approach. The first step is to decouple the full system matrices into two independent structures: the turbine  $\mathbf{M}_a, \mathbf{C}_a, \mathbf{K}_a$  and the foundation. Afterwards, a foundation designer reduces the original, detailed foundation model into the reduced one  $\tilde{\mathbf{M}}_j, \tilde{\mathbf{C}}_j, \tilde{\mathbf{K}}_j$  including the reduced wave loading  $\tilde{\mathbf{f}}_j$ . Due to the fact, that physically the models are coupled, the interface forces  $\mathbf{g}$  between two structures can be found. In order to fulfil the compatibility between the structures, the interface forces need to be in equilibrium. Mathematically, it can be expressed as in Eq. 1.2, where the subscript  $()_a$  and  $()_j$  denotes the turbine and foundation part, respectively.

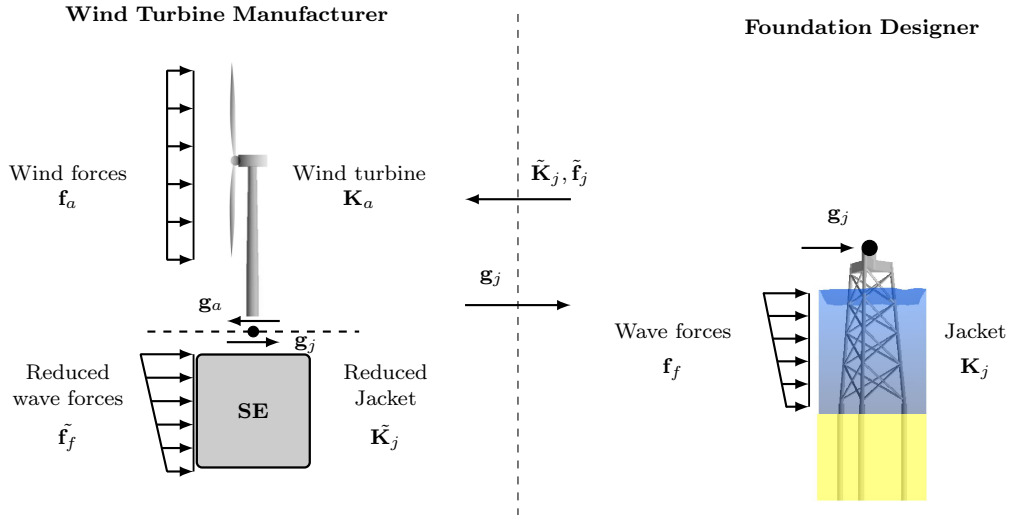


Figure 1.2: Integrated wind turbine model.

$$\begin{bmatrix} \mathbf{M}_a & \mathbf{0} \\ & \tilde{\mathbf{M}}_j \end{bmatrix} \begin{bmatrix} \ddot{\mathbf{u}}_a \\ \ddot{\tilde{\mathbf{u}}}_j \end{bmatrix} + \begin{bmatrix} \mathbf{C}_a & \mathbf{0} \\ & \tilde{\mathbf{C}}_j \end{bmatrix} \begin{bmatrix} \dot{\mathbf{u}}_a \\ \dot{\tilde{\mathbf{u}}}_j \end{bmatrix} + \begin{bmatrix} \mathbf{K}_a & \mathbf{0} \\ & \tilde{\mathbf{K}}_j \end{bmatrix} \begin{bmatrix} \mathbf{u}_a \\ \tilde{\mathbf{u}}_j \end{bmatrix} = \begin{bmatrix} \mathbf{f}_a \\ \tilde{\mathbf{f}}_j \end{bmatrix} + \begin{bmatrix} \mathbf{g}_a \\ \mathbf{g}_j \end{bmatrix}, \quad (1.2)$$

$$\mathbf{g}_a + \mathbf{g}_j = \mathbf{0}.$$

Note that providing the non-reduced foundation with non-linear soil, Eq. 1.2 is equivalent to Eq. 1.1. However, the foundation model is both, reduced, and linearized, therefore Eq. 1.2 provides the approximation, not the exact solution for the physical model. A reduced modelling approach can also be included in the turbine part. Some aero-elastic codes introduce the modal representation of e.g. tower and blades. That also corresponds to the model reduction and can lead to the decrease of the accuracy.

### 1.3 Aims of the thesis

The *Sequential Integrated* approach, which is the state-of-the-art method, introduces two strong assumptions:

- The reduced model of the foundation is dynamically equivalent to the non-reduced model.
- The reduced model of the foundation is linear, including soil and damping.

The validity of these assumptions guarantees that the accuracy of the design performed by using that approach is high. The first assumption is a matter of deriving the appropriate theory and implementing it. The second however, is inconsistent to the physics, since the soil is a non-linear material and for a high level of displacement the linearized model does not accurately describe the soil. Based on that consideration, the presented thesis defines the goal, which is investigated herein:

*Improved efficiency and accuracy of reduced models used in load calculations for an offshore wind turbine design.*

Out of many possible development fields within the offshore industry that specific has been chosen due to the fact that the foundation modelling seems the most primal. Investigation into the hydrodynamic or aerodynamic load is also essential, but without the proper foundation representation it is worth nothing. Therefore, assurance of the foundation model accuracy has been given priority. Only after that, further investigations into e.g. the load estimation, or more

complex damping models, makes sense. The general goal is achieved by investigating the three specific research scopes:

- Improve spectral and spatial convergence of the system reduction methods used
- Assess the accuracy of the modal tower representation in aero-elastic calculations
- Investigate the importance of the non-linear soil modelling on the coupled wind turbine dynamic response

The author believes that the foundation modelling is a key element for load calculation procedures and especially now, when the turbines are becoming larger than ever, additional effort is required within that field. The thesis mostly focuses on improving the *Sequential integrated* approach, by localizing the weak point of the state-of-the-art procedures and suggesting the improvements that can be implemented within reasonable effort.

Recently, there have been some publications suggesting that the reduced foundation models, especially for the dynamically sensitive structures, require additional improvement [5]. Moreover, the internal wave loading might not be accounted for in the most optimal way as suggested by e.g [6]. These issues are investigated by mean of the first research scope.

Based on the theoretical insight it is expected that the reduced tower model might not be able to properly describe the stiffness of the structure. This can lead to the erroneous aerodynamic wind forces and the interface forces. As the interface forces are crucial in the *Sequential Integrated* approach, it was decided to investigate that aspect as well, due to the fact that basically the same principle applies here, as for the foundation. That hypothesis is investigated by the second research scope.

There exist extensive literature in respect of the detailed, complicated soil models for the offshore foundation design [7, 8], whereas the soil model combined within the linear reduced model seems rather simplified. To the best of author's knowledge, there are not many publications where the more refined, yet simple soil model would be suggested for the specific offshore wind turbine design combined with a jacket foundation. Therefore, the field is investigated within the third research scope, where a special focus is given into the importance of non-linear soil modelling.

## 1.4 Thesis outline

The thesis has been divided into two main parts, whereupon the conclusion and appendices are presented.

In the first part, the theoretical basis for the methods used in the calculation procedures will be presented according to Fig. 1.3. Based on that part, the limitations of the currently used methods will be defined and possible improvements will be determined. The Dynamic Substructuring concept will be introduced with respect to different reduction methods. Procedures for recovering a non-reduced model response will be characterized.

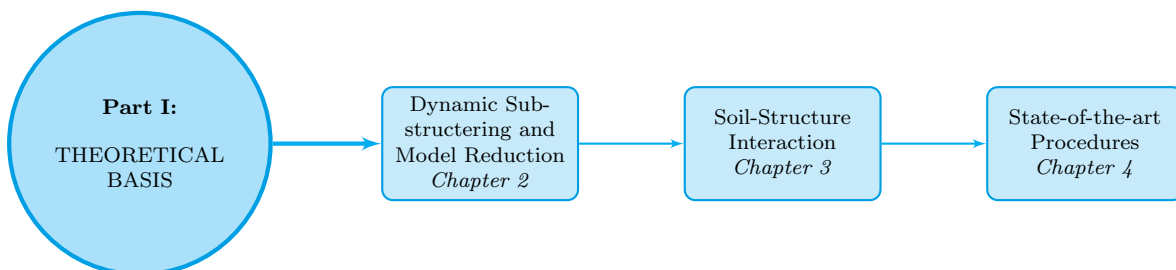
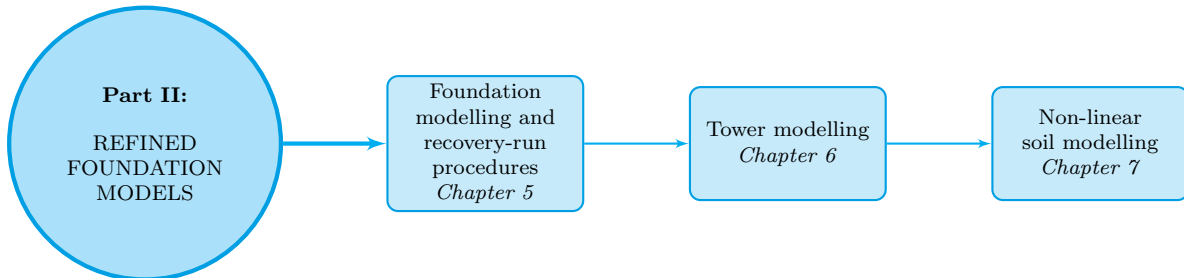


Figure 1.3: Outline of the Part I of the thesis.

Finally, a soil modelling review will be shortly sketched regarding how to efficiently reflect a state-dependent soil behaviour. The theory is followed by an overview of the state-of-the-art modelling procedures currently used by the industry. It will be described generally with more details given from a Foundation Designer perspective. Special interest will be given into shortcomings of the methods and possible pitfalls in every-day use. Afterwards, the weak spots will be analyzed in more detail in respect of both, theoretical and practical points of view.



**Figure 1.4:** Outline of the Part II of the thesis.

The structure of the second part is outlined in Fig. 1.4. It gives practical examples of a realistic offshore wind turbine model, where weaknesses of the currently used methods are demonstrated. Afterwards, suggestions of how the particular problems could be solved are presented. Finally, the reduced methods will be compared with the solution that corresponds to the most accurate model that is possible to obtain. A special interest will be given to reduced foundation models, tower modal representation in an aero-elastic code and a non-linear soil behaviour.

As the last part of the thesis, the conclusion is drawn from the analyses presented herein, see Fig. 1.5. The shortcoming of the state-of-the-art methods are pointed out and improvements are suggested. Finally, possible further research scopes are defined, which could serve as a starting point for additional investigations.

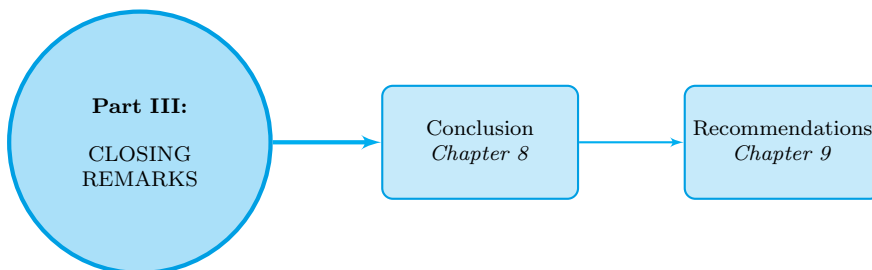


**Figure 1.5:** Outline of Part III of the thesis.

Part I

**THEORETICAL BASIS FOR  
LOAD CALCULATIONS**



# Roadmap

The currently used design methods in the wind turbine industry are based on the integrated method as introduced in the previous chapter. To fully understand the potentials and limitations of the methods, a theoretical background of the methods used in the load calculation procedures is presented in the following part of the thesis. The outline can be seen in Fig. 1.6.

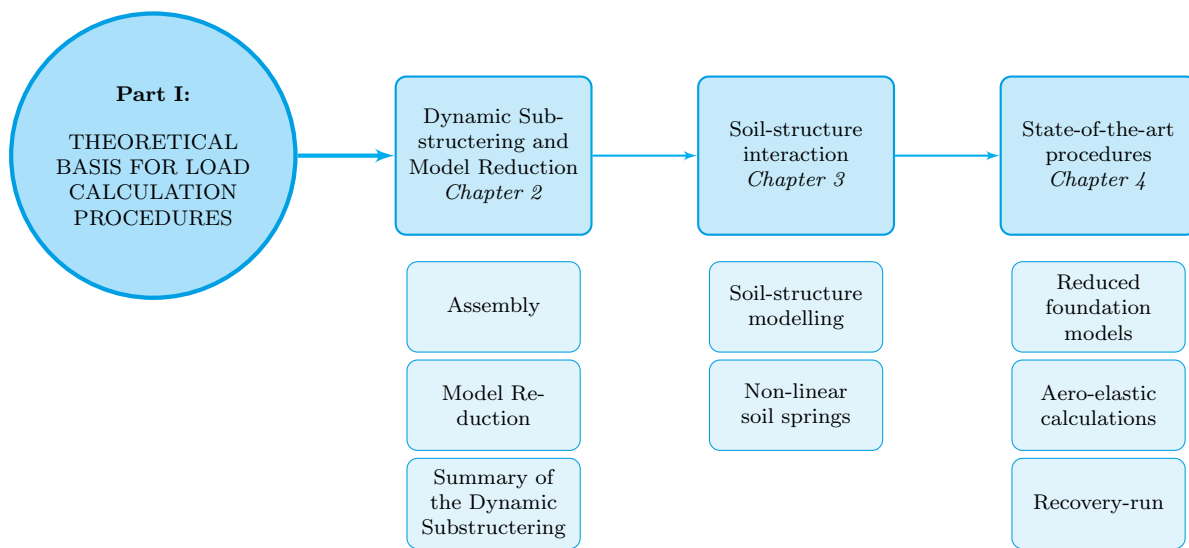


**Figure 1.6:** Detailed outline of Part I of the thesis.

The chapter consists of the Dynamic Substructuring concept, which allows to decompose a complex problem into a sequence of smaller models, reduce systems and finally couple them together in order to obtain the response corresponding to a coupled model. A number of reduction methods are described (Guyan, Craig-Bampton and Augmented Craig-Bampton), recovery-run procedures are described on how to recover full system response based on the reduced solution (Force-Controlled and Direct Expansion). The relevant theory for that part is outlined in Chapter 2.

Soil modelling approaches are illustrated afterwards as a significant part of the total wind turbine system. At first, a brief review of general soil modelling is given, followed by a more specific offshore application. Since soil is a material, which depends on the load level applied, the non-linear approach is described.

Finally, the state-of-the-art load calculation procedures are described, additionally stating the weak points of the methods.

The idea of including the theoretical part is in order to build up a reference, based on which the state-of-the-art methods can be assessed and points can be localized, where possible improvements can be included. Afterwards, the second part of the thesis uses the theoretical part to include new methods in order to increase accuracy of currently used procedures.



## Chapter 2

# Dynamic substructuring and model reduction

The concept of Dynamic Substructuring serves as a framework for many dynamic analysis applied to a numbers of industries, since it was first introduced in the early 1970s [9]. The basic idea that made the method so popular, is to divide the system into a number of subsystems that are less demanding to solve.

A sketch of the concept is presented in Fig. 2.1.

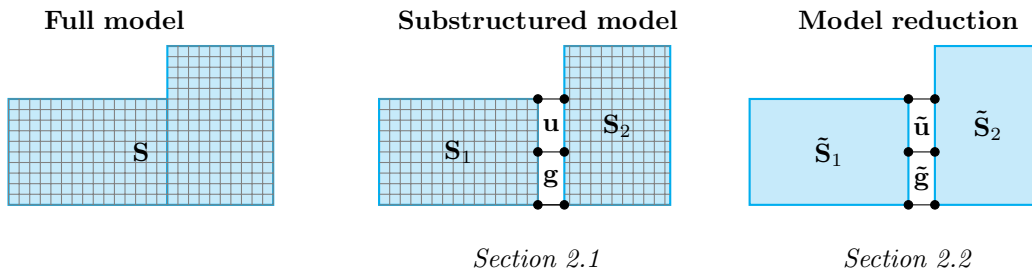


**Figure 2.1:** Dynamic substructuring concept.

Initially, the standard equation of motion of the full, finely discretized system  $\mathbf{S}$  has to be solved.

$$\mathbf{M}\ddot{\mathbf{u}} + \mathbf{C}\dot{\mathbf{u}} + \mathbf{K}\mathbf{u} = \mathbf{f}, \quad (2.1)$$

where  $\mathbf{u}$  are the displacements of the system,  $\mathbf{M}, \mathbf{K}, \mathbf{C}$  are the mass, stiffness and damping matrices of the full system and  $\mathbf{f}$  stands for the external excitation. However, the model might be setup for a detailed component analysis, and it may be too computationally demanding for a global dynamic analysis. One way to handle this type of analysis is to introduce a new, less refined mesh. It is time consuming, therefore, a decomposition of the system and the mathematical reduction can be performed instead.

The first step is to decompose the full model into a number of independent subsystems that can be analyzed separately.

$$\mathbf{S} = \begin{bmatrix} \mathbf{S}_1 & & \\ & \mathbf{S}_2 & \\ & & \dots \end{bmatrix}, \quad (2.2)$$

where each of the subsystems  $\mathbf{S}_i$  is represented by an independent equation of motion

$$\mathbf{M}_i\ddot{\mathbf{u}}_i + \mathbf{C}_i\dot{\mathbf{u}}_i + \mathbf{K}_i\mathbf{u}_i = \mathbf{f}_i + \mathbf{g}_i, \quad (2.3)$$

where the subscript  $( )_i$  corresponds to the matrices of the independent system. Certainly, it has to be assured that the systems are connected together and each component corresponds to the

global behaviour of the full system. It can be set up in terms of either  $\mathbf{u}$  displacements,  $\mathbf{g}$  forces, or a combination of both. That process is called the *assembly* and it is described in Sec. 2.1.

Afterwards, the subsystems can be simplified in order to reduce the computational time by disregarding redundant, detailed information. The method to obtain such a model reduction corresponds to reducing the original number of DOFs into a new reduced system. In principle the reduction method corresponds to the transformation of the physical  $\mathbf{u}$  DOFs into the generalized  $\mathbf{q}$  DOFs space

$$\mathbf{u} = \mathbf{T}\mathbf{q}. \quad (2.4)$$

The reduction is obtained by using the so-called reduction basis  $\mathbf{T}$ . There exists a number of reduction methods to obtain that basis and the most important ones are described in Sec. 2.2

At the time, when the Dynamic Substructuring was introduced, this was the only approach how the complex systems could be handled due to limited computational capacities. Therefore, the systems were not only substructured, but also reduced as much as possible to account only for the relevant aspects of the non-reduced models.

Even though the modern technologies overcame most of the limitations for the analysis over the time, engineers still use the very same concept, therefore the following chapter will introduce the basis of the relevant theory in order to build up on this later in relation to the offshore wind industry application.

## 2.1 Assembly

The first step in the process of Dynamic Substructuring is to divide the complex problem into a number of smaller, easier to handle substructures. Once the system described by Eq. 6.1 is divided into the independent systems, the dependency on the adjacent structures appears in terms of the interface forces  $\mathbf{g}_i$ . These forces, combined with the interface displacements  $\mathbf{u}$  uniquely define the relationship between the substructures. The equations of motion for the individual substructure combined with the relationship equations in the general form are:

$$\begin{array}{ll} \mathbf{M}_1 \ddot{\mathbf{u}}_1 + \mathbf{C}_1 \dot{\mathbf{u}}_1 + \mathbf{K}_1 \mathbf{u}_1 = \mathbf{f}_1 + \mathbf{g}_1, & \\ \text{compatibility equation} & \mathbf{u}_1 - \mathbf{u}_2 = \mathbf{0}, \\ \text{equilibrium equation} & \mathbf{g}_1 + \mathbf{g}_2 = \mathbf{0}. \end{array} \quad (2.5)$$

The two relationship equations are the compatibility equation and the equilibrium equation. The first one enforces that the interface displacements of substructure 1  $\mathbf{u}_1$  are equal to the displacements of the adjacent substructure 2  $\mathbf{u}_2$ . Additional requirement is to enforce the equilibrium in terms of the interface forces  $\mathbf{g}_1$  and  $\mathbf{g}_2$  between the substructures, which is fulfilled by using the latter.

The complete set of the equations for the full system is composed of a number of substructures can be written in the form:

$$\begin{array}{ll} \mathbf{M}\ddot{\mathbf{u}} + \mathbf{C}\dot{\mathbf{u}} + \mathbf{K}\mathbf{u} = \mathbf{f} + \mathbf{g}, & \\ \text{compatibility equation} & \mathbf{B}\mathbf{u} = \mathbf{0}, \\ \text{equilibrium equation} & \mathbf{L}^T \mathbf{g} = \mathbf{0}. \end{array} \quad (2.6)$$

Here the individual substructures have been combined in the block diagonal matrix form:

$$\mathbf{M} = \begin{bmatrix} \mathbf{M}_1 & \\ & \mathbf{M}_2 \end{bmatrix}, \quad \mathbf{u} = \begin{bmatrix} \mathbf{u}_1 \\ \mathbf{u}_2 \end{bmatrix}, \quad \dots, \quad (2.7)$$

where the substructure's matrices  $\mathbf{M}_i$  are disassembled and the assembly is fulfilled by the explicit compatibility and equilibrium equations.

The  $\mathbf{B}$  matrix is the Boolean matrix that defines the relation of the displacements and ensures the interface displacements compatibility. The  $\mathbf{L}$  matrix is responsible for defining a unique set of the displacement for the full system. Normally, each of the substructures has nodes at the interface as seen in Fig. 2.2a. The mirror of the nodes is depicted in the adjacent substructure. In order to not double the number of nodes, the  $\mathbf{L}$  matrix is created. More details on construction of these matrices can be found in App. A.

Among others, there exist two methods on how to fulfil the relationship equations, namely the Primal and Dual assembly.

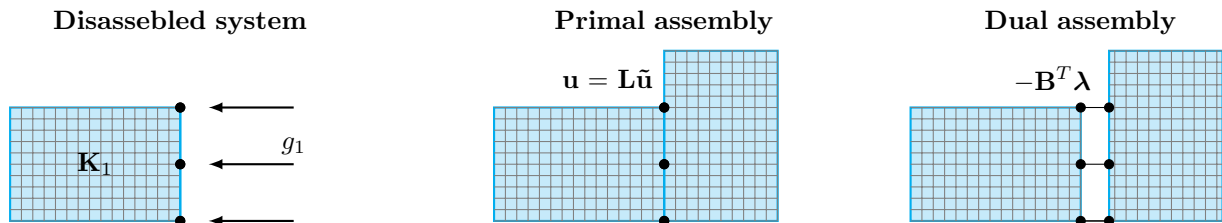


Figure 2.2: The idea of primal and dual assembly.

### Primal assembly

The primal assembly uses the assumption that the disassembled substructures with independent DOFs can be combined into one system by rearranging the DOFs and constructing the unique set of nodes numbering. Basically, it corresponds to *glueing* the interface DOFs into one node as presented in Fig. 2.2b.

Mathematically, it can be constructed by using the  $\mathbf{L}$  transformation matrix:

$$\text{assumption } \mathbf{u} = \mathbf{L}\tilde{\mathbf{u}} \rightarrow \tilde{\mathbf{M}} = \mathbf{L}^T\mathbf{M}\mathbf{L} \quad , \quad \tilde{\mathbf{K}} = \mathbf{L}^T\mathbf{K}\mathbf{L}. \quad (2.8)$$

As noted earlier, it corresponds to reducing the original decoupled DOFs  $\mathbf{u}$  into coupled DOFs  $\tilde{\mathbf{u}}$ . In this case Eq. 2.6 is reduced to:

$$\tilde{\mathbf{M}}\ddot{\tilde{\mathbf{u}}} + \tilde{\mathbf{C}}\dot{\tilde{\mathbf{u}}} + \tilde{\mathbf{K}}\tilde{\mathbf{u}} = \tilde{\mathbf{f}}, \quad (2.9)$$

which fully determines the assembly between the substructures.

### Dual assembly

When the assumption regarding the interface forces is used instead, the assembly is called Dual:

$$\text{assumption } \mathbf{g} = -\mathbf{B}^T\boldsymbol{\lambda}. \quad (2.10)$$

Again the Eq. 2.6 reduces into:

$$\begin{aligned} \mathbf{M}\ddot{\mathbf{u}} + \mathbf{C}\dot{\mathbf{u}} + \mathbf{K}\mathbf{u} &= \mathbf{f} - \mathbf{B}^T\boldsymbol{\lambda}, \\ \mathbf{B}\mathbf{u} &= \mathbf{0}, \end{aligned} \quad (2.11)$$

and can be used as the equivalent of Eq. 2.9.

### Implementation

When it comes down to the implementation of the Primal or Dual Assembly, each has its advantages and drawbacks.

The Primal assembly is most widely used in the *Finite Element* codes, due to the straightforward implementation and reduction of a number of the interface nodes. It might not be an

important factor in beam models, however, when the model uses shell or solid elements, the reduction actually can be significant. Especially in the case, where there is a large number of substructures, therefore the interface nodes number is high.

The Dual assembly is mostly used, when the meshes between the substructures are not matching [10]. Therefore, it is more beneficial to keep the original *double* set of DOFs rather than restructure the mesh in the interface region.

The graphical interpretation of Primal and Dual equations 2.9 and 2.11 is presented in Fig. 2.3.



Figure 2.3: Matrix formulation of primal and dual assembly.

The primal assembly fulfils coupling a priori by *overlapping* the interface DoFs, which is creating a new set of DOFs  $\mathbf{u} = \mathbf{L}\tilde{\mathbf{u}}$ , therefore the compatibility and equilibrium equations are enforced. Thereby, the Dual assembly has to introduce additional explicit equations that are realized by the use of  $\mathbf{B}$  matrices and the interface forces assumption  $-\mathbf{B}^T\boldsymbol{\lambda}$ .

## 2.2 Model Reduction

Once the full system is assembled into a number of substructures, a reduction procedure can be applied. As mentioned in the introduction to the chapter, the reduction is used in order to increase the efficiency of the dynamic analysis without remeshing the original system. Usually, the mesh is prepared based on the detailed design, therefore it must be accounted for complicated geometry and stress concentration, or very local effects of the substructure. As long as the overall goal of the dynamic analysis is to determine the global behaviour of the total system, that level of accuracy is not necessary. Therefore, the reduction methods are used in order to transform the complicated mesh into a reduced space by accounting only for significant factors.

The basic idea used in the reduction method is to transform the physical DOFs  $\mathbf{u}$  into a number of the generalized DOFs  $\mathbf{q}$  as introduced in Eq. 2.4. The assumption is that by using a proper number of modes that are representing all of the physical aspects, the displacements of the non-reduced system can be described as:

$$\mathbf{u} = \sum_{i=1}^n \psi_i q_i = \mathbf{T}\mathbf{q}, \quad (2.12)$$

where  $\psi_i$  represents a mode and  $q_i$  stands for the corresponding amplitude. The choice of the modes  $\psi_i$  included in the reduction basis should account for the most significant aspects of the global displacements and is described in more details in herein. By applying the reduction equation (6.2) into the non-reduced system (6.1) the following can be obtained:

$$\mathbf{M}\mathbf{T}\ddot{\mathbf{q}} + \mathbf{C}\mathbf{T}\dot{\mathbf{q}} + \mathbf{K}\mathbf{T}\mathbf{q} = \mathbf{f} + \mathbf{g} + \mathbf{r}. \quad (2.13)$$

As long as the reduction basis includes all modes  $n = N$ , the equation is exact, however, the purpose of the reduction is to increase the efficiency by decreasing the size of the matrices. Therefore, when reducing the system the approximation of the exact solution is obtained. The

introduced error is given in terms of residual forces  $\mathbf{r}$ . It is assumed that the residual forces are orthogonal to the reduction basis, which mathematically can be expressed as:

$$\text{Galerkin assumption} \quad \mathbf{T}^T \mathbf{r} = \mathbf{0}. \quad (2.14)$$

Applying that assumption into Eq. 2.13 the reduced equation of motion is received.

$$\tilde{\mathbf{M}}\ddot{\mathbf{q}} + \tilde{\mathbf{C}}\dot{\mathbf{q}} + \tilde{\mathbf{K}}\mathbf{q} = \tilde{\mathbf{f}} + \tilde{\mathbf{g}}, \quad (2.15)$$

where:

$$\tilde{\mathbf{M}} = \mathbf{T}^T \mathbf{M} \mathbf{T} \quad , \quad \tilde{\mathbf{C}} = \mathbf{T}^T \mathbf{C} \mathbf{T} \quad , \quad \tilde{\mathbf{K}} = \mathbf{T}^T \mathbf{K} \mathbf{T} \quad , \quad \tilde{\mathbf{f}} = \mathbf{T}^T \mathbf{f} \quad , \quad \tilde{\mathbf{g}} = \mathbf{T}^T \mathbf{g}. \quad (2.16)$$

It is important to notice that the Galerkin assumption 2.14 holds as long as the reduction basis well describes the system. Practically, it means that a type combined with a number of modes included has a significant impact on the correctness of the approach. If the assumptions are not fulfilled (the number of modes is not sufficient, or the types do not correspond to the physical system), the error of the method is significant.

Therefore, in order to be able to successfully apply the Dynamic Substructuring within the field of offshore wind engineering, a brief description of the currently used methods is presented, followed by the potential method that might improve the load calculation procedures. The description is intended to provide an essential mechanical understanding of the methods, not the extensive mathematical derivation. More details can be found in [11, 12, 13].

Even though the examples and possible considerations are mostly addressed to the offshore application, the framework is general and can be applied into a number of different applications.

## Guyan

The Guyan method is historically the first used in the Dynamic Substructuring [11]. The reduction basis uses the so-called *constraint modes*. These modes describe the internal deformation of the subsystem subject to unit displacements of the fixed interface DoFs.

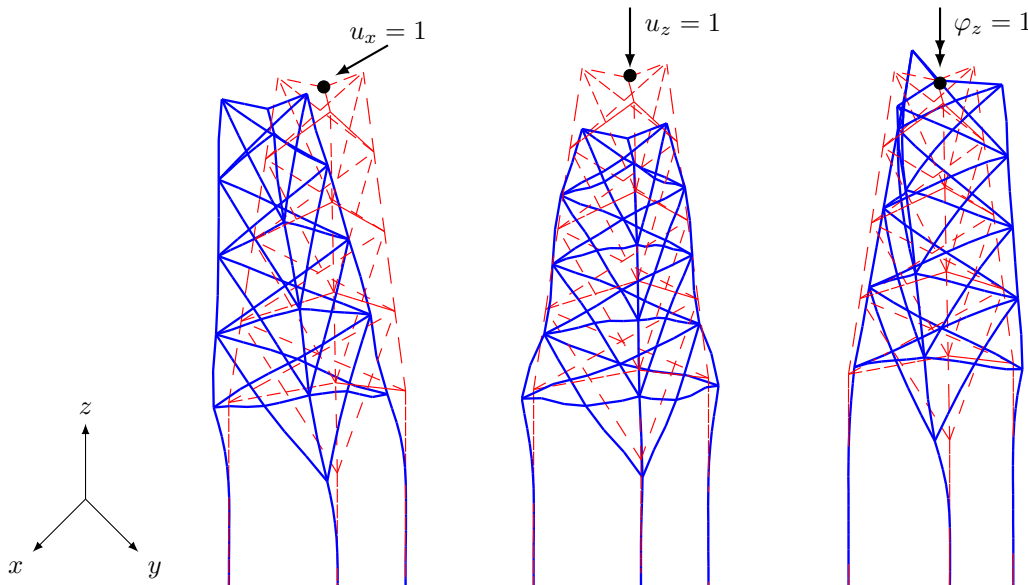


**Figure 2.4:** Static constraint modes ( $\Psi_C$ ) for the Guyan reduction basis.

The columns of the reduction basis  $\Psi_C$  correspond to the displacements of the substructure, subject to unit deformation of the specific interface DoFs, constraining the rest of the boundary

displacements  $\mathbf{u}_b$ . The exemplary modes that are corresponding to a horizontal, vertical and torsional deformation, are presented in Fig. 2.4.

The basic idea of the Guyan method is to describe the internal deformation of the structure based on solely the interface displacements. In order to do so, the general equation of motion has to be split into the interface (boundary) DOFs  $\mathbf{u}_b$  and the internal DOFs  $\mathbf{u}_i$ .

$$\begin{bmatrix} \mathbf{M}_{bb} & \mathbf{M}_{bi} \\ \mathbf{M}_{ib} & \mathbf{M}_{ii} \end{bmatrix} \begin{bmatrix} \ddot{\mathbf{u}}_b \\ \ddot{\mathbf{u}}_i \end{bmatrix} + \begin{bmatrix} \mathbf{K}_{bb} & \mathbf{K}_{bi} \\ \mathbf{K}_{ib} & \mathbf{K}_{ii} \end{bmatrix} \begin{bmatrix} \mathbf{u}_b \\ \mathbf{u}_i \end{bmatrix} = \begin{bmatrix} \mathbf{f}_b \\ \mathbf{f}_i \end{bmatrix}, \quad (2.17)$$

where the non-reduced system matrices follow the boundary  $()_{bb}$ , internal  $()_{ii}$  and mixed  $()_{ib}$  terms. The general equation is reduced by using the following restriction:

- fixed interface  $\mathbf{u}_b = \mathbf{0}$
- inertial forces are neglected  $\ddot{\mathbf{u}} = \mathbf{0}$
- load is only applied to the boundary nodes  $\mathbf{f}_i = \mathbf{0}$

When the assumptions are applied to Eq. 2.17, the internal displacements can be described by using only the boundary static displacements:

$$\mathbf{u}_i = \Psi_C \mathbf{u}_b, \quad (2.18)$$

where:

$$\Psi_C = -\mathbf{K}_{ii}^{-1} \mathbf{K}_{ib}, \quad (2.19)$$

are called static constraint modes. When the modes are applied into the form as in Eq. 6.2, the Guyan reduction basis takes shape as:

$$\mathbf{T}_G = \begin{bmatrix} \mathbf{I} \\ \Psi_C \end{bmatrix}, \quad (2.20)$$

and the final equation for the Guyan reduction is as follows:

$$\begin{bmatrix} \mathbf{u}_b \\ \mathbf{u}_i \end{bmatrix} = \mathbf{T}_G \begin{bmatrix} \mathbf{u}_b \end{bmatrix}. \quad (2.21)$$

Based on Eq. 2.19 it can be noticed that the Guyan builds the reduced model only on the stiffness matrix. This will lead to neglecting of inertia terms. As a result the Guyan method will not be able to capture the dynamic behaviour of the full model.

The Guyan reduction method can only deliver acceptable results, when the quasi-static excitation is applied. That could be the case, when the frequency content of the excitation is below the first eigenfrequency of the structure. Practically, it corresponds to a wind turbine with a monopile foundation. However, when a jacket foundation is applied, the local dynamics can have a significant influence on both, the global response and the localized effect. Therefore, for a jacket foundation, a more refined reduction method is required.

### Craig-Bampton

In order to increase the accuracy of the result for the dynamically sensitive structures, Craig and Bampton [12] suggested to augment the Guyan reduction method by introducing the *fixed interface modes* as illustrated in Fig. 2.5. They account for the internal dynamic that has been disregarded in the Guyan method.

Compared to the Guyan method, the number of restrictions has been reduced:

- fixed interface  $\mathbf{u}_b = \mathbf{0}$

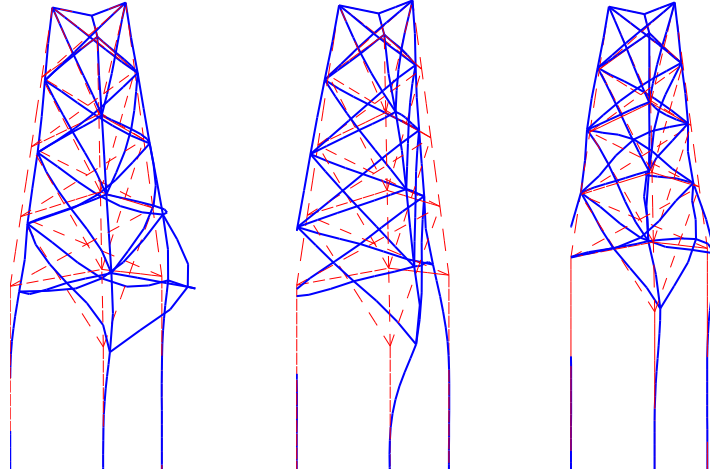


**Figure 2.5:** Fixed interface eigenmodes ( $\Phi_i$ ) for the Craig-Bampton reduction basis.

- load is only applied to the boundary nodes  $\mathbf{f}_i = \mathbf{0}$

The *fixed interface modes* can be found by solving the eigenproblem of the substructure, where the interface nodes have been fixed:

$$(\mathbf{K}_{ii} - \omega_j^2 \mathbf{M}_{ii}) \Phi_i = \mathbf{0}, \quad (2.22)$$

where  $\Phi_i$  are the fixed interface modes obtained by introducing a limited number of eigenmodes from the non-reduced model.

$$\mathbf{u}_i = \Psi_c \mathbf{u}_b + \sum_{i=1}^n \Phi_i \eta_i. \quad (2.23)$$

The reduction basis for the Craig-Bampton method can be written as:

$$\mathbf{T}_{CB} = \begin{bmatrix} \mathbf{I} & \mathbf{0} \\ \Psi_c & \Phi_i \end{bmatrix}. \quad (2.24)$$

The displacements of the full system therefore, can be found according to:

$$\begin{bmatrix} \mathbf{u}_b \\ \mathbf{u}_i \end{bmatrix} = \mathbf{T}_{CB} \begin{bmatrix} \mathbf{u}_b \\ \boldsymbol{\eta}_i \end{bmatrix}. \quad (2.25)$$

It can be noticed that in the Craig-Bampton method an additional generalized set of DOFs has been introduced. The  $\boldsymbol{\eta}_i$  correspond to the internal dynamic DoFs, represented by the modal coordinates.

### Augmented Craig-Bampton

The Guyan and Craig-Bampton methods neglect the internal loading  $\mathbf{f}_i = \mathbf{0}$ . Therefore, the methods does not explicitly account for it in the calculation process. In order to obtain accurate results, a rather large number of internal dynamic modes should be included. To overcome this problem an additional, load dependent component  $\Phi_{MTA}$  in the reduction basis is suggested to include the loading in a more elegant and efficient way [14, 13].

The  $\Phi_{MTA}$  vectors, in a simple mechanical interpretation, represent the structure deformation caused by the internal loading as presented in Fig. 2.6. Similarly, as for the internal dynamic in the classical Craig-Bampton, it is assumed that the internal loading can be decomposed into a number of modes.

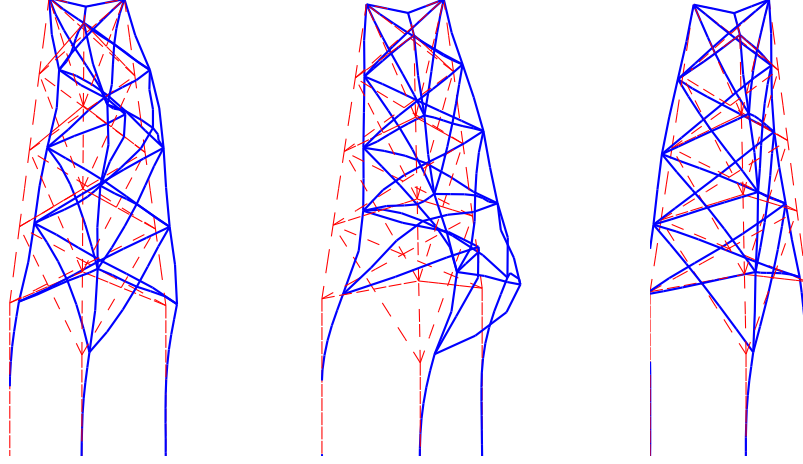


**Figure 2.6:** Load-dependent vectors for the Augmented Craig-Bampton reduction basis ( $\Phi_{MTA}$ ).

The internal force  $\mathbf{f}_i(t)$  is represented by a superposition of the time invariant spatial components  $\mathbf{f}_j$  and corresponding time dependent amplitudes  $\alpha_j(t)$ :

$$\mathbf{f}_i(t) = \sum_{j=1}^p \mathbf{f}_j \alpha_j(t) = \mathbf{F}_i \alpha(t). \quad (2.26)$$

By including a number of these components the  $\mathbf{F}_i$  matrix can be built which represents the internal loading. The challenge in that approach is how to transform the time dependent, correlated load vector  $\mathbf{f}_i(t)$  into a representative time-invariant and uncorrelated load vectors  $\mathbf{F}_i$ . One of the method is to use the so-called *Proper Orthogonal Decomposition* as described in App. C and e.g. [15].

When the load vectors are established, the augmentation to the reduction basis can be calculated as:

$$\Phi_{MTA} = \mathbf{P} \mathbf{K}_{ii}^{-1} [\mathbf{Y} \quad \mathbf{F}_i], \quad (2.27)$$

where  $\mathbf{Y}$  corresponds to the additional acceleration contribution from the interface

$$\mathbf{Y} = \mathbf{K}_{ib} - \mathbf{K}_{ii} \mathbf{M}_{ii}^{-1} \mathbf{M}_{ib}, \quad (2.28)$$

and  $\mathbf{P}$  is the orthogonalizing operation, which assures that no information overlapping is included with the fixed vibration modes  $\Phi_i$

$$\mathbf{P} = \mathbf{I} - \Phi_i \Phi_i^T \mathbf{M}_{ii}. \quad (2.29)$$

Equation 2.27 can be seen as a twofold augmentation of the classical Craig-Bampton. The first contribution is due to the interface dynamics  $\mathbf{K}_{ii}^{-1} \mathbf{Y}$ , where the second corresponds to the internal loading  $\mathbf{K}_{ii}^{-1} \mathbf{F}_i$ . Note that in both cases, the columns represent the deformation shapes due to the *generalized excitation* (interface dynamic and time-invariant load vectors).

By applying the augmentation, the internal displacements  $\mathbf{u}_i$  are represented by the static part  $\Psi_c$ , the internal dynamics  $\sum_{i=1}^n \Phi_i$  and the internal load vectors  $\sum_{j=1}^p \Phi_{MTA} \zeta_i$ :

$$\mathbf{u}_i = \Psi_c \mathbf{u}_b + \sum_{i=1}^n \Phi_i \eta_i + \sum_{j=1}^p \Phi_{MTA} \zeta_i. \quad (2.30)$$

The reduction basis for the classical Craig-Bampton can now be augmented to account for the internal dynamic by introducing the MTA vectors:

$$\mathbf{T}_{ACB} = \begin{bmatrix} \mathbf{I} & \mathbf{0} & \mathbf{0} \\ \Psi_C & \Phi_i & \Phi_{MTA} \end{bmatrix}. \quad (2.31)$$

When applied to the previously used matrix formulation, the total displacements of the structure can be found as:

$$\begin{bmatrix} \mathbf{u}_b \\ \mathbf{u}_i \end{bmatrix} = \mathbf{T}_{ACB} \begin{bmatrix} \mathbf{u}_b \\ \boldsymbol{\eta}_i \\ \boldsymbol{\zeta}_i \end{bmatrix}. \quad (2.32)$$

## 2.3 Summary of the Dynamic Substructuring concept

In the presented chapter, the concept of the Dynamic Substructuring has been introduced as a general framework, serving in the load calculation procedures for the offshore wind application.

Two different assembly procedures have been presented: primal and dual. The basic difference between them is in handling the substructures compatibility. The Primal method assumes unique sets of the DOFs for the global system, which can correspond to the standard FE assembly. The Dual method a priori fulfils the interface forces equilibrium. The choice of the assumption has a consequence concerning the implementation afterwards, therefore for the clarity the methods are summarized in Tab. 2.1.

**Table 2.1:** Review of the assembly methods summarized in the chapter.

Method	Assumption	Pros	Cons
Primal	$\mathbf{u} = \mathbf{L}^T \tilde{\mathbf{u}}$	easy implementation	
Dual	$\mathbf{g} = -\mathbf{B}^T \boldsymbol{\lambda}$	non-conforming meshes	double interface DoFs

The second aspect of the Dynamic Substructuring that is addressed in the chapter are the reduction methods. Three methods are presented: the Guyan, the Craig-Bampton and the Augmented Craig-Bampton. The first two are widely known and acknowledged in the industry, however, both have problems when internal loading plays an important role in the calculations. Therefore, an improvement is suggested in order to include the internal loading, which corresponds to the Augmented Craig-Bampton method.

To obtain accurate results within the least amount of time it should be considered, which reduction method has to be used. In order to assess this, a helpful flow chart is presented in Fig. 2.7.

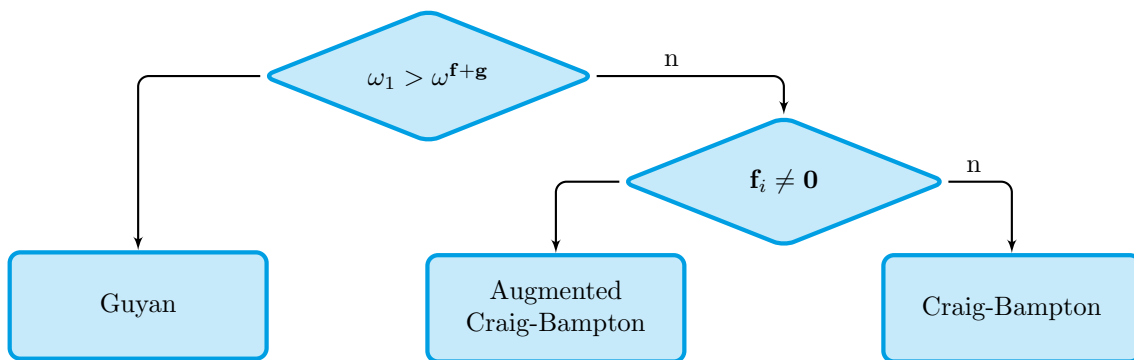


**Figure 2.7:** Decision process for choosing the most appropriate reduction method [16].

The first criterion that should be considered before reducing the model, is the dynamics importance. It can be based on the comparison of the structural eignefrequencies and the frequency content of the excitation. If the first structural eigenfrequency  $\omega_1$  is above the excitation frequency, the structure is likely to behave quasi-statically, therefore the Guyan method can be used. Otherwise, the internal dynamic should be included by using the Craig-Bampton or Augmented Craig-Bampton. The distinction between the methods is made by assessing the importance of the internal loading. If it has a significant influence on the global response, the load

dependent vectors should be included, by using the Augmented Craig-Bampton. Otherwise, the Craig-Bampton method can be successfully used.

## Chapter 3

# Soil-structure interaction

Every engineering structure requires a clear definition of the boundary conditions. These conditions serve as a support/constraint for the structure based on which an equilibrium is obtained and energy can be transferred from point, where the load is applied through the structure further to another medium. The boundary conditions can be seen as a support of a bridge, a foundation of a house, an offshore wind turbine, etc.

The definition of the boundary condition has a paramount importance on both, the global and the local behaviour of the structure. An engineer should decide on the detail level for the boundary condition modelling. The boundary condition can be represented as a fixed support, when the displacements are fully restrained  $\mathbf{u} = \mathbf{0}$ , partially restrained, where e.g. rotations are free, or flexible support represented by a spring, where the displacements are proportional to the applied force  $\mathbf{F} \propto \mathbf{kx}$ .

The applied boundary condition should represent the physical deformation of the structure and properly account for all physical phenomena related to the structure. Depending on the application of the boundary condition, the response of the structure will be different as seen in Fig. 3.1. Therefore, an engineer should assure the proper representation of the boundary condition.

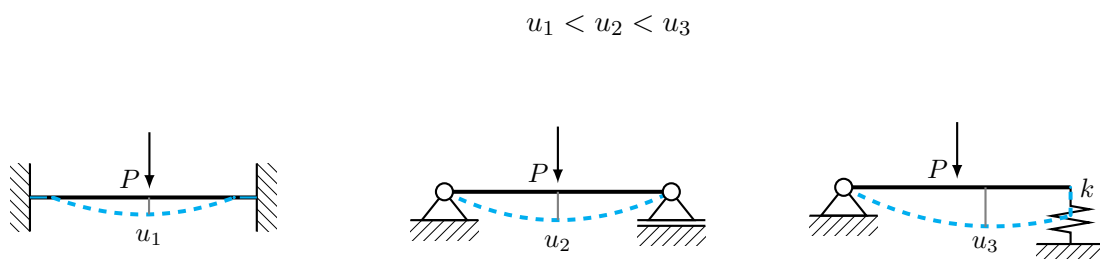


**Figure 3.1:** Influence of the boundary conditions on the response of the structure.

### 3.1 Modelling approaches

At some point most of the civil engineering structures are settled in the soil, therefore there exists a clear need for defining the boundary condition of the surrounding soil as well as the interaction between the structure and the soil. The literature on that matter is very extensive, it can even be said that the soil mechanics is an independent engineering branch. The following chapter is intended to give a basic overview of the soil-structure modelling used in the offshore application, not the comprehensive soil mechanics guide.

In general, the soil is a non-linear material, therefore the interaction between the pile and the soil is highly complex. Non-linearities arise from both the soil as well as from the soil-structure

**Table 3.1:** Non-linear soil phenomena.

Material based	Interaction based
three-phase	pile group
time-variant	gap
frequency-variant	contact
cyclic effects	slip
plasticity	geometric damping

interaction as summarized in Tab. 3.1. The soil non-linearities result from the material texture. It consists of three phases (solid, water, voids), which can vary over the time. The system is not only time variant, it can also depend on the frequency content of the excitation.

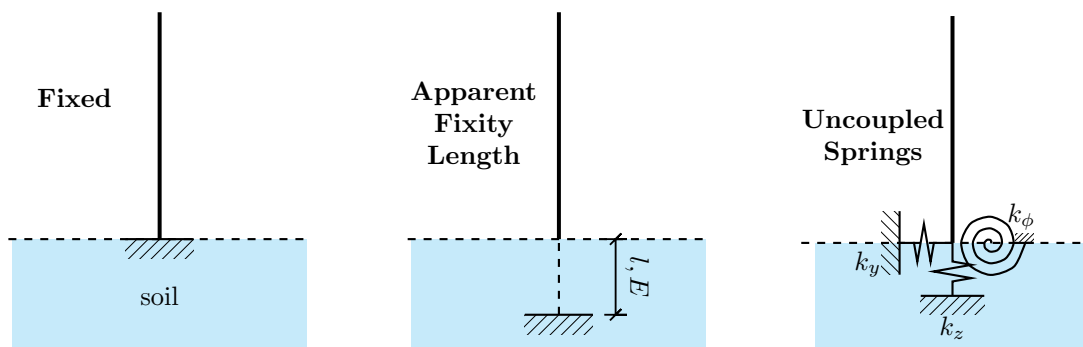
Apart from the material non-linearities, the geometrical non-linearities are also possible. The material itself is strongly inhomogeneous and depth dependent, moreover the piles interact between themselves, if spaced closely.

In terms of the soil-pile interaction, a number of non-linear phenomena can also appear. The most obvious is a contact between the soil and pile. It is non-linear due to the possible gap that can arise, especially in the cohesive soil, i.e. clay. Moreover, the axial displacements between the soil and a pile cause the slip, if the displacement level is significant.

The aforementioned phenomena affect not only the stiffness of the soil, but also the damping and mass. All of these parameters are crucial for the dynamic analysis, but accounting for all of them is infeasible in the engineering model due to the limited computational effort. Therefore, the simplified models have been developed. A brief overview of the approaches for the soil-structure interaction for the offshore structures is given below.

### Simple models

The discussion starts with simple models presented in Fig. 3.2.

**Figure 3.2:** Simplistic soil-structure models.

The easiest approach in soil modelling is to completely deny its existence by fully restraining the structure (Fig. 3.2a). That is sometimes useful, if the soil has negligible influence on the structure, i.e. when the deformation does not influence the structure. A **Fixed** structure introduces no additional computational effort, therefore is the easiest way to apply the soil boundary condition.

If the soil and structure stiffness are comparable to the influence of the boundary condition, then it can be applied by adjusting the fictitious pile length  $l$  by using the **Apparent Fixity Length** (Fig. 3.2b). The combination of a fictitious pile length  $l$  and stiffness  $E$  can be chosen to resemble the real structure displacements at the mudline. It can improve the results of the structure above the soil, however, the underlying part is not modelled properly.

A more representative method is the **Uncoupled Springs** method (Fig. 3.2c). In that case the foundation is modelled by using the uncoupled spring constants  $k$  for each DOFs separately. It can independently fit the rotation and the displacements of the mudline, not by the coupling of the translation and the rotation of a pile.

### Refined models

The above-mentioned models do not introduce significant modelling difficulties, therefore they can be used for the simple analyses, where the soil does not significantly influences the solution. However, none of these models properly accounts for the pile modelling nor damping, therefore when the dynamic analysis has to be performed, a more refined model has to be applied. The overview of the models is presented in Fig. 3.3.

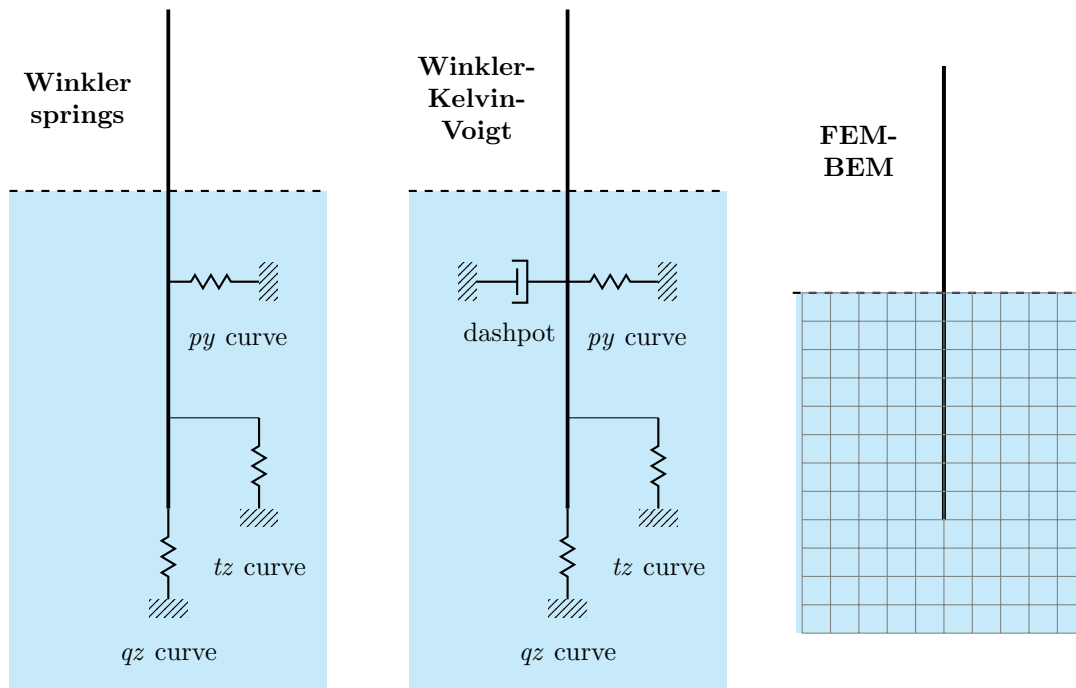


**Figure 3.3:** More refined soil-structure interaction models.

The state-of-the-art soil modelling for the offshore application is the **Winkler** approach (Fig. 3.3a). The assumption is that the soil can be discretized into a number of nodes, where the stiffness is described via a decoupled (non-) linear spring. The improvement compared to the Uncoupled Springs model accounts for depth varying soil non-linearity due to the fact, that multiple springs are applied. Because the pile is properly described by using the combined beam (Bernoulli-Euler, Timoshenko) and soil components, both for stiffness  $\mathbf{K}$  and mass  $\mathbf{M}$  matrices, the simple damping  $\mathbf{C}$  formulation can be included. Most frequently, the Rayleigh damping is used:

$$\mathbf{C} = \alpha\mathbf{M} + \beta\mathbf{K}, \quad (3.1)$$

where  $\alpha$ ,  $\beta$  are the mass and stiffness proportional terms. The model can use both, the linear and the non-linear soil formulation. The non-linear force-displacement curves ( $py$ -,  $tz$ - and  $qz$ - curves), based on which the stiffness is derived, are adopted in the standards [17, 18].

The Winkler model is used widely in the industry, however some studies work on the improved Winkler model, accounting on the more sophisticated damping model as well as on the non-linear contact soil-pile phenomena [19]. The idea of the improvement is twofold:

- Dashpots- instead of the simple Rayleigh damping model, by introducing dashpots (dampers) to the system, a more realistic hysteretic, velocity (viscous) dependent damping can be introduced. The combination of the spring-dashpot system can be set up either parallel or series. If the parallel layout is used, the model includes so-called visco-plastic or visco-elastic **Kelvin-Voigt** material.
- Near- and far-field- by combining a series of Kelvin-Voigt elements (Fig. 3.3b), the additional phenomena can be described, e.g. wave propagation, radiational damping, slip zone, which were impossible to account for in the Winkler model.

The presented models are in the development phase, but could actually increase the soil-modelling accuracy, therefore they have been mentioned here. The significant advantage of the model is the non-complicated application and similarity to the currently used Winkler model. Therefore, the possible implementation should not significantly decrease the computational efficiency of the model.

The final modelling approach is the fully three-dimensional **FEM-BEM** (Fig. 3.3c), coupled soil-structure models. The soil is modelled as a continuum field, therefore no lumping to a pile node is necessary. That model accounts for all non-linearities mentioned in Tab. 3.1. Therefore, it is the most exact and universal approach for modelling the soil. However, the level of complexity is so high, that the computational time is unreasonable, therefore the models cannot be applied in the load calculation procedures. Moreover, the calculations are highly dependent on the soil parameters, therefore to obtain the correct results additional soil tests are required. For these reasons, the method is mostly used to validate the simplified models and test new approaches.

The comparison of the above-mentioned methods is summarized in Tab. 3.2.

**Table 3.2:** Soil-structure modelling approaches overview.

Approach	Pros	Cons
Fixed	fast	soil is totally disregarded
Apparent Fixity Length	soil indirectly accounted for	neglect soil-structure interaction
Uncoupled Springs	simple soil representation at the boundary node	does not account for soil inhomogeneity
Winkler Springs	soil precisely modelled over the depth	simple damping model
Winkler-Voigt-Kelvin	improved damping model	no pile interaction and wave reflection
FEM	account for all important non-linearities	labor-intensive, time-consuming

Based on the general overview of the soil-structure modelling approaches, the Winkler Springs has been chosen to be investigated in more details. The state-of-the-art in terms of soil modelling for offshore application, is to represent soil as a series of uncoupled linear springs. However, the soil is linearized according to the initial soil stiffness, when as mentioned before due to many phenomena the material is non-linear. Therefore, the idea is to investigate the influence of including non-linear soil models in the load calculation procedures.

In the following section, the Winkler approach is briefly introduced, followed by the standard [17, 18] guidelines in terms of soil curves approximations. Finally, the discussion of the limitations of the Winkler method is given.

### 3.2 Non-linear Winkler Springs

The state-of-the-art method to model soil-structure interaction in the offshore applications, is the Winkler approach combined with the  $py$  curve method.

The Winkler approach [20] is an old method developed in 19<sup>th</sup> century to analyze the response of a beam on an elastic foundation. It accounts for the soil interaction by means of a series of springs.

The properties of the spring, given in terms of its stiffness  $k$ , is provided by the  $py$  curve method. The method describes the interaction between the soil and a pile. The method is based on the empirical results of the experiment conducted in 1966.

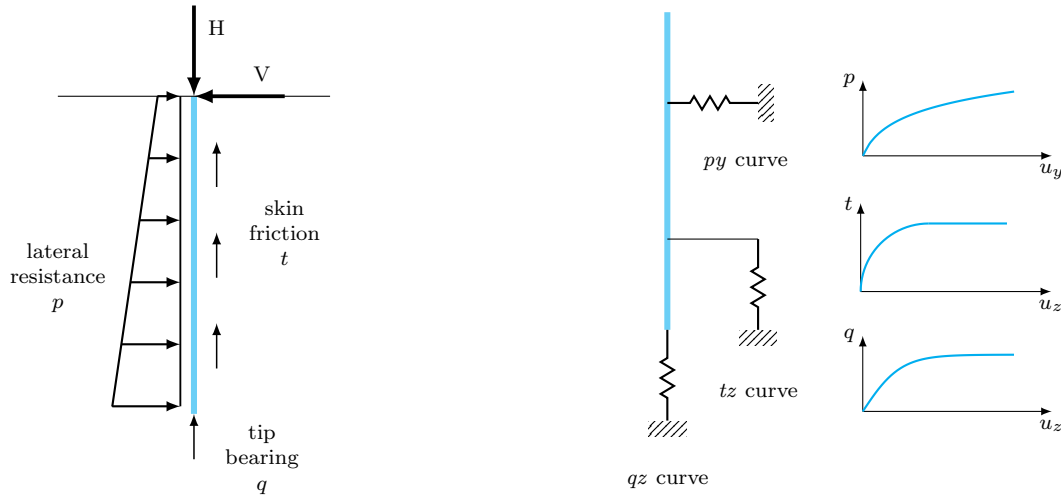


**Figure 3.4:** Non-linear soil-structure model. a) physical model, b) Winkler model with  $py$  curves.

Starting from the physical problem of a beam, submerged in the soil, which is presented in Fig. 3.4a, the lateral pile resistance  $V$  can be described as:

$$V = \int_0^l p(u_y, z) D dz, \quad (3.2)$$

where  $D$  is the pile diameter,  $p(u_z, z)$  is the soil resistance depending on the depth  $z$  and the deflection  $u_y$ . The soil profile can differ over the depth that is why in general the relation is difficult to estimate. Moreover, the soil resistance is dependent on the load level due to the plasticity of the soil.

Similar expression can be set up for the axial pile resistance:

$$H = H_t + H_q = \int_0^l t(u_z, z) C dz + q(u_z) A_t. \quad (3.3)$$

In the axial case, the total resistance  $H$  consists of two components:  $H_t$  skins friction between the soil and the shaft of the pile and  $H_q$  pile tip end bearing capacity. The skin friction component is based on the skin friction resistance  $t(u_z, z)$ , depending on the axial displacements  $u_z$  and the depth  $z$  and the shaft area that is estimated by the use of the circumference  $C$  and the pile length. The end bearing capacity is based on the end bearing curve  $q(u_z)$  and the gross area of the tip  $A_t$ .

The governing equation of the pile as in Fig. 3.4b can be set up in order to estimate the pile deflection and consequently the pile capacity.

$$EI \frac{d^4 u_y}{dz^4} - N \frac{d^2 u_y}{dz^2} - p(u_y) = 0. \quad (3.4)$$

The lateral pile deflection is governed by Eq. 3.4, where  $EI$  is the bending stiffness of the pile,  $u_y$  is the lateral deflection,  $z$  is the depth,  $N$  the axial force and  $p(u_y)$  represents the soil curve. It is a modified version of the Bernoulli-Euler beam with an additional component representing the soil. The first term is related to the bending of the pile, the second takes the axial forces into account and the last term represents the soil-pile interaction.

The same equation can be set up by using of the Timoshenko beam theory that is accounting for the pile shear force. That approach is advised to use, if monopiles with a low  $L/D$  ratio are used. However, in the thesis, the jacket with slender piles is considered, therefore, the Bernoulli-Euler formulation is sufficient.

The axial direction is governed by Eq. 3.5:

$$EA \frac{d^2 u_z}{dz^2} - t(u_z)C - q(u_z)A_t = 0, \quad (3.5)$$

where  $EA$  is the axial pile stiffness,  $u_z$  is the axial displacement,  $t(u_z)$  the skin friction soil curve,  $C$  is circumference and the last term describes the end bearing capacity.

The governing equations can be solved in both analytical and numerical ways. In the presented study, the numerical *Finite Element* approach is used. The schematic description of the implementation is given below.

### FE implementation

The governing equations for the deflection of the beam is solved by using the standard *Finite Element* method. It is assumed that the reader has a basic knowledge of the method, therefore the general principles are not explained herein.

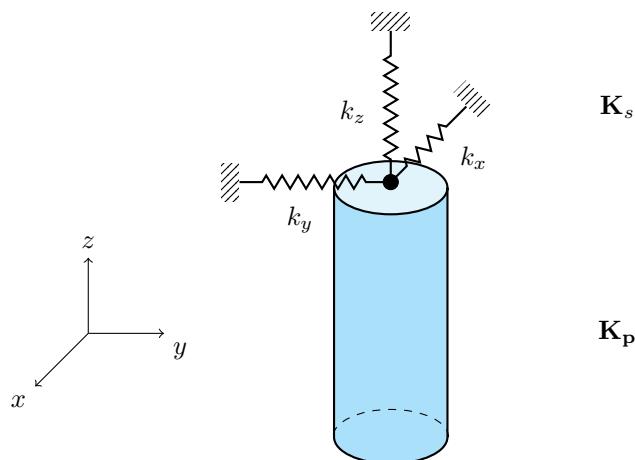


**Figure 3.5:** Composite soil-structure element.

What is explained though, is the combination of the structural beam element and the surrounding soil. The pile element is treated as a composite, non-linear element consisting of the structural and the soil part, see Fig 3.5. The structural component can be represented by a linear Bernoulli-Euler or Timoshenko beam, but can also include the second order non-linear effects. The soil component is modelled as a set of non-linear, decoupled springs.

The stiffness  $\mathbf{K}$  of that composite element is described as

$$\mathbf{K}(\mathbf{u}) = \mathbf{K}_p + \mathbf{K}_s(\mathbf{u}), \quad (3.6)$$

where  $\mathbf{K}_p$  is the structural pile stiffness and the  $\mathbf{K}_s$  stands for the soil part. As mentioned, the structural part can in general be non-linear, however in the study a linear element is used. The soil stiffness contribution is non-linear, depending on the displacement level  $\mathbf{u}$ .

In the matrix form the stiffness of the element is as follows:

$$\mathbf{K}_p = \begin{bmatrix} k_{11} & 0 & 0 & 0 & k_{15} & 0 \\ & k_{22} & 0 & k_{24} & 0 & 0 \\ & & k_{33} & 0 & 0 & 0 \\ & & & k_{44} & 0 & 0 \\ & & & & k_{55} & 0 \\ & & & & & k_{66} \end{bmatrix} \quad \mathbf{K}_s(\mathbf{u}) = \begin{bmatrix} k_x(u_x) & 0 & 0 & 0 & 0 & 0 \\ & k_y(u_y) & 0 & 0 & 0 & 0 \\ & & k_z(u_z) & 0 & 0 & 0 \\ & & & 0 & 0 & 0 \\ & & & & 0 & 0 \\ & & & & & 0 \end{bmatrix}. \quad (3.7)$$

The  $\mathbf{K}_p$  corresponds to the Bernoulli-Euler beam element (for simplicity only DoFs that are corresponding to the first node are presented) and the  $\mathbf{K}_s$  presents the soil springs. The  $k_{ij}$  coefficient are provided by the standard beam formulation and the spring stiffness coefficients  $k_i(u_i)$  are derived based on the  $py$  curves.

### Soil curves

The *FEM* implementation requires the spring stiffness  $k$  to represent the surrounding soil. That value is obtained by differentiating the force-displacement soil curves:

$$k_x(u_x) = \frac{dp(u_x)}{dx} \quad k_y(u_y) = \frac{dp(u_y)}{dy} \quad k_z(u_z) = \frac{dt(u_z)}{dz}. \quad (3.8)$$

Many experiments have been conducted that are in line with the theoretical attempts, in order to provide the general and robust description of the general soil interacting with the general structure. One of the approach,  $py$  curves, is adapted in the offshore standards [17] and is used in the study.

The  $py$  curves describe the load transfer between the pile and the surrounding soil, see Fig. 3.6. The curves predict the deflection based on the applied force. Due to the fact that the curves are non-linear, the stiffness that is obtained by using Eqs. 3.8, depends on the displacement level. That makes the calculations non-linear as well.

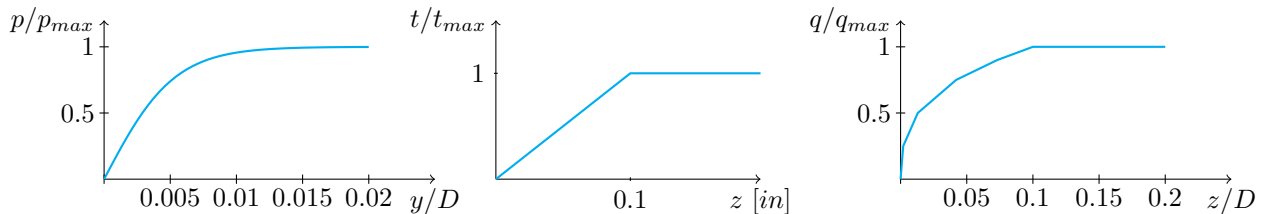


**Figure 3.6:** Soil curves suggested by the standards.

The curves in Fig. 3.6 are the generalized version of the original experiments [21] and improved afterwards by e.g [22]. The guidance on obtaining the specific curves for the pile diameter, soil type and specific depths are given in [17]. An excerpt from the standards is given below in Tab. 3.3 and 3.4.

**Table 3.3:** Force–displacement relation for the axial spring according to API standard [18].

$z$ [in]	0.0	0.1	$\infty$
$t/t_{max}$	0.0	1.0	1.0

The  $py$  relation is modelled as a constant function, where the axial curves are piece-wise linearized [17]. Note that the skin friction is governed by a very strict condition of an axial deformation corresponding to 0.1 in. By the time, the limit displacements are reached, the skin friction stiffness is constant, afterwards it is zero. That corresponds to the physical phenomenon

**Table 3.4:** Force–displacement relation for the end bearing spring according to API standard [18].

$z/D$	0.000	0.002	0.013	0.042	0.073	0.100	$\infty$
$q/q_{max}$	0.00	0.25	0.50	0.75	0.90	1.00	1.00

of losing friction contact between the soil and the pile after a certain limit displacement is reached (0.1 inch [18]).

Due to the fact, that the curves are based on the experiment that was conducted on a limited number of samples and a rather small number of load cases, it is questioned whether the *py* method can accurately describe the soil-pile interaction.

### Limitation of the method

The *py* method has some uncertainties, the Winkler method also provides a number of assumption. Therefore, the main shortcomings of the used approach is briefly described, based on the discussion from [19, 23].

- **Shearing force between soil layers**– the soil acts as a continuum, while the Winkler approach discretizes it into a series of uncoupled springs. Therefore, the displacements of a specific point do not depend on the surrounding points. That approach disregards the shearing forces between the soil layers. Pasternak [24] suggested a modified approach, which accounts for shearing forces, the model has been implemented by Belkhir [25] and the results of 5% differences has been found.
- **The ultimate soil resistance**– one of the significant parameters used in the *py* methods, is the ultimate soil resistance, which is defined by the assumption of the soil stability failure mode. The assumption is that the surface between the soil and the pile is either perfectly smooth or perfectly rough. However, the reality is rather the combination of these conditions, therefore the results might be affected. Nevertheless, that effect has neglected the importance for slender piles, it may however be important for monopiles.
- **Effect of soil-pile interaction**– even though the pile bending stiffness  $EI$  is taken into account in the *FEM* application, the *py* methods do not account for it. Therefore, there is no difference if the pile behaves flexible, or deflects rather as a rigid body. The studies by Ashour [26], Fan [27] question this assumption by showing the results, where the pile response depends on the pile stiffness.
- **Developed for static lateral capacity**– the *py* method is originally developed for a static lateral capacity estimation, but is now also used for the dynamic FLS calculation. To account for it, a rather simplistic solution was suggested, where the cyclic degradation is applied to the static curves. That approach has recently been questioned by Buren in [19] and the dynamic version of the *py* curve is under development.

## Chapter 4

# State-of-the-art procedures

The goal of the thesis is to contribute to the improvement of the quality of reduced models, which are used in the design procedures for an offshore wind turbine. One of the stages on the path to obtain that goal, is to critically present the currently used design procedure that is implemented by the industry. As mentioned in the introductory chapter, the integrated design, which serves as a framework for a load calculation procedure, might not be the most precise method. However, it is the most widely used method to design wind turbines, hence it is of great importance to briefly summarize the key points of a design procedure.

The main reason why the method might raise some concerns of the quality of the results comes from the fact, that a wind turbine model is decomposed into a series of simpler, independent structures. As described in the introduction a multiphysics wind turbine model ought to act as a coherent model with proper coupling. The integrated model for a wind turbine application is repeated here for convenience.

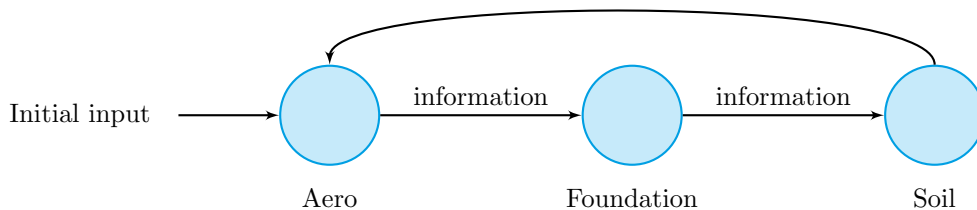


**Figure 4.1:** Information flow in Sequential Integrated approach.

To some extent that coupling is fulfilled in the integrated approach by means of the information that is shared between different parties involved in a design process as sketched in Fig. 4.1. Due to the fact that the information is shared only after an integration of the whole time period of the analysis (usually 600 s), the intermediate stiffness adjustments are not possible, therefore any non-linearities are not feasible to account for. The process is also called *iterative*, because after the full sequence of integrations, the initial input must be checked whether it corresponds to the *real* one from the analysis. In case a significant change has been discovered, an additional iteration is necessary. One of the significant shortcomings of the method that will be investigated in more details in the thesis, is the above mentioned non-linearities in respect of the soil.

Another aspect analyzed is the quality of the information shared. That is an essential part of the method, because based on the information quality and the ability to properly describe the model behaviour, the coupling will be set up. Information combines system matrices and interface forces, a description of the system is a matter of agreement between parties. Certainly, the amount of information to share, due to the confidential and practical reason, is minimized. Therefore the models are not given in a full representation, but in a reduced sense with the so called *superelement*. As described in the previous theoretical part, many types of *superelements*



and can therefore not be used in the integrated approach, it has to be linearized according to a specific load level. That is usually done for a initial stiffness corresponding to the stiffest possible soil. Whether this is the correct method is questioned and will be assessed in the latter part of the thesis. When soil and wave forces are obtained, the model can be reduced in a sense of specific *superelement* theory, usually Guyan for a monopile and Craig-Bampton for a jacket.

- **Aero-elastic calculation**– The information from a previous step is given to a Wind Turbine Manufacturer, who applies it to a model and performs aero-elastic calculations. The model consists of a wind turbine, tower and an integrated, reduced foundation model. An aero-elastic code is implemented to evaluate a wind forces combined with a controller code and certainly a structural part. The model should include all relevant properties such as non-linear blades stiffness, servo system for a nacelle, etc. During that analysis a tower dimensioning is being performed. This is the only site-specific element of a wind turbine except the foundation that has to be adjusted based on the local conditions. As an output of that analysis, a Wind Turbine Manufacturer should deliver an interface force time series that is given to a Foundation Designer.
- **Detailed foundation design**– as a first step of that part of the analysis, a Foundation Designer needs to recover an input into a full jacket response. This procedure is called *recover-run* and can be done either as the *Force/Displacement-Controlled* method, or the *Direct-Expansion*. Once the jacket displacements are recovered, a detailing design can be performed in order to fulfil a necessary designing criteria, such as element utilization, fatigue lives, serviceability conditions, pile penetration and so on. Depending on the results from that part of the jacket is either optimized or strengthen to meet all of the requirements with a minimum allowable steel amount. Usually, an optimized jacket is significantly different and an additional load iteration is necessary to obtain updated interface forces for a site-specific foundation model. Depending on how much a foundation model changed, the interface forces might vary and correspond to a new foundation model. The *iterative* procedure lasts as long as the foundation model converges.

After a general overview of the procedures, some more specific and practical issues will be addressed in the following chapters. For convenience of a reader each main part of the procedures corresponds to a separate chapter, so the the input-output relation between parties can be addressed.

## 4.1 Reduced foundation models

The following chapter describes procedures performed by a Foundation Designer in order to obtain a reduced foundation model, which afterwards serves as a boundary condition for a Wind Turbine Manufacturer. The reduced model consists of a system matrices fully describing a system in case of a dynamic analysis (stiffness, damping and mass matrices) and a reduced interface forces, which describe all internal loading imposed to the jacket (waves, current, buoyancy).

With respect to the foundation it is assumed that the piles and surrounding soil is also included in the model, since the current design is not ready for a method with multiple interface nodes (other than an interface between a tower and a jacket). Therefore, an integrated pile model will be presented here. The problem with that approach is that it does not account for complicated pile models such as suction buckets. A suggestion for a better model of such a foundation will be given in the next part of the thesis.

A procedure for obtaining a *superelement* is described in Fig. 4.3. Initially, an interface node is chosen, which will be a connection point between a foundation and a tower, afterwards piles are linearized, since a *superelement* theory can only handle linear models. Finally, the proper

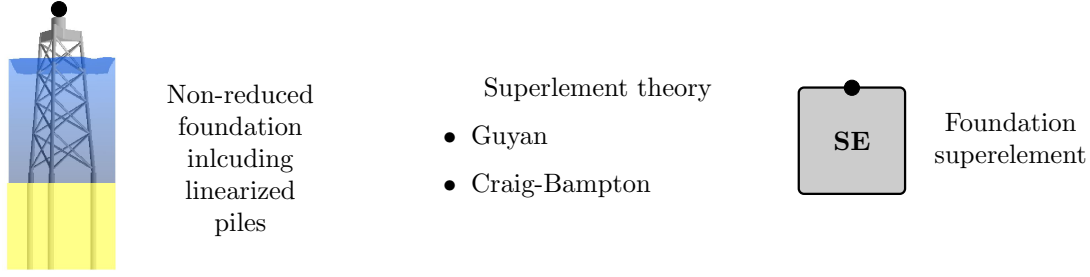


**Figure 4.3:** Procedure for obtaining a superelement of a foundation including linearized piles.

theory is used in order to reduce both, a foundation matrices and a load vector. The description of different methods is given in the theoretical part of the thesis.

Creating a *superelement* is nothing more than translating a physical DoFs into a generalized DoFs. The first describes the translation and rotations of each individual node and can require more than 1,000 DoFs for a complex foundation structure like a jacket. The generalized DoFs are associated with magnitudes of dynamic modes of a foundation. Usually less than 50 generalized DoFs are enough to precisely describe a foundation motion, therefore that reduction is very effective and practical.

A transformation is described as:

$$\mathbf{u} = \mathbf{T}\mathbf{q}, \quad (4.1)$$

where  $\mathbf{u}$  is the jacket physical DoF,  $\mathbf{T}$  the transformation matrix and  $\mathbf{q}$  the generalized jacket DoF. The system matrices and force vector are reduced by projecting the original matrices on the reduced generalized space:

$$\tilde{\mathbf{K}} = \mathbf{T}^T \mathbf{K} \mathbf{T}; \quad \tilde{\mathbf{C}} = \mathbf{T}^T \mathbf{C} \mathbf{T}; \quad \tilde{\mathbf{M}} = \mathbf{T}^T \mathbf{M} \mathbf{T}; \quad \tilde{\mathbf{f}} = \mathbf{T}^T \mathbf{f}, \quad (4.2)$$

where superscript  $(\tilde{\cdot})$  denotes the reduced matrices.

The quality of the reduced system and ability to properly describe the non-reduced one lays only within the transformation matrix, therefore it is of great importance to make sure that the proper method and parameters were used. Derivation and more details on how to create that matrices are addressed in the theoretical part, both for the Guyan and Craig-Bampton method.

For a jacket foundation, where internal dynamic is important, Guyan method does not provide sufficient accuracy, therefore it is advised to use the Craig-Bampton *superelement*. The Craig-Bampton reduction basis consists of static part which describes the interface displacements  $\Psi_C$  and number of modes for internal dynamic  $\Phi_i$

$$\mathbf{T} = \begin{bmatrix} \mathbf{I} & \mathbf{0} \\ \Psi_C & \Phi_i \end{bmatrix}. \quad (4.3)$$

An important parameter for that method is the number of internal dynamic modes  $i$ . If all internal nodes are included, the reduced and the full system should have the exact same response, but the size of the reduced model would be the same. Therefore to get a more effective one the number of modes need to be truncated and thereby the system is reduced. To use the optimal number of internal modes, a sensitivity analysis should be performed, where the convergence of the reduced system should be checked in terms of two aspects:

- **spectral convergence**– when truncating a model its *freedom* of deformations is limited, therefore the stiffness is artificially increased which results in the increased eigenfrequency of the system. Therefore, a sufficient number of modes should be included in order to converge the frequency up to a certain level. An engineering rule of thumb is to converge all frequencies up to 1.5 times the highest relevant frequency of the excitation. For a jacket

excited with wind and wave that might correspond to approximately 10 Hz, but it should be checked for a every specific case.

- **spatial convergence**– corresponds to a spatial distribution of internal loads. It will be responsible to properly describing wave loads that are internally imposed to a jacket. One way to check it, is to compare a response of some specific nodes (preferably brace nodes) from reduced and non-reduced models. The problem with the Craig-Bampton method is that for localized effects the convergence might be slow, therefore, a high number of internal dynamic modes might be important to include.

Once the number of internal modes is chosen, one should also pay attention to a proper description of the soil. As mentioned in the theoretical chapter, the soil is a non-linear material, which softens when the load level is increased. As long as piles are integrated in the foundation model, they have to be included in the reduced as well. Since the reduction theory is linear it can only describe a constant stiffness of the soil. Therefore, it need to be decided what would be the most *representative* soil stiffness that characterizes the soil the best over the total period of the simulation.

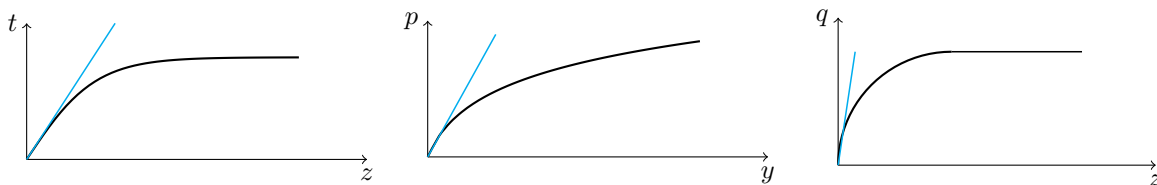


**Figure 4.4:** Linearization of the soil for the purpose of creating the *superelement*. The black plot corresponds to a non-linear curves, cyan to a linearized curve with initial soil stiffness.

In some cases one the initial soil stiffness is used in order to describe the soil as depicted in Fig. 4.4 . That assumes that the soil does not soften when a load level increases. That might be an accurate approach, when a load level does not correspond to a high level of displacement and a softer, non-linear soil response. This might be the case when FLS load cases are considered. However, when the interest is in assessing the ULS utilization, the soil might not be properly described by using the initial (high) stiffness. The current practice is that one superelement is used both for ULS and FLS cases with initial stiffness. That means that soil for the ULS might act as overly stiff in the analysis. The question that arises is what is the influence of that compared to the non-linear solution, because from the theoretical point of view it might result in a significant misestimation of the soil.

To summarize that part of load calculation procedures it is important to:

- properly describing all important physical phenomena of the non-reduced model,
- if relevant, including dynamic abilities of the model (jacket foundation) by the using correct *superelement* type,
- ensuring the spectral and spatial convergence by including enough dynamic modes,
- constructing the correct soil *representative* model to be linearized.

In order to help choosing the correct *superelement* a brief characteristic of each is given below.

- **Guyan**- very compact (matrices size 6x6) representation of the reduced model. The *superelement* is precise for cases where the structure can be described by using a quasi-static response. That model can be used for monopiles, where internal dynamics do not influence the total response significantly.

- **Craig-Bampton**- On top of the quasi-static of Guyan theory, the *superelement* can also describe internal dynamics of the model by including a number of internal eigenmodes. That significantly increase accuracy for a jacket type foundation. The size of the reduced model is  $6 + i$ , where  $i$  is the number of internal modes. Usually 50 and less modes are enough to describe a complex jacket foundation.

The two mentioned methods are successfully used in reduced foundation modelling, however they also have some limitations as seen in Tab. 4.1.

**Table 4.1:** Ability of the superelement to describe different phenomena.

Superelement	quasi-static	dynamic	internal load	non-linear piles
Guyan	+	-	-	-
Craig-Bampton	+	+	+/-	-

Both *superelements* can describe quasi-static response, when using Craig-Bampton also a dynamic one can be included. However, when dynamic, internal loading plays an important role the Craig-Bampton method requires significantly higher number of internal modes (200 based on the internal Rambøll investigation) to properly describe the brace motion. Both *superelements* cannot account for non-linear soil behaviour, therefore a linearized soil model has to be implemented instead.

## 4.2 Aero-elastic calculations

Once the foundation model is reduced, it can be integrated into an aero-elastic code. The integrated equations of motion that combine the tower and the foundation, can be presented in a *dual-format* as it was derived in the theoretical basis for the general case and introduced as a basic idea in the introductory chapter.

$$\begin{bmatrix} \mathbf{M}^a & 0 & 0 \\ 0 & \tilde{\mathbf{M}}^f & 0 \\ 0 & 0 & 0 \end{bmatrix} \begin{bmatrix} \ddot{\mathbf{u}}_a \\ \ddot{\mathbf{q}} \\ \ddot{\lambda} \end{bmatrix} + \begin{bmatrix} \mathbf{C}^a & 0 & 0 \\ 0 & \tilde{\mathbf{C}}^f & 0 \\ 0 & 0 & 0 \end{bmatrix} \begin{bmatrix} \dot{\mathbf{u}}_a \\ \dot{\mathbf{q}} \\ \dot{\lambda} \end{bmatrix} + \begin{bmatrix} \mathbf{K}^a & 0 & \mathbf{B}_a^T \\ 0 & \tilde{\mathbf{K}}^f & \mathbf{B}_f^T \\ \mathbf{B}_a & \mathbf{B}_f & 0 \end{bmatrix} \begin{bmatrix} \mathbf{u}_a \\ \mathbf{q} \\ \lambda \end{bmatrix} = \begin{bmatrix} \mathbf{f}_a \\ \tilde{\mathbf{f}}_f \\ 0 \end{bmatrix}. \quad (4.4)$$

The equations combine the tower model  $(\cdot)^a$  with the reduced foundation model  $(\cdot)^f$ . Coupling is fulfilled by the kinematic constraint (last equation), where the interface displacements are equal in both subsystems. An illustration of the integrated system can be seen in Fig. 4.5a. By combining equations 4.4 with the illustration it can be clearly seen how the integrated approach is set up for an offshore wind turbine.

The quality of coupling and finally the results depend on the quality of the models used in the calculations. For aero-elastic calculations, the foundation is modelled as the reduced system, therefore the quality of final results for the foundation depends on the quality of the reduced system. Therefore, it so important which *superelement* is used and what are the limitations/shortcomings.

The aero-elastic calculation is performed based on a model equivalent to Eq. 4.4, where both wind and reduced wave forces are applied simultaneously. The outcome of the calculations corresponds to time series of displacements for the tower part and the foundation part and the interface forces. Depending on what type of system representation was used, it can be either physical DoFs or generalized DoF. Usually the tower is represented by a physical coordinates, but for some cases (FLEX software) it might be modal coordinates.

If a dual assembly procedure is used, the outcome will correspond to:

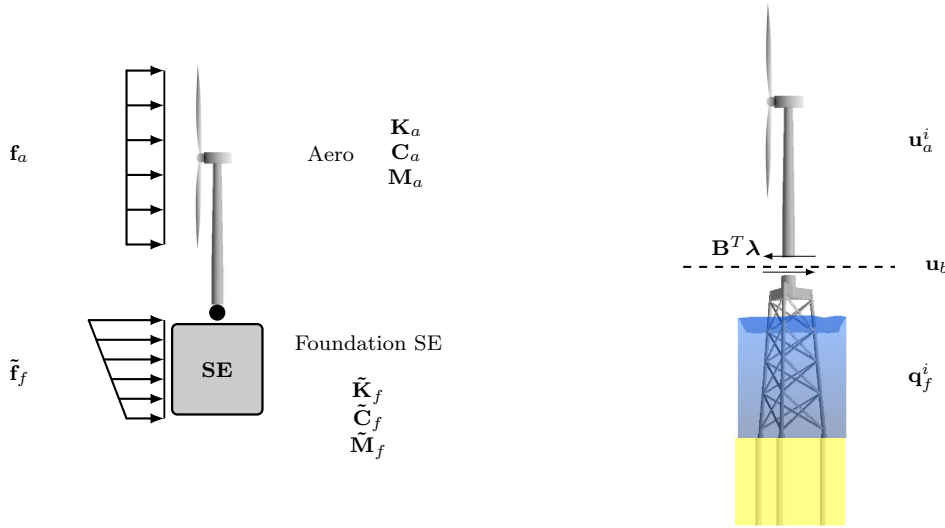


Figure 4.5: a) Integrated wind turbine model b) Information sharing procedure.

$$\begin{aligned} \mathbf{u}_a(t) &= [\mathbf{u}_a^i \quad \mathbf{u}_b], \\ \mathbf{q}(t) &= [\mathbf{u}_b \quad \mathbf{q}_f^i], \\ &\boldsymbol{\lambda}(t), \end{aligned} \quad (4.5)$$

where the first line represents tower displacements, the second reduced foundation generalized displacement and the last one the interface forces. Certainly, the derivatives of displacements in terms of velocities and accelerations are also obtained. It can be observed that the displacements of both structures include the interface  $\mathbf{u}_b$ . That lays in the nature of the *dual* assembly where the interface node is defined twice. This might lead to an unnecessary increase of the system size, therefore usually due to a practical reason *primal* assembly is used. However, the dynamic results obtained from both systems are identical.

It can be noticed that the solution for the foundation consists of two main terms: physical interface displacements  $\mathbf{u}_b$  and the magnitude of the foundation modeshapes  $\mathbf{q}_f^i$ . This corresponds to the format of the reduced model is used, in this case the Craig-Bampton one. If one would use Guyan, the output would be in terms of only interface displacements, therefore the system could only respond quasi-statically. However, when Craig-Bampton is used, the system is additionally described in terms of internal dynamic modes. At this point the influence of the superlement on the load calculation procedures can be explicitly noticed.

Finally, the most important outcome of the integrated analysis for the current approach is the time series of the interface forces. Based on that information, a foundation designer can apply it combined with synchronized wave loads to the non-reduced system and integrate inside of the software and obtain the full response.

### 4.3 Recovery-run procedures

In order for a Foundation Designer to be able to perform a detailed design of the foundation structure, forces that are representing the wind loading need to be obtained. These forces are provided by a Wind Turbine Manufacturer in terms of the interface forces  $-\mathbf{B}^T \boldsymbol{\lambda}(t)$  from an integrated aero-elastic analysis.

As explained in the previous section, forces provide a coupling between two substructures and constitute enough information to properly describe all relevant influences of the tower and turbine model that is coupled to the foundation. Therefore, if they are applied by a Foundation Designer and combined with reduced wave forces, the result will be exactly the same as if the

models would be coupled. That in fact yields of solving the second equation of integrated system Eq. 4.4

$$\tilde{\mathbf{M}}_f \ddot{\mathbf{q}} + \tilde{\mathbf{C}}_f \dot{\mathbf{q}} + \tilde{\mathbf{K}}_f \mathbf{q} - \tilde{\mathbf{f}}_f = -\mathbf{B}_f^T \boldsymbol{\lambda}. \quad (4.6)$$

Usually however, a Foundation Designer uses a non-reduced jacket as a post-processing model, while for the aero-elastic analysis the model is reduced. Hence, the results will not be exact, but within a marginal difference as long as the reduced model is properly set up as described in Sec. 4.1. That corresponds to yet another argument to emphasize the importance of the quality of the reduced model.

Once the interface forces are applied together with the wave excitation to the non-reduced foundation model an integration can be performed to obtain displacements of the foundation model.

$$\mathbf{M}_f \ddot{\mathbf{u}}_f + \mathbf{C}_f \dot{\mathbf{u}}_f + \mathbf{K}_f \mathbf{u}_f - \mathbf{f}_f = -\mathbf{B}_f^T \boldsymbol{\lambda}. \quad (4.7)$$

Based on that model, cross section forces can be obtained as a standard procedure and a detailed design of the foundation can be performed. That procedure will not be described here, since it does not lay in the scope of the thesis. Instead a brief discussion will be presented on how to perform control check-ups ensuring that the integration procedure between a Foundation Designer and a Wind Turbine Manufacturer was set up correctly.

The simplest check would be to assure that the interface displacements, calculated by a Foundation Designer, from Eq. 4.7 and a Wind Turbine Manufacturer from 4.5, are the same. However, the interface match usually does not say much about the internal displacements that are also important. A Wind Turbine Manufacturer is not able to calculate the internal displacements of the foundation model, because he does not have physical matrices of a foundation system, only a reduced one. However, assuming a Foundation Designer would deliver the reduction basis, which was used to reduce the system, an internal displacements could be recovered. A Wind Turbine Manufacturer would perform a back transformation from a reduced modal coordinates into a physical, non-reduced coordinates according to Eq. 4.1 (repeated for convenience)

$$\mathbf{u}_f = \mathbf{T} \mathbf{q}, \quad (4.8)$$

and internal displacements could also be compared. Provided that also the internal displacements are the same, it can be assumed that the models are set up properly. A difference between solutions 4.7 and 4.8 might be seen as an indirect measure of the reduced model quality. The difference should be negligible, in any other case the procedure should be checked in great details, because a significant error was committed at some point of the analysis.

At this point of the analysis, it is also a good practice to check the pile displacements with soil curves and asses how much non-linearities is expected for that specific displacement level. If the solution is far from a linear part of the soil curve, it means that the initial assumptions for the soil were incorrect. If this is the case, a load calculation procedure should be repeated for the updated reduced model that is corresponding to the new soil linearization or updated pile design.

**Part II**

**REFINED REDUCED  
FOUNDATION MODELS**



# Roadmap

The goal of the thesis is to improve the quality of the reduced models used in the design procedures for wind turbine structures. Once the state-of-the-art procedures are defined in the previous chapter and weak points are pinpointed it is high time to investigate the possible improvements. The outline of the upcoming part is given in Fig. 4.6.

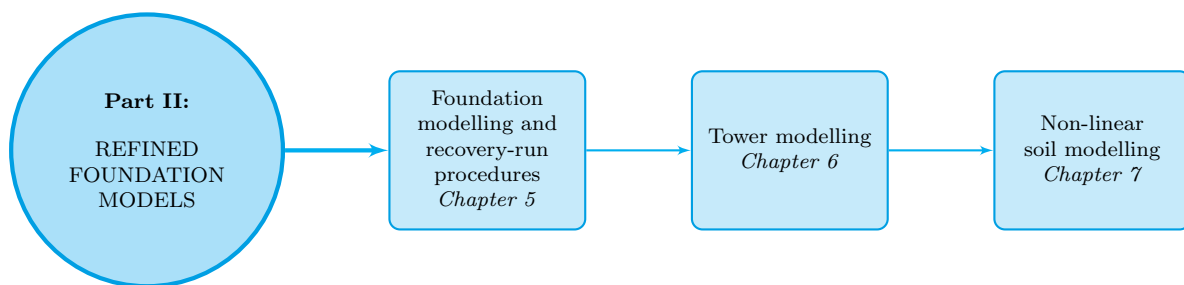


Figure 4.6: Outline of Part II of the thesis.

There are four main areas which will be investigated in order to contribute to the development of the wind turbine industry:

1. **Reduced foundation models** - as mentioned in the state-of-the-art description the reduction theory used to represent a foundation model has significant importance on the quality of results, therefore it is important to strive for a more efficient and accurate representation. **Chapter 5** provides a total load calculation procedure using different reduced foundation, including the currently used Guyan and Craig-Bampton. Moreover, to overcome the problem with internal wave loading experienced by Craig-Bampton an improved Augmented Craig-Bampton method is suggested. Afterwards, results are compared and a set of recommendations is given in order to provide some practical guidance.
2. **Recovery-run procedures** - final step of the load calculation procedure is to recover displacements of the non-reduced foundation model using information from a Wind Turbine Manufacturer. Currently, a time consuming Force-Controlled approach is used, requiring an additional time integration performed by a Foundation Designer. The integration is not necessary to recover the integral displacements of the jacket, hence the more time-efficient, yet accurate Direct Expansion recover-run procedure is assessed in **Chapter 5** as well.
3. **Tower modelling** - in spite of the fact that is up to a Wind Turbine Manufacturer to choose the tower modelling approach the influence of that decision has a significant effect on the wind force transfer from a nacelle to the foundation. Therefore, **Chapter 6** investigates a number of internal dynamic modes on the quality of wind force transferred to the interface.
4. **Non-linear soil-pile modelling** - since soil modelling has the significant impact on the dynamic behaviour of a wind turbine and currently is implemented in a rather simplified linearized manner the investigation of the importance of a non-linear modelling is included



## Chapter 5

# Foundation modelling and recovery-run procedures

As the initial investigation, the efficiency and accuracy of the different reduced foundation models are assessed. The theoretical chapter outlined the importance of the *superelement* on the final results of the integrated wind turbine model. The practical aspect of foundation modelling is addressed in more details in the following chapter. Once the reduced models are integrated in the system, the natural part of the procedure to recover the full foundation displacements. Parallel to the prior investigation, additional interest is given to the more efficient recovery-run procedure. The scope of the presented chapter is in line with the currently used methods as presented in Fig. 5.1.

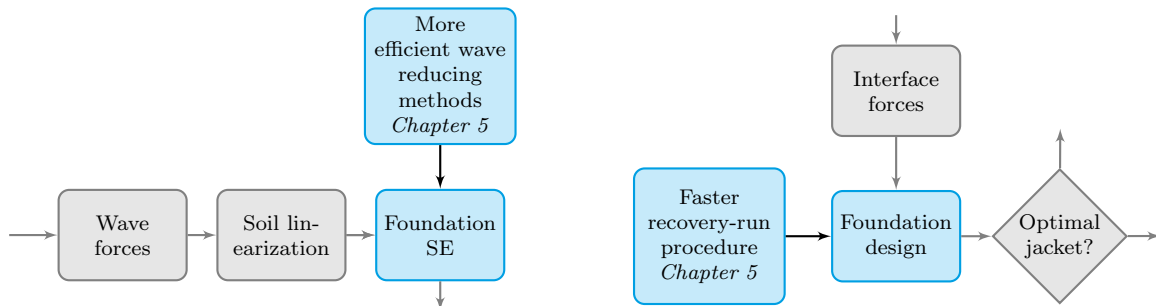


**Figure 5.1:** Focus of the chapter in relation to the state-of-the-art procedures.

The left figure presents how the foundation reduced models gives an input to the load calculation procedures, where the right one contributes to the recovery-run procedures based on the aero-elastic inputs. One of the goals of the presented investigation is to increase the efficiency of the reduced models in terms of representing the internal (wave, current) loading.

### Internal wave loading

As outlined in the theoretical basis, the reduction methods divide the model into interface and internal nodes. The first represents the *key* points of the model responsible for fulfilling the integrity between adjacent substructures. The latter is the second priority *slave* nodes as described indirectly by the interface displacement and the additional components in the reduction basis.

When the excitation is applied directly to the interface node, the exact representation of the forces is transferred into the model. However, when there exists the significant internal loading, it is projected to the interface nodes via the reduction basis. The procedures for the offshore application are sketched in Fig. 5.2. Firstly, the wave and current excitation is generated based

on the non-reduced model. Afterwards the reduction method is applied and the internal loading is reduced based on the reduction basis  $\mathbf{T}$ . Finally, the reduced load vector  $\tilde{\mathbf{f}}$  is obtained.

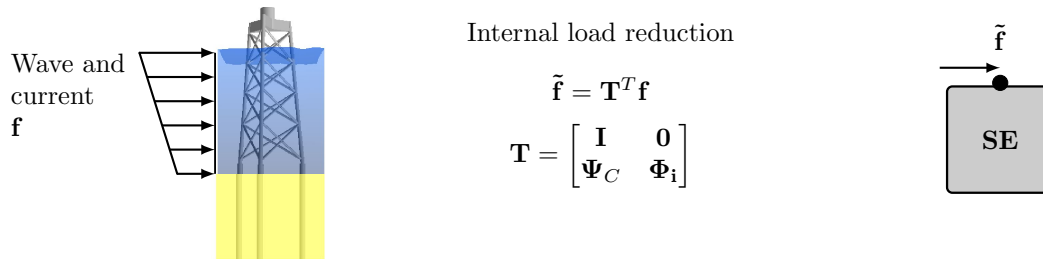


**Figure 5.2:** Reduction of the internal loading for the Guyan and the Craig-Bampton methods.

Basically, the quality of the internal load representation is fully determined by the reduction basis components, for e.g. Craig-Bampton they correspond to  $\boldsymbol{\Psi}_C$ - the quasi-static and  $\boldsymbol{\Phi}_i$  the internal dynamic terms. To obtain that components in the derivation process (Eq. 5.1 and Eq. 5.2) an important assumption has been made.

$$\mathbf{K}_{ib}\mathbf{u}_b + \mathbf{K}_{ii}\mathbf{u}_i = \mathbf{f}_i \quad \text{assumption} \quad \mathbf{f}_i = 0 \quad \Rightarrow \quad \boldsymbol{\Psi}_C = -\mathbf{K}_{ii}^{-1}\mathbf{K}_{ib}, \quad (5.1)$$

$$(\mathbf{K}_{ii} - \omega^2\mathbf{M}_{ii})\boldsymbol{\Phi} = \mathbf{f}_i \quad \text{assumption} \quad \mathbf{f}_i = 0 \quad \Rightarrow \quad \boldsymbol{\Phi} = [\boldsymbol{\Phi}_1 \quad \dots \quad \boldsymbol{\Phi}_i]. \quad (5.2)$$

The assumption holds that the internal loading is assumed to be zero. Therefore, the reduction basis is derived based on the situation, where the loading is only applied to the interface nodes. Due to that fact, when the above mentioned methods were applied to the case, where internal loading is important, the approximation is obtained instead of the accurate solution. In cases where the internal loading is governing, more internal modes  $\boldsymbol{\Phi}_i$  should be used than would be required in other cases.

One possible solution to overcome this inconvenience may be the introduction of additional interface nodes, where the wave loading is applied. However, for the offshore jacket application that method is infeasible, because the computational effort is proportional to the number of interface nodes.

A more efficient solution is suggested in the thesis by introducing an additional component in the reduction basis (Eq. 5.3), which is derived directly from the internal loading vectors.

$$\mathbf{T} = \begin{bmatrix} \mathbf{I} & \mathbf{0} & \mathbf{0} \\ \boldsymbol{\Psi}_C & \boldsymbol{\Phi}_i & \boldsymbol{\Phi}_{MTA} \end{bmatrix}. \quad (5.3)$$

The procedure to obtain that component is described in App. B herein or in [28] and corresponds to the Augmented Craig-Bampton reduction method. The method is currently investigated for the offshore wind application in many publications [29, 6, 30]. Therefore, it is also tested in the thesis as a potential method for the improvement of the state-of-the-art procedures.

## Recovery-run

Another aspect of the load calculation procedures investigated in the chapter, is the way how the full foundation displacements are recovered from the aero-elastic calculations. In the aero-elastic code, the total wind turbine model is integrated and solved to obtain the displacements of the system.

Currently, a Wind Turbine Manufacturer provides a Foundation Designer with the interface forces between the structures. The latter applies them in the full foundation model and performs

an additional time-integration in order to obtain the time series of the non-reduced foundation model. The method provides with the correct results, however the question to be asked is whether it is the most efficient method, since the equation of motions are in fact solved twice.

Theoretically, once the system is correctly set up and a Wind Turbine Manufacturer solves the equation of motions as described in Ch. 4, the foundation displacements are obtained. The problem is that displacements do not corresponds to the physical, but rather to the generalized DOFs. However, there exist the method [31], where the displacements can be expanded into the non-reduced models, without performing a redundant time-integration.

The idea is sketched in Fig. 5.3. Based on the output provided by a Wind Turbine Manufacturer, a Foundation Designer can either perform the Force-Controlled method (interface forces  $\lambda$ ), or the Direct Expansion (generalized foundation DOFs  $\mathbf{q}$ ).

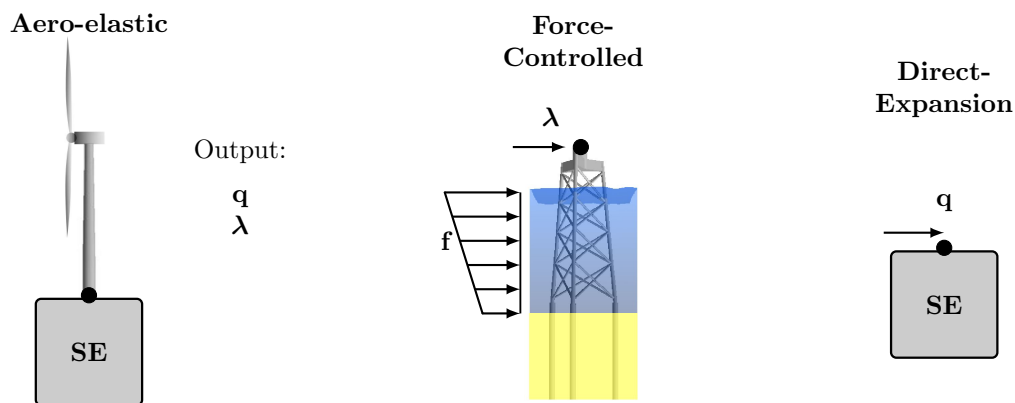


**Figure 5.3:** Procedures to obtain the non-reduced foundation displacements, based on the output from the aero-elastic calculations.

## Objectives of the investigation

The presented chapter tries to provide an answer to the following questions:

- How accurately do the reduced foundation models describe the non-reduced system?
- Can spatial convergence be obtained more efficiently?
- Can internal displacements be recovered more efficiently?

The first question is answered based on the comparison of different foundation reduction methods with the referenced foundation model integrated in the aero-elastic code. The second question searches for the more efficient internal wave loading representation by using an additional load-dependent term in the reduction basis for the Augmented Craig-Bampton method. The latter uses the Direct Expansion recovery run method, which does not require additional time-integration. However, it can recover the non-reduced foundation displacements directly from the output of the aero-elastic calculation. The question is whether the accuracy of the results is comparable to the reference solution.

Based on some of the analyses described in the following chapter the conference paper [32] has been prepared.

## 5.1 Methodology

The main aim of this chapter is to evaluate the accuracy and efficiency of the methods used in the load calculation procedures. A special interest is given into investigating the performance of three foundation reduction methods, namely: the Guyan, the Craig-Bampton and the

Augmented Craig-Bampton. Of these methods, the first two are widely used in the industry, the Guyan is being already used for a long time, whereas the Craig-Bampton was introduced relatively recently. The latter has never had an industrial application, however the recent publications indicate some potential in the Augmented Craig-Bampton method for the offshore wind application.

The additional investigation is set up in order to improve the efficiency of the post-processing method which was used to recover the full displacements of the foundation. The currently used Force-Controlled method will be compared with the potentially more efficient Direct Expansion method.

In order to leave no doubts while assessing the accuracy of the reduction and post-processing method, as a reference the non-reduced foundation model is used to provide the *true* solution. The following set up is proposed as stated in Fig. 5.4 to perform calculations and afterwards compare the solutions from the methods. The set up is fully in line with the integrated load calculation procedures used in the industry. The only modification is that additionally to the reduced models, the reference, the non-reduced foundation is used as well, and on top of the Force-Controlled method, the Direct Expansion, is also used as the post-processing method.

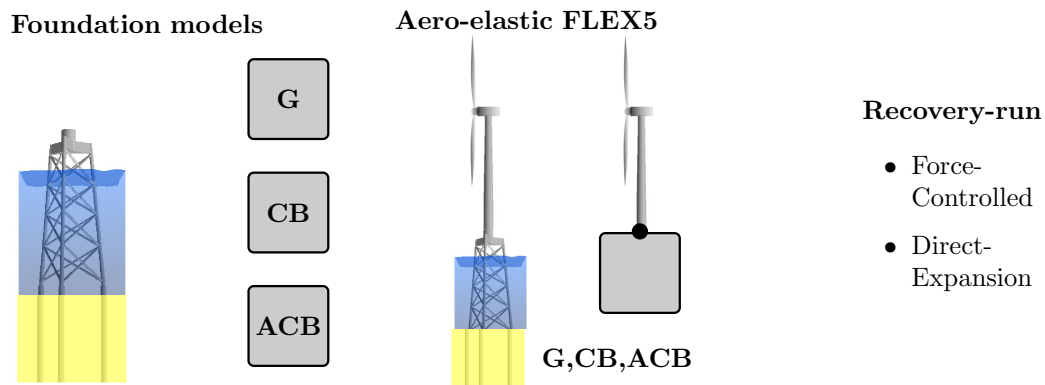


**Figure 5.4:** Outline of the investigation for different foundation reduction methods and post-processing methods.

As for the first step, four foundation models are prepared:

- **Referenced-** the non-reduced foundation model, which serves as the reference solution for the following reduced models.
- **Guyan-** the most simplistic foundation model with the reduced matrices size of 6
- **Craig-Bampton-** the state-of-the-art reduced foundation model that is currently used in the jacket projects. The size of the matrices is  $6 + n_i$ , where  $n_i$  is a number of internal modes included to represent the dynamic behaviour of the foundation.
- **Augmented Craig-Bampton-** the new foundation reduction method, which is tested in order to increase the ability to more effectively include internal wave loading. The size of the reduced model is  $6 + n_i + n_f$ , where  $n_i$  is the Craig-Bampton parameter for internal dynamic and  $n_f$  is a number of internal loading components included.

Once the foundation models are prepared they are integrated, in the aero-elastic code. The aero-elastic code used in the study is a Rambøll modified version of FLEX5 [33]. The FLEX5 is a code developed by a DTU professor S. Øye and is widely acknowledge in the offshore wind industry. The code is able to model the wind turbine with all relevant aero-elastic features such as turbulent wind, pitch controller, etc. The Rambøll modification concerns the possibility to include a complex foundation model by coupling it with the physical interface.

The four foundation models are assembled in the code and the *realistic* load cases are setup in order to model the loads, which later are used in the post-processing part. As output of the calculations, the interface force  $\lambda$  and the foundation displacements are given. The displacements are provided either for the physical  $\mathbf{u}$  or the generalized  $\mathbf{q}$  DOFs, for the non-reduced model, the physical DOFs are given, where for the reduced model the generalized DOFs.

Therefore, as for the last step the post-processing of the results is performed in order to recover the reduced, generalized DOFs into the non-reduced, physical DOFs. Two methods are used, the current one- Force-Controlled and the Direct Expansion.

After the analyses, the results are compared to the reference, non-reduced system and the conclusions are drawn.

## Load case definition

In pursuance of the most diverse test for the methods, three load cases are set up as summarized in Tab. 5.1. Wind varies from zero via a cut-in 3 m/s up to the rated wind speed of 15 m/s. The wave corresponds to the ULS wave for the site.

The first load case, where only wave is applied, assesses how well the methods represent the internal wave loading. The second case is intended to test the situation where both wind and wave are applied, however, the wave is the determinant for the design. The last one corresponds to the normal power production case for the turbine, with the ULS wave. Direction of wind and wave is fully aligned.

**Table 5.1:** Load cases definition for the analyses

Load case	Wind speed	Wave period	Wave height
Wave only	0 m/s	14 s	18 m
Cut-in	3 m/s	14 s	18 m
Rated	15 m/s	14 s	18 m

## Foundation and turbine model

In the analysis a generic jacket model is used, which is modelled in the state-of-the-art Rambøll's in-house software. The ROSAP (Rambøll Offshore Structural Analysis Package) software is a robust finite element based code, which allows to model all important aspects of the foundation structures, supported by piles.

**Table 5.2:** Jacket geometry and turbine parameters.

Jacket		Turbine	
Parameter	Value	Parameter	Value
Footprint	25 m	Rating	5MW
Topprint	16 m	Blades number	3
Leg diameter	1422 mm	Rotor diameter	126 m
Leg thickness	35 mm	Cut-in wind speed	3 m/s
Brace diameter	813 mm	Rated wind speed	11.4 m/s
Brace thickness	21 mm	Nacelle mass	240,000 kg
Can section	70 mm	Tower mass	347,460 kg
Pile penetration	48 m	Rotor mass	110,000 kg

The foundation is a 3-legged jacket with 4 brace levels as seen in Fig. 5.5. The essential geometric parameters are summarized in Tab. 5.2 and in App. D. The foundation is supported by the 48 m piles with a diameter of 2134 mm. The soil condition for the site is modelled as

medium sand with a friction angle of  $\phi = 35^\circ$ , water depth is 40 m. The added mass, marine growth is also included.

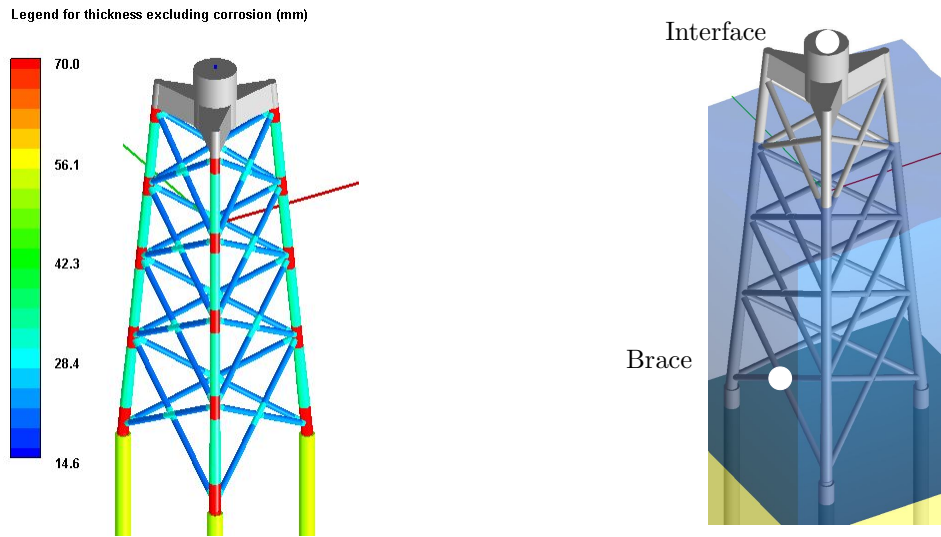


Figure 5.5: Jacket geometry and node naming.

The turbine used in the analyses is the reference 5 MW NREL turbine. It is a three bladed offshore turbine with a 87.6 m tower which corresponds to the 90 m hub height. More details on the turbine can be found in Tab. 5.2 or in the detailed description [34].

Damping of the turbine is implemented in terms of the modal damping as specified in [34]. Damping of the jacket structure is implemented by using the Rayleigh method,

$$\mathbf{C}_j = \alpha \mathbf{M}_j + \beta \mathbf{K}_j = 0.0001 \mathbf{M}_j + 0.001 \mathbf{K}_j, \quad (5.4)$$

where  $\mathbf{C}_j$ ,  $\mathbf{M}_j$ ,  $\mathbf{K}_j$  are the damping, mass and stiffness jacket matrices, including piles. The mass and the stiffness proportional terms are  $\alpha = 0.0001$  and  $\beta = 0.001$ , respectively.

## 5.2 Foundation reduction and Recovery-Run

In the following section, methods and parameters which are used to reduce the foundation model are described, followed by the recovery-run procedures. According to Fig. 5.4 three reduced foundation models are used: Guyan, Craig-Bampton and Augmented Craig-Bampton. The models are reduced as described in Ch. 2 by using:

$$\tilde{\mathbf{M}} = \mathbf{T}^T \mathbf{M} \mathbf{T}, \quad \tilde{\mathbf{C}} = \mathbf{T}^T \mathbf{C} \mathbf{T}, \quad \tilde{\mathbf{K}} = \mathbf{T}^T \mathbf{K} \mathbf{T}, \quad \tilde{\mathbf{f}} = \mathbf{T}^T \mathbf{f}.$$

In the equation, the reduction basis  $\mathbf{T}$  is needed, which includes vectors describing the internal dynamics  $\Phi_i$ . The quality of the reduced models depends on the number of dynamic modes included.

For the Guyan method the internal dynamic is not included, therefore, the only parameter that determines the size of the reduced model is the number of interface nodes included. However, that parameter is determined a priori, depending on how the substructures are connected. In the offshore case, the top of the transition piece connects with the tower bottom in the one node. Therefore, the Guyan model consists of only 6 modes.

In order to determine how many modes should be taken into account in the Craig-Bampton method, a sensitivity study should be performed in order to see whether the spectral convergence test is fulfilled.

As mentioned in the theoretical basis, the more system is reduced, the higher are the eigenfrequencies. Therefore, a simple test should be performed, where the number of internal modes

is increased and the corresponding eigenfrequencies are compared with the referenced system. The more internal modes are included, the better the reduced model will fit with the eigenfrequencies of the non-reduced model. The engineering *rule of thumb* says that the convergence should be fulfilled up to 2 times the highest frequency of the excitation.

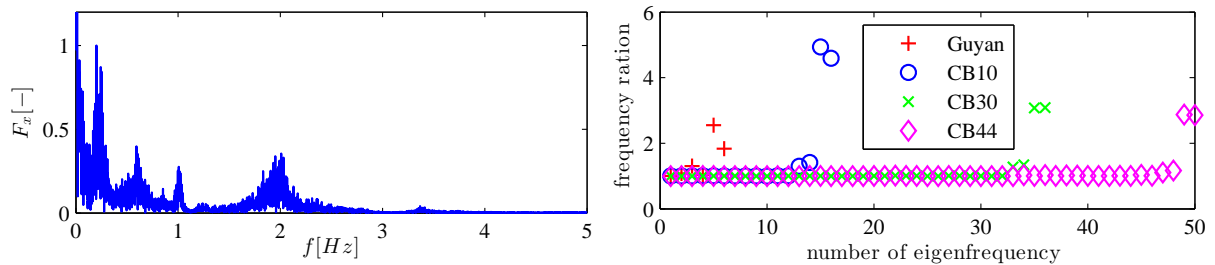


Figure 5.6: Spectral convergence test.

For the analyzed case, the frequency spectra of the excitation forces (combined wind and wave) is presented in Fig. 5.6a. It can be seen that the highest relevant frequency in the force spectra is about 4 Hz. Therefore, the convergence up to  $2 \cdot 4 \text{ Hz} = 8 \text{ Hz}$  is expected for a properly converged reduced model. That corresponds to the 20<sup>th</sup> eigenfrequency of the non-reduced model.

To include a sufficient number of internal dynamic modes in the Craig-Bampton method, the results from the spectral convergence are shown in the Fig. 5.6b. The figure shows the normalized eigenfrequencies in respect to the non-reduced model vs. the number of internal modes included. It can be seen that  $n = 30$  is the sufficient number of internal modes to fulfil the spectral convergence.

However, also the spatial convergence should be fulfilled, which is responsible for a proper representation of the internal loading. There exists no strict method on how to easily estimate that value, therefore to be on the safe side additional internal modes are included and the final number of internal modes  $n = 44$  was decided to account for.

In the Augmented Craig-Bampton method additional parameter besides the one used in the Craig-Bampton, is a number of the load dependent vectors  $\Phi_{MTA}$ . Therefore, in that case, the quality of the solution is a combination of the two above mentioned parameters: internal modes, and load dependent vectors. One method to assesses the required number of the load dependent vector, is to measure the energy associated with the corresponding modes and compare it to the total energy of the load applied to the non-reduced model. More details on that method can be found in [29]. Based on the sensitivity study a total number of 9 load dependent vectors  $\Phi_{MTA}$  was included.

Table 5.3: Reference and reduced foundation models.

Foundation model	static modes	dynamic modes	load modes	Matrice size	Reduction level
Reference				1128	0
Guyan	6			6	99%
Craig-Bampton	6	44		50	95%
Augmented Craig-Bampton	6	35	9	50	95%

The four models used in the analyses are summarized in Tab. 5.3. It can be seen that the reduction level is significant compared to the reference model size. When combining the information regarding the 95% of reduction level in the matrices size and the fact, that the calculations for the industrial offshore wind turbine are using cloud computing, which can last

up to several hours, it can be realized how important is to keep the reduction as high as possible.

### Recovery-run

The final comparison is obtained via the displacements of the full foundation, therefore, the Force-Controlled and Direct Expansion methods are used to recover the internal displacements. The procedure for implementing the methods is sketched in Fig. 5.3.

As described in the theoretical basis, the Force-Controlled method is obtained by solving the equation of motion of the non-reduced system applied with the interface forces  $-\mathbf{B}_f^T \boldsymbol{\lambda}$  and the internal wave forces  $\mathbf{f}_f$  according to the equation:

$$\mathbf{M}_f \ddot{\mathbf{u}}_f + \mathbf{C}_f \dot{\mathbf{u}}_f + \mathbf{K}_f \mathbf{u}_f - \mathbf{f}_f = -\mathbf{B}_f^T \boldsymbol{\lambda}.$$

The same approach is adopted in the presented study.

The new method is used to recover the internal foundation displacements directly from the aero-elastic solution. The expansion of the generalized  $\mathbf{q}$  DOFs is performed via the reduction basis  $\mathbf{T}$  according to equation:

$$\mathbf{u}_f = \mathbf{T}\mathbf{q}.$$

The damndest benefit of the method is that the redundant, time-consuming integration is avoided by a simple matrix calculation, which for the computer takes no time to perform. The only problem that might occur is the fact, that the internal displacements, recovered in the methods are based solely on the reduction basis, therefore the quality will strongly depend on the reduction method used. However, the final results will be assessed in terms of the accuracy with the reference solution.

## 5.3 Results

In the following section the results from the analyses are presented. The first load case includes only wave excitation, with no wind forces. It provides with an idea of how significant the waves are and what is the quality of the wave representation in the state-of-the-art methods. The following load cases simulate the normal production of the wind turbine combined with the ULS wave.

### Wave-only load case

The first load case includes only wave loading on the jacket. Even though it might seem unrealistic to include only wave without wind the purpose of this investigation is to determine the quality of the reduced model in terms of the internal loading representation. The internal loading is responsible for the spatial convergence criterion, which is one of the important tests, that has to be conducted before the correct analyses starts.

The easiest method to determine the spatial convergence is to perform a sensitivity analysis as described in the previous section. Therefore, the sensitivity analysis was performed for the Craig-Bampton method, where a number of internal dynamic modes  $\boldsymbol{\Phi}_i$  were increased. Each of the reduced models was applied with the reduced internal wave loading and time-integrated, afterwards the Direct-Expansion method was performed and the full displacements vector was obtained. As a measure of quality, the time-averaged elastic energy of the jacket,

$$\mathbf{E}(t) = \mathbf{u}(t)^T \mathbf{K} \mathbf{u}(t), \quad (5.5)$$

was stored and compared with the elastic energy of the non-reduced foundation. The elastic energy is a simple yet accurate measure of the total deformation of the structure, therefore is used to represent the quality of the reduced models to represent the internal loading.

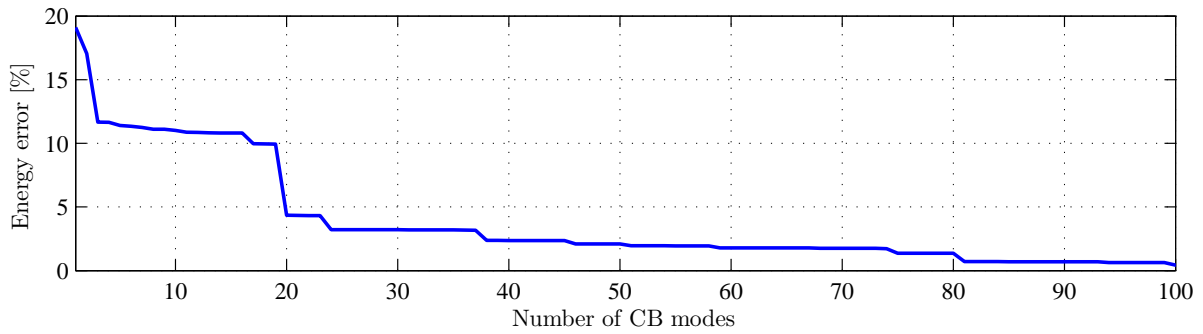


**Figure 5.7:** Spatial convergence test for the Craig-Bampton method.

The results of the test, where  $i = [1, \dots, 100]$  internal dynamic modes were included, are presented in Fig. 5.7. The case where  $i = 0$  corresponds to the Guyan method, where  $i > 0$  represents the Craig-Bampton method. The energy error for the Guyan method is 19% and the Craig-Bampton varies from 18% to 0.8%.

The error plot has three characteristic regions, which can be clearly explained based on the reduction methods theory:

- **quasi-static error**- when internal dynamics is not well described by excluding relevant dynamic modes, the error is the largest. It corresponds to  $i = [0 \ 1 \ 2]$  dynamic modes, where the error is from 19% to 12%. The error is characteristic for the Guyan method and not properly converged Craig-Bampton method.
- **dynamic error**- when the internal dynamic is converging to the number of internal modes that provides the correctly converged Craig-Bampton reduced model. In the figure it corresponds to  $i = [3, \dots, 20]$  dynamic modes and is represented by the 12% to 5% energy error.
- **internal loading error**- the error due to improper internal dynamic load representation. In the plot it corresponds to  $i = [20, \dots, 100]$ , but in fact the error is still present up to  $i = n_{DOF}$  modes included, that means as long as the model is reduced. The corresponding error is 5% to 0.8%.

It can be observed that the quasi-static error is eliminated by including just a few internal modes. The internal dynamic error can also be easily limited, by including in this case around  $i = 20$  modes. However, the internal loading error is converging significantly slower. That is due to the fact, that the loading in the Craig-Bampton method is trying to be represented by the uncorrelated structural modes. In the other words, one try to describe arbitrarily internal loading by the a priori prescribed structural modes. Therefore, the convergence is not obtained in the modest efficient way and requires in this case up to a 100 of internal modes to achieve the error level less than 1%.

Note that the measure used in the analysis is the global, averaged error, where the local effects can be significantly more severe. In order to also guarantee the full convergence on the local level, even more nodes should be considered.

The solution for the slow spatial convergence can be the proposed Augmented Craig-Bampton reduction method, which includes the load-dependent vectors directly in the reduction basis. In the following analysis two factors were included. One is the standard number of internal dynamic modes  $\Phi_i$  as in the Craig-Bampton, and the additional one, describing the internal loading  $\Phi_{MTA}$ . Therefore, in this case the elastic energy error is described by using a surface, rather than the line as in the previous example.

The error is plotted in Fig. 5.8. In fact in the plot the all three analyzed methods are included. The figure presents the error for  $i = [0, \dots, 30]$  internal dynamic modes and

$MTA = [0, \dots, 25]$  load dependent vectors. The  $MTA = 0$  corresponds to the Craig-Bampton and Guyan methods as in Fig. 5.7. The efficiency of the load dependent vectors is significantly higher compared to only the dynamic modes. After including just one  $MTA$  mode, the error drops to 2% and including  $MTA = 2$  modes the error is below 1%. NB that the same accuracy level for the Craig-Bampton method requires 100 modes.

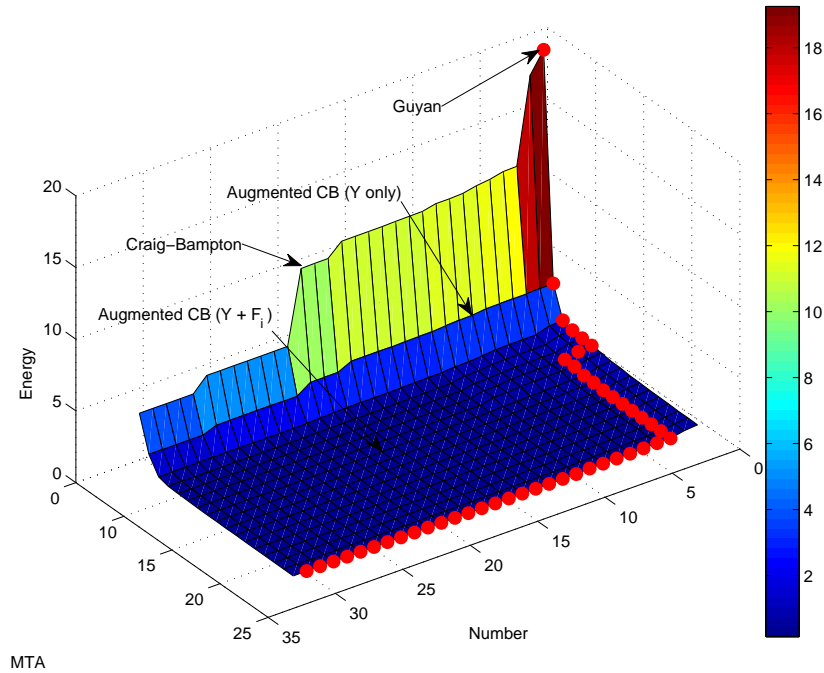


Figure 5.8: Elastic energy error for the Augmented Craig-Bampton method.

## Wind and waves load case

Once the importance of the wave representation is tested based on the wave only load case, the more realistic and design relevant examples are presented. In the following section the three reduced tests were subjected to both turbulent wind and hydrodynamic excitation. Afterwards, the full jacket displacements were recovered using both, the Force-Controlled and the Direct Expansion method.

In the figures a 50 s section from the original 600 s analyses is presented combined with the corresponding frequency spectra. The quality of the solution is based on the comparison of the out-of-plane mid-node cross brace displacements. Moreover, in the latter part also the interface displacements are compared. The specific nodes are highlighted in Fig. 5.5b. The results are presented separately for the two post-processing methods.

The reason for focusing on the lower part of the jacket is that this part of the foundation is typically the most relevant for the fatigue calculations. The stress ranges in the braces used in the fatigue assessment, it will be mostly affected just by the out-of-plane displacements. Therefore, estimating that parameter is the crucial part of the load calculation procedure and requires high accuracy in order to fulfil the design criteria.

Firstly, the Direct Expansion method is presented in Fig. 5.9. The Guyan method significantly underestimates the displacements in a way that the method is not suitable for the design purposes. The Craig-Bampton performs significantly better, however it can be noticed, that with respect to the peaks, the method slightly underestimates the displacements. The Aug-

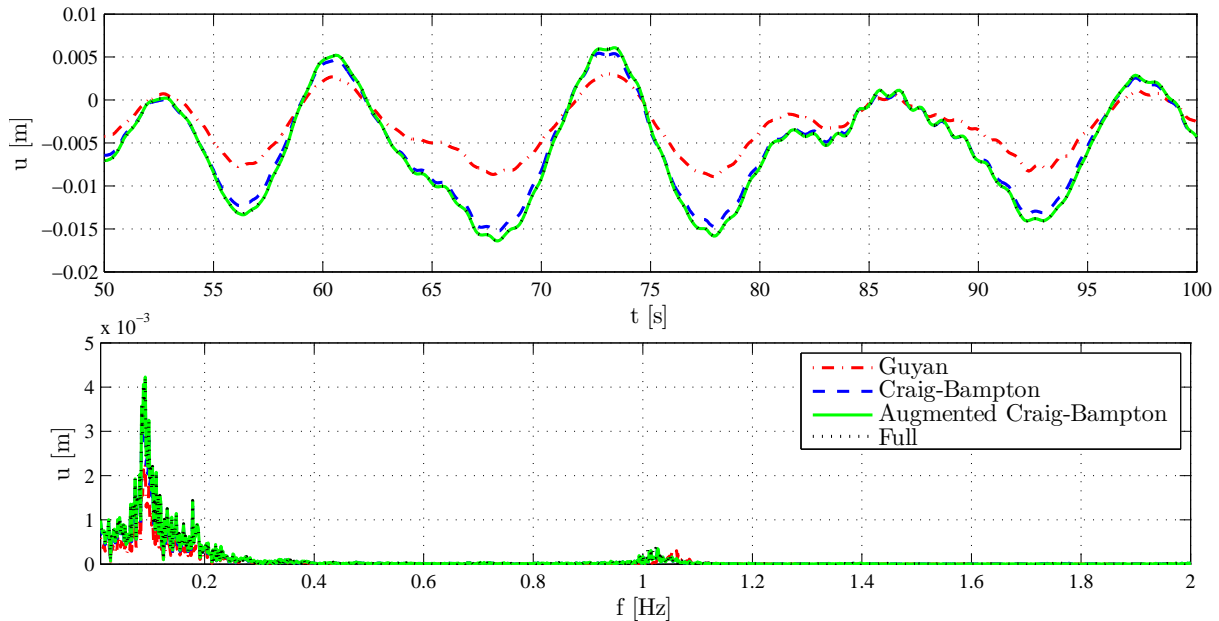


**Figure 5.9:** Comparison of the out-of-plane displacement for different reduced models by using the Direct Expansion recover-run method.

mented Craig-Bampton is indistinguishable from the reference solution. The explanation of the results is that the displacements are derived solely on the reduction basis. Therefore, the quality of the result depends only on the ability of the method to properly describe all relevant physical phenomena.

Due to that fact the Guyan method, which is the most reduced one, cannot capture the dynamic effects as well as part of the energy associated with the internal loading. As a result, the *superelement* appears overly stiff and significantly underestimates the displacement. The Craig-Bampton, which includes the dynamic modes, can significantly better describe the overall foundation displacements including the brace displacements. The peak underestimations are due to the truncation of the dynamic modes, which results in reducing the higher frequency modes and inability to precisely describe the internal wave loading.

The Force-Controlled method includes time-integration of the full model with the non-reduced hydrodynamic excitation. Therefore, the results are expected to be with better quality. The results are presented in Fig. 5.10.

As expected the results seem to be more consistent with the reference solution at least in terms of the magnitudes. However, the Guyan method exhibits an artificial dynamic excitation around frequency of 1 Hz. That might be due to a global resonance between the tower and the foundation, which is caused by overestimation of the Guyan foundation model. As for the Craig-Bampton and Augmented Craig-Bampton method, the results are indistinguishable from the reference solution. This is as expected, because the only difference between these methods is in the internal load representation and since in the Force-Controlled recovery-run the internal load is applied directly to the non-reduced model, the advantage of the Augmented Craig-Bampton is not used.

As mentioned in the introduction to this section, the interface displacements are also compared. Moreover, the additional load case with rated wind speeds should be presented. These results are presented in the tabular form, since for the interface displacements the differences between the methods are not observable, and the rated wind speed load case presents the same patterns as for the cut-in wind speed.

Therefore, Tab. 5.4 summarizes the maximum error between the reduced foundation models and the reference solution for both load cases, where the turbulent wind was combined with the

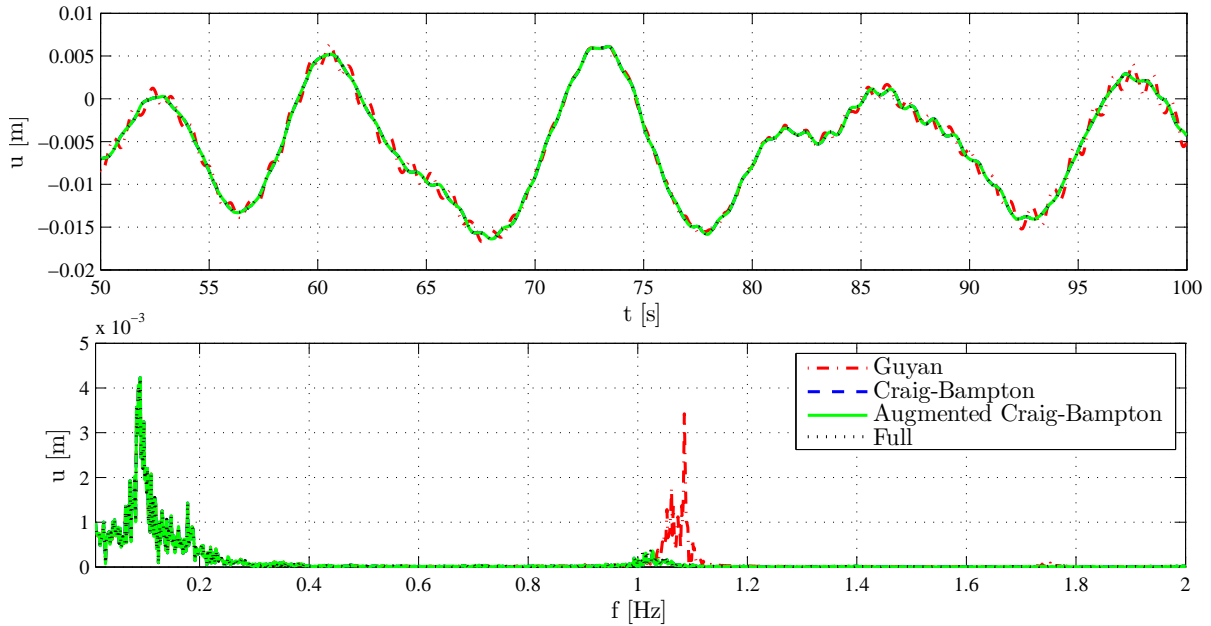


**Figure 5.10:** Comparison of the out-of-plane displacement for different reduced models by using the Force Controlled recover-run method.

**Table 5.4:** Quantitative comparison of the wind and wave load cases.

	Cut-in wind + wave				Rated wind + wave			
	Force-Controlled		Direct Expansion		Force-Controlled		Direct Expansion	
	Interface	Brace	Interface	Brace	Interface	Brace	Interface	Brace
Guyan	9.5	48.1	3.9	33.4	52	100	20	29.8
Craig-Bampton	0.1	0.2	0.1	10.7	0.2	0.5	0.7	6.3
Augmented Craig-Bampton	0.1	0.2	0.1	0.3	0.2	0.2	0.7	0.9

hydrodynamic excitation. What can be seen is that for all cases the Guyan method introduces significant error in the order of magnitude of 50%. The Craig-Bampton introduces 10% error for the Direct Expansion and 0.7% for the Force-Controlled. The Augmented Craig-Bampton for both load cases and recovery-run methods introduces a maximum error of 0.7%.

## 5.4 Discussion

Based on the results from the analyses presented in the chapter, the following three question asked in the beginning are addressed:

- **How accurately do the reduced foundation models describe the non-reduced system?**

The accuracy of the reduced model significantly depends on the method that is used to reduce the model. From the three investigated methods the Guyan delivers undoubtedly the lowest quality of the results. If the jacket foundation is considered, it is strongly advised to avoid using the Guyan due to the significant stiffness overestimation in the Direct Expansion method and artificial resonance in the Force-Controlled method. The error mainly comes from the poor dynamic representation of the Guyan method, therefore whenever a dynamically sensitive structure e.g. jacket is considered, the method should be

avoided. The Craig-Bampton delivers significantly better results and combines the Force-Controlled method with the spectrally converged reduced model. It delivers comparable results with the referenced model, therefore it can be seen as a proper method in that case. The Augmented Craig-Bampton not only delivers the best results, but also performs on the same level of accuracy for both post-processing methods. Therefore, from the three analyzed methods is the most reliable and robust method to reduce the foundation.

- **Can spatial convergence be obtained more efficiently?** The currently used Craig-Bampton method has a problem of properly describing the internal loading. That problem is solved, by using the time-consuming Force-Controlled post-processing method, where the non-reduced method is solved with the non-reduced hydrodynamic, internal loading. However, the issue of the internal loading representation is not solved for the Craig-Bampton and can be noticed when the Direct Expansion method is used, which depends only on the modes included in the reduction basis. In that case, unacceptable slowly spatial convergence is obtained by using the Craig-Bampton method. The solution for that problem is suggested by using the Augmented Craig-Bampton, which include load-dependent vectors and obtain significantly faster convergence compared with the Craig-Bampton. In the analyzed case for the same system size, the Augmented Craig-Bampton has an error of 0.3%, while the Craig-Bampton method delivers 10.7% error.
- **Can internal displacements be recovered more efficiently?** The Force-Controlled method as mentioned above, is not the most efficient method to recover the internal foundation displacements. In order to increase the efficiency, the Direct Expansion was suggested instead. The question however, was whether the Direct Expansion can deliver the same accuracy level as the Force-Controlled method. As seen for the analyses, the Direct Expansion method combined with a foundation reduced method using the Augmented Craig-Bampton can deliver the same level of accuracy as the Force-Controlled method significantly reducing the computational time. Therefore, that setup can significantly improve the efficiency without a loss on the quality.



# Chapter 6

## Tower modelling

The two previous chapters focused on the load calculation aspects concerning sensu stricto a foundation modelling. In the following chapter the investigation is set into a part of the aero-elastic code and a tower representation, see Fig. 6.1.

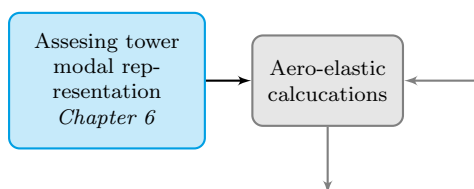


**Figure 6.1:** Tower modelling investigation in respect of the load calculation procedures.

The aero-elastic code in the current procedures lays within the responsibility of a Wind Turbine Manufacturer, which includes a tower modelling. However, due to the fact mentioned many times in the thesis, the independent parties solve the coupled model and the modelling approach, which is used by one party involves the other parties as well. Some tower modelling approaches use a system reduction, which might lead to the introduction of the error.

The tower modelling approach may significantly influence the interface forces, which in the state-of-the-art serves as the only coupling between a Wind Turbine Manufacturer and a Foundation Designer. Therefore, the following chapter assesses the modal tower representation, which is used by the industry. That approach is implemented in e.g. FLEX5, which is used by e.g. VESTAS.

### Modal vs. physical coordinate system

The system can be represented by a standard physical coordinate system, where each node in the three-dimensional case has six DoFs (three translation and three rotations). The equation of motion in that case is:

$$\mathbf{M}\ddot{\mathbf{u}} + \mathbf{C}\dot{\mathbf{u}} + \mathbf{K}\mathbf{u} = \mathbf{f}, \quad (6.1)$$

where  $\mathbf{M}$ ,  $\mathbf{C}$ ,  $\mathbf{K}$ ,  $\mathbf{f}$  are the system matrices and force vector. The displacements  $\mathbf{u}$  that are solved for, represent the physical displacements of each node. However, when the dynamic analysis are considered and many nodes is used for the analysis, the calculations can be time consuming. In the case of the wind turbine modelling (tower + RNA + blades), the system can properly be represented by 250 nodes, which correspond to  $250 \cdot 6 = 1500$  DoFs. For modern day standards that is definitely not much, but 20 years ago, where the first aero-elastic codes being developed, it could cause efficiency problems.

In order to speed-up the calculations, again the reduction methods were used. In this specific case, the modal coordinate transformation has been implemented. The idea is to represent the system in terms of a special type of modes that corresponds to the dynamic excitation of the

turbine. It is possible, when the structure deformation is known a priori to the analysis. The assumption is that the wind turbine responds to the turbulent wind by means of the limited number of mode shapes.

In that case the physical DoFs  $\mathbf{u}$  are transformed into a generalized  $\mathbf{q}$  DoFs:

$$\mathbf{u} = \sum_{i=1}^n \psi_i q_i = \mathbf{T}\mathbf{q}. \quad (6.2)$$

The transformation equation is in fact the very same that is used in the general model reduction as used in the theoretical basis. This time the reduction basis  $\mathbf{T}$  consists of the dynamic modes only.

When the reduction is applied to the general equation of motion it becomes the reduced equation:

$$\tilde{\mathbf{M}}\ddot{\mathbf{q}} + \tilde{\mathbf{C}}\dot{\mathbf{q}} + \tilde{\mathbf{K}}\mathbf{q} = \tilde{\mathbf{f}}, \quad (6.3)$$

where:

$$\tilde{\mathbf{M}} = \mathbf{T}^T \mathbf{M} \mathbf{T} \quad , \quad \tilde{\mathbf{C}} = \mathbf{T}^T \mathbf{C} \mathbf{T} \quad , \quad \tilde{\mathbf{K}} = \mathbf{T}^T \mathbf{K} \mathbf{T} \quad , \quad \tilde{\mathbf{f}} = \mathbf{T}^T \mathbf{f}. \quad (6.4)$$

As in the Guyan, Craig-Bampton, etc. reduction methods the quality of the reduced solution depends on the modes included in the reduction basis. The modes have to be the most representative to the non-reduced model deformation. In FLEX5 the total wind turbine is simplified into the 22 modes representing the tower, RNA and blades plus additional foundation modes. The overview is outlined in Tab. 6.1

**Table 6.1:** LACflex degrees of freedom

Interface	Tower	Blades	RNA	Foundation
translation $u_x$	Fore-aft 1 <sup>st</sup>	Flap-wise 1 <sup>st</sup>	Tower-nacelle jaw	internal
translation $u_y$	Fore-aft 2 <sup>nd</sup>	Flap-wise 2 <sup>nd</sup>	Nacelle tilt	foundation
translation $u_z$	Side-side 1 <sup>st</sup>	Edge-wise 1 <sup>st</sup>	Shaft rotation	DoFs
rotation $r_x$	Side-side 2 <sup>nd</sup>	Edge-wise 2 <sup>nd</sup>	Shaft bending $r_x$	
rotation $r_y$			Shaft bending $r_y$	
rotation $r_z$			Shaft torsion	

It can be seen that the tower is represented by only 2 bending modes in 2 perpendicular directions. The stiffness of the tower has a significant importance for the quality of the solution, because the aerodynamic forces are dependent on the structural stiffness  $\mathbf{f}(\mathbf{K})$ . Moreover, the force transfer from the nacelle to the tower base influences the interface forces, which serve as the interaction between the tower and the foundation. Therefore, if the tower stiffness is not properly described, the global response of a wind turbine can suffer in the accuracy.

## Objectives of the chapter

Based on the theoretical considerations of the modal system reduction, this chapter investigates the accuracy of the tower modelling approach in the FLEX5 aero-elastic code. It is assumed that the RNA representation is accurate and the considerations are given in the tower representation:

- How many tower bending modes should be included to properly describe the tower?
- Could a more accurate tower modelling approach be implemented?

## 6.1 Methodology

In order to estimate the error, introduced by reducing the tower down to two bending modes, the FLEX reduced model is compared with the reference model, where the tower is modelled as a non-reduced *FEM* model. The comparison will be given in terms of the aerodynamic forces, tower top deflection and interface reaction forces at the bottom of the tower.

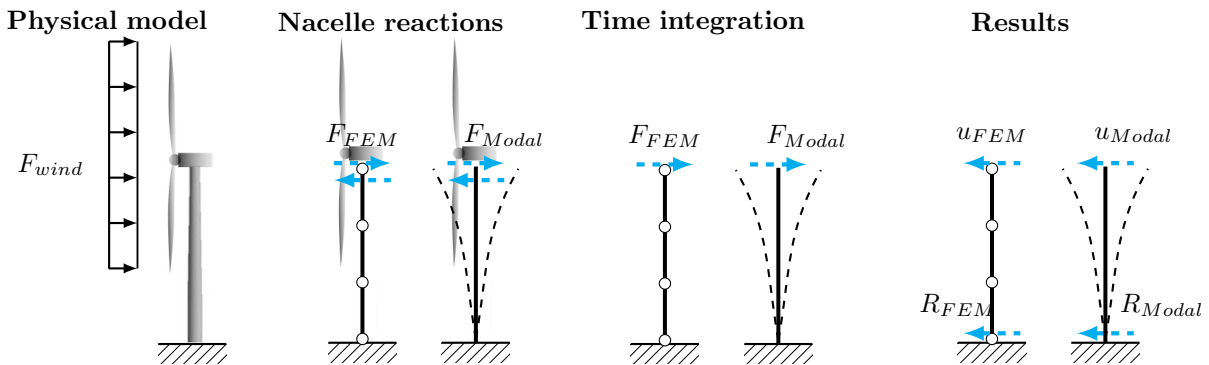


Figure 6.2: Tower assessment methodology.

The suggested setup is presented in Fig. 6.2 and can be described in the following steps:

- The turbine model is assumed to consist only of the RNA and the tower clamped at the bottom. That simplified model was decided to be used in order to include only the relevant elements, any possible disturbance from the more complicated foundation models i.e the monopile and jacket can be avoided. The turbine is excited with a 15 m/s turbulent wind, which corresponds to the rated wind conditions.
- Two models in FLEX are analyzed: the standard modal system, where the tower is clamped, and the model, where the *FEM* representation of the tower is implemented. The aerodynamic nacelle reactions  $F_{Modal}$  and  $F_{FEM}$  are extracted from both models.
- The reactions afterwards are applied to the tower only model in MATLAB code and time integration is performed in order to obtain the internal tower displacements.
- As the final step, the tower top displacements and the tower base reactions are extracted from both models. The comparison of the results gives the error that is introduced in FLEX by using only 2 tower bending modes.

Following the comparison between FLEX modal representation and the FEM tower model, the sensitivity analysis is presented, where the number of tower modes is gradually increased and the corresponding error is measured in terms of the tower top displacement and the reaction forces convergence. Based on that analysis, the question of how many tower modes should be included is answered.

## 6.2 Numerical model

There is no problem with obtaining the results using the currently used modal approach in FLEX. However, in order to implement the FEM model of the tower, as well as the augmented modal approach, additional code modifications are necessary. The modifications are implemented in Rambøll's in-house LACflex code [33], which uses the FLEX5 engine.

The FEM and augmented modal tower approach are modelled in external MATLAB code and imported to FLEX as external foundation matrices. That possibility was originally implemented in order to include a complicated foundation i.e. the jacket. In the presented analysis, that

feature is used in order to exclude the limited FLEX tower model and implement an arbitrarily tower from the external model.

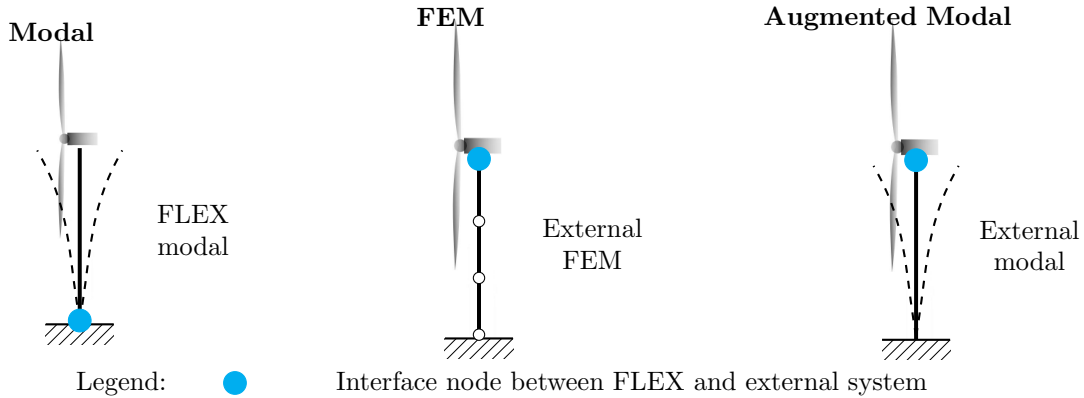


**Figure 6.3:** Tower modelling approaches.

The modelling approaches are outlined in Fig. 6.3. The **Modal** model is the standard FLEX approach, where the tower is modelled by using two bending modes in perpendicular directions. The **FEM** model introduces a modification, where the FLEX interface is artificially moved at the tower top node. The tower than is modelled in the external code and the system matrices are implemented with the FLEX code at the interface node. The **Augmented Modal** approach also uses the external module, where the tower is represented with a varying number of modes assembled with the FLEX code using the same approach as for the previous model.

The two custom models in principle introduce external tower models into the FLEX code. That basically corresponds to the case, where the tower is modelled by a Foundation Designer and afterwards implemented into the aero-elastic code. That approach is not used in the state-of-the-art method, but a discussion has been started recently about the possible advantages of that approach. Therefore, the results of this study can afterwards serve as an argument in the discussion.

## Parameters

In the analysis the same 5 MW NREL turbine [34] was used as in the previous chapter. As for the tower, the conical cylinder is used with varying the outer diameter and the thickness. The tower geometrical properties are outlined in Tab. 6.2

The tower height is 87.6 m, which corresponds to the 90 m hub height of the turbine. The outer diameter varies from 6 m at the bottom to 3.87 m at the top, where the thickness is 35.1 mm and 24.7 mm for the corresponding points.

**Table 6.2:** Tower geometrical properties

Outer diameter		Thickness	
H = 0	H = 87.6	H = 0	H = 87.6
6.00 m	3.87 m	35.1 mm	24.7 mm

The intermediate points are the linear interpolation of the tower top and tower bottom. The geometrical parameters varying over the tower height are presented in Fig. 6.4.

The results were obtained by using the Generalized- $\alpha$  [35] method with an integration time step of  $\Delta t = 0.01$ s and a high frequency spectral radius limit of  $\lambda_\infty = 0.8$ . The wind excitation is modelled by using the FLEX normal turbulence model (Kaimal), with a mean wind speed of 15 m/s, a wind shear coefficient 0.1 and a turbulence intensity 0.1573.

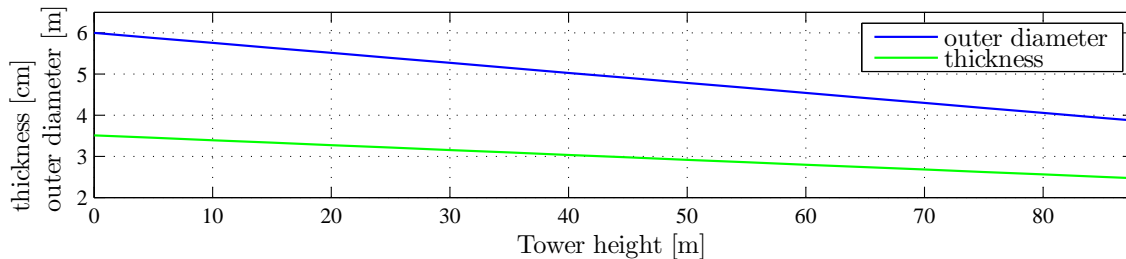


Figure 6.4: Variation of the tower outer diameter [m] and wall thickness [cm] over the height.

## 6.3 Results

In the following section, the results from the analyses, which are described above, are presented. The analyses are intended to evaluate two aspects of the tower representation:

- Influence of the tower stiffness representation on the **aerodynamic forces**. As mentioned in the introduction to this chapter, due to the aero-elastic coupling between the structure and the aerodynamic wind excitation, the wind forces at the nacelle  $\mathbf{f}(\mathbf{K})$  are dependent on the stiffness of the system. Mostly depends on the blades stiffness, but also on the stiffness of the underlying system i.e. the tower. Therefore, the comparison of the aerodynamic forces obtained from the non-reduced FEM tower model and the reduced modal representation evaluate the quality of the reduced system.
- Afterwards, the sensitivity study of the **Augmented Modal** representation is described. In the analysis, the modal tower is described by using a varying number of internal modes and is compared with the reference solution. The aim of the sensitivity study is to answer the question of how many internal tower modes are necessary to properly describe the tower bottom reactions. In this study, the tower representation does not only influence the aerodynamic forces, but also the ability of the tower to properly transfer the forces into the tower-foundation interface point.

### Aerodynamic forces

Firstly, the nacelle aerodynamic forces are compared. The accuracy of the reduced modal representation is measured by means of the six components of the nacelle reactions (three forces and three moments). The selected 50 s of the original 600 s analysis is presented in Fig. 6.5 and Fig. 6.6 for both, time and frequency spectrum, respectively.

The quality of the modal representation depends on the component. The axial direction has the best match between the modal and the FEM representation, however that is due to the fact that no significant dynamic excitation is present in that direction, therefore, it can be assumed that it is a quasi-static case. As for the lateral direction, the noticeable difference can be spotted.

In the wind direction  $x$ , the drag force  $F_x$  is underestimated by the modal representation by around 25% in the dominant 2P frequency range (0.4Hz). The P frequency is the rotor frequency, and the 2P and 3P represents the frequency of the passing blades. In the side  $y$  direction the lateral  $F_y$  force is underestimated even more significantly by the modal representation. The maximum error is introduced again around the 2P frequency and the difference between the modal and FEM representation is 75% in terms of the magnitude.

Similar conclusions can be drawn in terms of the bending moments, since they are coupled with the translation direction. Therefore, the torsional moment is in the best agreement between two models, where the  $M_x$  bending moment introduces a significant error in the 2P frequency.

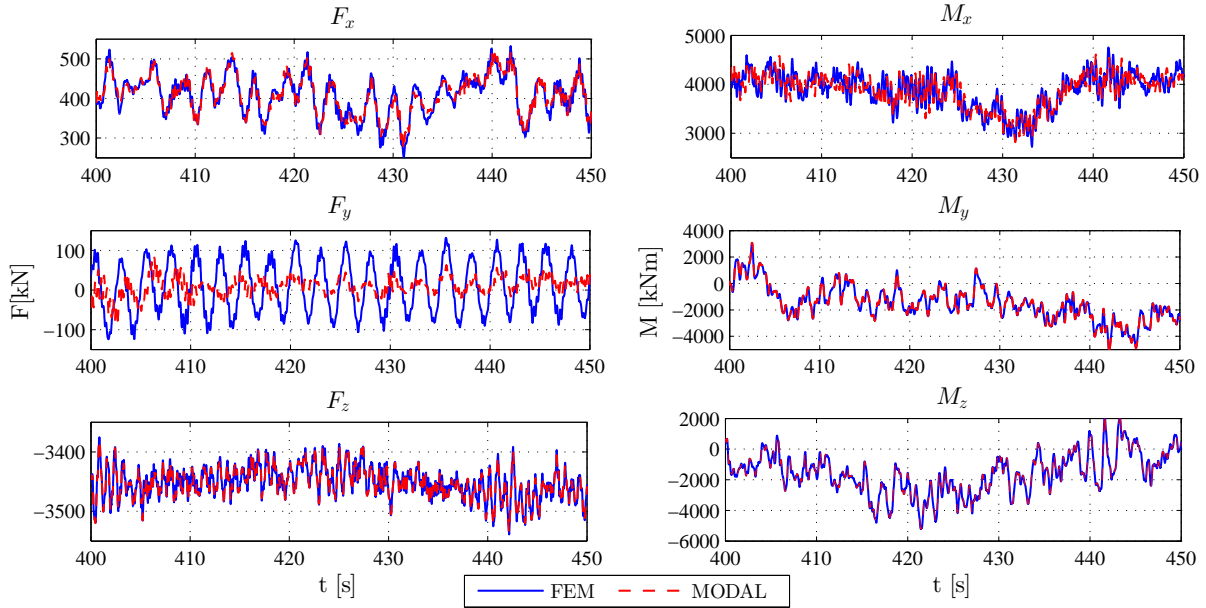


**Figure 6.5:** Time-series of the nacelle reactions for FEM and modal tower representation.

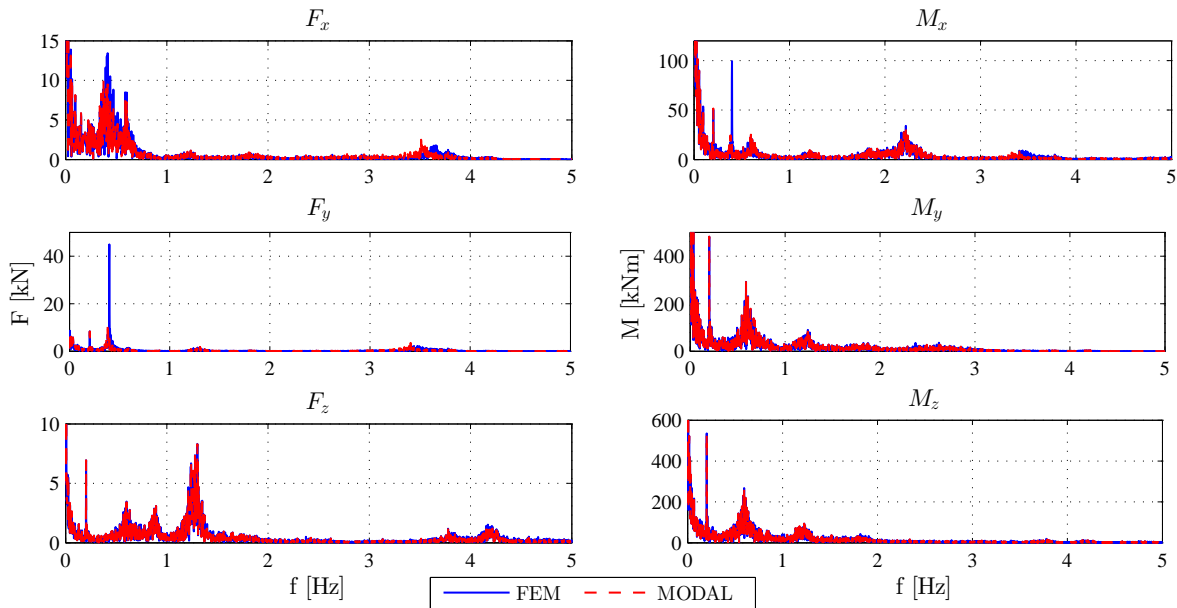


**Figure 6.6:** Frequency spectrum of the nacelle reactions for FEM and modal tower representation.

### Augmented Modal approach

In the previous section the comparison between the non-reduced FEM model and the FLEX modal representation with 2 bending modes are presented. In the following section, the FLEX modal representation is augmented with additional tower modes. The non-reduced tower model is discretized by using  $k = 50$  nodes, which corresponds to the total number of  $n = k \cdot 6 = 50 \cdot 6 = 300$  DoFs (internal modes). Therefore, the sensitivity analysis measures the convergence of the reduced modal representation, when more internal modes are included.

The first analysis presents the convergence of the tower top node in terms of the displacements in the wind direction  $u_x$  and the corresponding rotation  $\varphi_y$ . The results are outlined in Fig. 6.7. The translation DoF converges fast- including only 2 modes that are corresponding to an error

of only 3%. Therefore, solely based on these results, it may be said that 2 modes are enough. However, the rotational convergence is significantly slower. For the 2 tower modes, the error for the rotation is 40%. Due to the fact that the rotation and translation are coupled, the nacelle reaction includes the error of both components. Therefore, 2 tower modes should not be seen as the sufficient number of modes to properly describe the nacelle reaction.

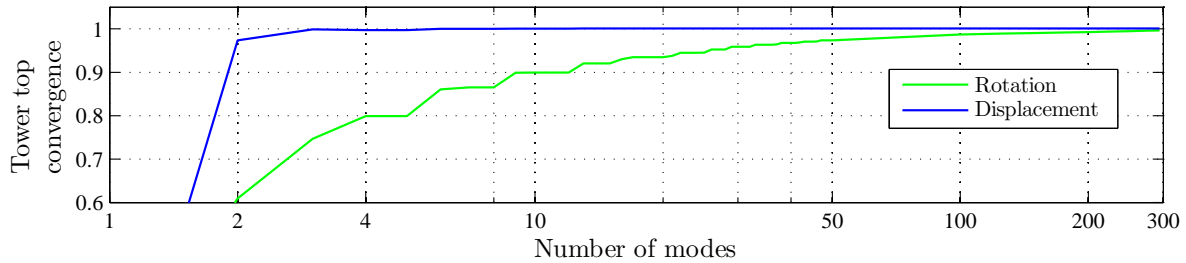


**Figure 6.7:** Tower top node convergence in terms of internal tower modes included.

The tower node convergence is an important parameter, especially for the aerodynamic forces. However, what is the most important in terms of the global turbine analysis, is the quality of the reactions at the tower bottom. This point is the interface between a Wind Turbine Manufacturer and a Foundation Designer, therefore based on that result the global coupling between a turbine and a foundation is utilized.

The quality of that result is investigated in terms of the tower bottom reaction convergence. In the presented study, the wind direction  $F_x$  reaction is considered, since that direction is dominant in the wind forces.

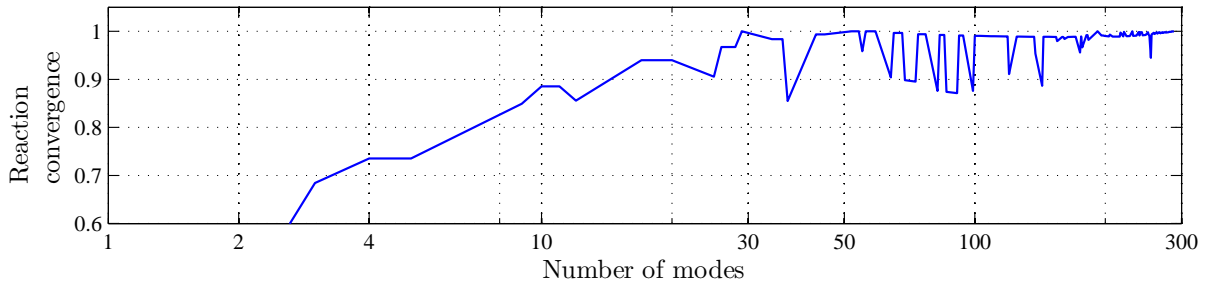


**Figure 6.8:** Tower bottom reaction convergence in terms of internal tower modes included.

The convergence of the tower bottom reaction  $F_x$  in respect of the tower modes included, is presented in Fig 6.8. The general observation is that the more internal modes are included the better the reduced model describes the reaction. The insignificant exceptions can be noticed, when including additional modes, the results actually worsen. The reason for that is hard to find. What is also confirmed is that when a total number of modes is included, the modal system is not a reduced one anymore, by only transferred into a different coordinate system. In that case, the error is zero.

What can be concluded from the analysis is that when a number of approximately  $n = 30$  is included, the modal representation delivers the same results as the non-reduced FEM model. In that case, the modal system has a size of  $30 \times 30$  matrix, compared to the original size of  $300 \times 300$ , it is the reduction of 90% in size. Therefore, it can be noticed why the idea of a modal reduction has been introduced in the first place in FLEX code. However, the number of the modes included in FLEX, corresponds to 2 bending modes in both directions, equals 4 total bending modes. Thus, it is significantly too low, based on the results from the presented analysis.

## 6.4 Discussion

In the presented chapter, an influence of the tower modelling approach on the load calculation procedure has been evaluated. The use of the reduced modal tower representation influences the load calculation procedures in two main aspects: aerodynamic force estimation and the wind force transfer to the tower bottom interface point. The possible error introduced decreases the accuracy of the wind excitation and this might influence the interface forces.

The significant error has been found by using the FLEX5 modal approach with the tower represented by using only 2 tower bending modes. The fore-aft force error in FLEX has been found up to 25 %, while the less important side-side direction introduced up to 75% error compared to the non-reduced reference solution.

The possible improvement in the accuracy of the results can be implemented by including an additional number of tower bending modes. Based on the sensitivity study, it has been found, that by including a full sets of internal tower modes up to the 30<sup>th</sup> mode the error can be eliminated. The tower base reaction error is reduced to only 2%. Moreover, the main contribution to the accuracy improvement are the tower bending modes. Therefore, it is suggested to include only these modes, in order to maximize the efficiency-accuracy ratio.

**Table 6.3:** Error introduced due to a modal truncation.

Bending mode	Global mode		Error [%]	
	fore-aft	side-side	$u$	$F_x$
1 <sup>st</sup>	1	2	3	65
2 <sup>nd</sup>	3	4	1	25
3 <sup>rd</sup>	6	7	0	20
4 <sup>th</sup>	9	10	0	14
5 <sup>th</sup>	12	13	0	12
6 <sup>th</sup>	16	17	0	7
7 <sup>th</sup>	21	22	0	6
8 <sup>th</sup>	25	26	0	4
9 <sup>th</sup>	29	30	0	2
10 <sup>th</sup>	33	34	0	1

Table 6.3 presents the error in the tower bottom reaction vs. the number of internal tower bending modes included in the modal representation. In the current state of the FLEX5 software, the 2 bending modes introduce 25% error. By introducing 10 tower bending modes, the error can be reduced up to the 1%. That corresponds to the global number of 34 modes. However, the axial and the torsional modes are excluded, which correspond to only 20 modes. As mentioned before, in the specific wind turbine case, where the excitation is mostly in lateral direction, and the structure is axis-symmetric, the torsional and axial modes do not have a significant importance, therefore can be excluded.

In relation to the chapter objectives, two questions have been asked:

- **Can a reduced modal tower representation be used in aero-elastic calculations?**

Based on the analysis performed in the FLEX5 code, where both, the modal tower representation and the referenced non-reduced FEM tower formulation were used, it can be stated that the modal tower representation can deliver accurate results. However, the accuracy of the results strongly depends on the number of the internal tower modes included in the analysis. The FLEX code represents the tower by using only 2 bending modes. Based on the results, it can be stated that this number is not sufficient.

- **How many internal tower modes should be included in the modal tower representation in order to deliver accurate results?**

Based on the realistic wind turbine analysis, it can be stated that the reasonable number of internal tower bending modes is 10 for both directions. This corresponds to the total number of 20 DoFs to properly represent the tower. The question can be asked, whether this number is low/high and if another, more efficient approach exists. The alternative approach is to represent the tower by using the non-reduced FEM model. However, to properly describe the frequency of the tower within the area of interest (10 Hz), around 50 nodes should be introduced. This corresponds to the  $50 \cdot 6 = 300$  DoFs. Compared to the 20 DoFs in the modal representation, it appears that the modal approach is still the most efficient.



## Chapter 7

# Non-linear soil modelling

The soil-structure interaction is undoubtedly an essential aspect that needs to be considered in an offshore wind turbine design process. As outlined in the theoretical basis, there exist many methods of how to model the interaction between a structure and the surrounding soil continuum. The currently implemented approach represents the soil as a series of independent non-linear springs attached to a pile. The method can successfully be applied to model piles. The problem however, arises when piles and the surrounding soil need to be implemented into the linearized reduced model.

Soil is a non-linear material due to e.g. plasticity, contact between soil and pile, therefore when it has to be represented by a linear model, it cannot maintain its non-linear abilities any more. In that case a soil model has to be linearized by finding a *representative* stiffness. Thereby, one should decide what is the most appropriate soil stiffness for a particular case. This is part of the process when creating a reduced foundation model during load calculation procedures as recalled in Fig. 7.1. The following chapter questions the linear soil representation and investigates the importance of the more sophisticated, non-linear soil modelling.

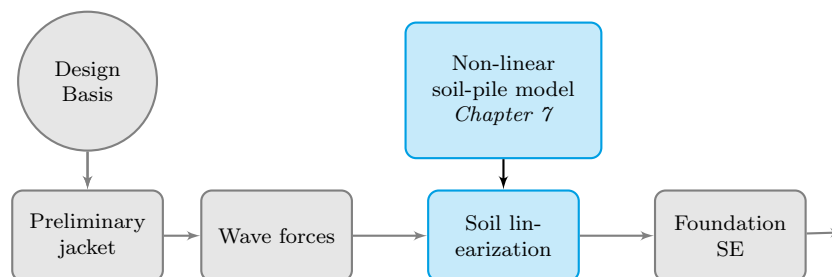


**Figure 7.1:** Outline of the initial load calculation step for creating a reduced foundation model.

The reason for such an investigation is that the soil influences the design in a multiple ways. It may seem obvious that it is important for a local pile design such as determination of dimensions like diameter, penetration, etc. But even more important may be the influence of the soil on the global dynamics of the system.

Figure 7.2 illustrates an exemplary influence of the soil on the turbine response. The study presents the wind turbine represented by the jacket foundation with the 5MW NREL turbine (both described in Ch. 5) subject to the rated wind-speed. Three different cases were analyzed with different soil profiles (sand  $\varphi = 30^\circ$ , sand  $\varphi = 35^\circ$ , and sand  $\varphi = 40^\circ$ ). The left figure shows a time series of pile head displacements in the wind direction, while the right one shows a frequency content of that displacement.

One can notice that the soil type (stiffness) has a significant influence not only for the amplitudes of displacements, but also on the frequency content. The reason for the difference between the cases is related to the different soil stiffness, which serves as a boundary condition for the turbine. It is expected to observe the same, if the linearized case is applied instead of the

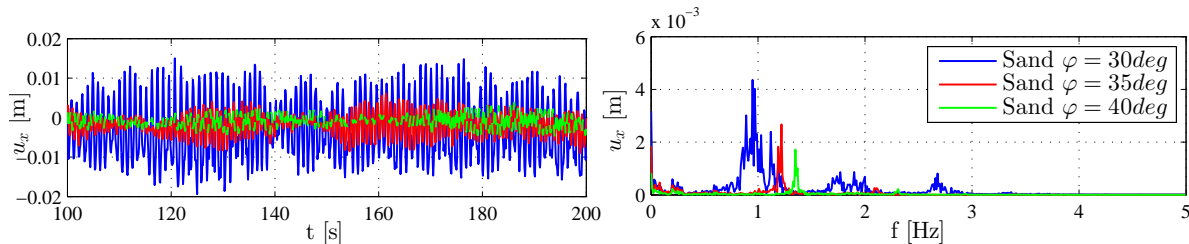


**Figure 7.2:** Influence of the soil stiffness on the response of the integrated wind turbine. a) pile head displacement, b) frequency spectrum

non-linear soil model, because then a representative soil stiffness model should be used, which in principle would correspond to stiffer or softer soil.

## 7.1 Methodology

The aim of the study is to investigate the importance of soil non-linearities on the response of the integrated wind turbine model.

In order to best describe a physical model, wind forces should be estimated based on a non-linear foundation to account for a soil stiffness variation during especially large pile displacements. Therefore, the application of a linear foundation *superelement* is not the method how the wind forces can be obtained. Therefore, the customized MATLAB code is used, which should resemble procedures used in the industrial wind turbine analysis as described in Ch. 4.

The priority of the thesis is to develop the method that can be afterwards implemented in the existing procedures, without significant modifications. Therefore, a procedure of combining a linear jacket with non-linear piles has to be developed as well. It will consist of creating a multi-interface *superelement*, which afterwards will be integrated to the tower and the piles model. The procedure is described in more details in the following sections.

Three models are implemented and illustrated in Fig. 7.3:

- **FEM<sub>NL</sub>** - a non-reduced model with non-linear soil curves. It corresponds to the non-reduced, non-linear, integrated turbine model and is considered as the most accurate solution as can be modelled with respect to the integrated method. Therefore, it serves that the reference solution to which the rest of the models are compared to.
- **SE<sub>LIN</sub>** - a linear reduced model, where the jacket and piles are represented by the Craig-Bampton *superelement*, and a non-reduced tower. It corresponds to the state-of-the-art method, including linearized piles in the foundation reduced model.
- **SE<sub>NL</sub>** - a non-linear reduced model, where the jacket is modelled by using the Craig-Bampton reduction method with  $n = 20$  internal modes, non-linear piles and a non-reduced tower. This is the suggested model, which is tested against the referenced solution and the currently used approach. The expectation of that model is to obtain the same accuracy as the non-reduced non-linear model due to the non-linear piles attached, yet has the efficiency not significantly worse than the currently used, linear model.

The performance of all three models is compared in terms of displacements at the selected characteristic locations of the model. The emphasis is on the case where significant difference between the linear and non-linear solutions can be noticed. The main goal of that investigation is to investigate whether a moderately/strongly non-linear model can be represented accurately with the linearized reduced foundation model external non-linear piles attached.

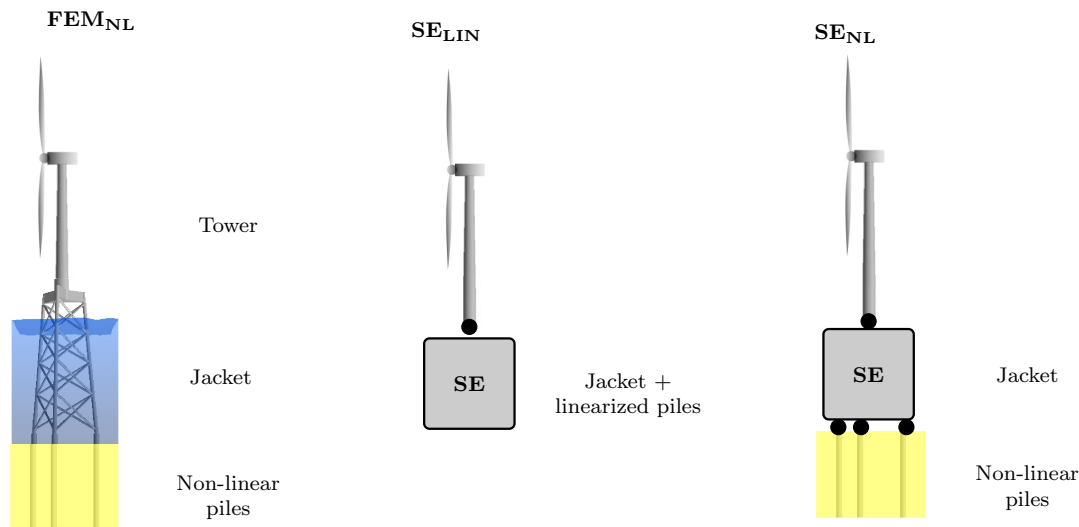


**Figure 7.3:** Implementation of non-linear soil model in the integrated wind turbine model.

## 7.2 Numerical model

The code to analyze the above described problem is set up in a standard *Finite Element Analysis* way. The tower and the jacket are modelled as Bernoulli-Euler beam elements. The structural properties for the tower, the jacket and piles are the same as used in the previous chapters (Ch. 5 and Ch.6). The more specific description on the jacket is provided in App. D, the turbine is also described in [34]. Piles are modelled as beams and the interaction between the structural part and the soil is realized using the Winkler approach with non-linear soil springs as described in Ch. 3. The sketch of the pile element is illustrated in Fig. 7.4.

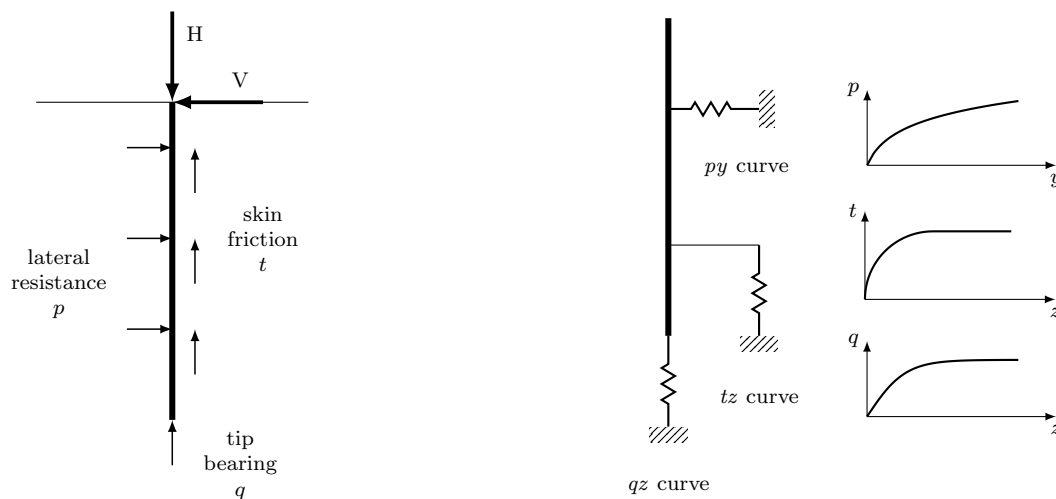


**Figure 7.4:** Non-linear soil-structure model.

The soil used in the analyses is the medium sand with friction angle  $\varphi = 35^\circ$ . The soil curves were obtained by using the API [18] and DNV [17] standards as described in Ch. 3. More details on the soil parameters is given in App. D.

The linear results were obtained by using the Generalized- $\alpha$  method [35] with integration time step of  $\Delta t = 0.01s$  and a high frequency spectral radius limit of  $\lambda_\infty = 0.8$ . The non-linear influence was adopted by modifying the stiffness matrix for each time step. That corresponds to the Euler non-linear solver method [36] adopted in the Generalized- $\alpha$  method. The sensitivity study has been performed to fulfil that the  $\Delta t = 0.01s$  time step is sufficient.

## Wind forces

Modelling of wind forces is all but a trivial process. One should account for many multi-physics coupling between the wind pressure field and the structure, pay attention to the non-linear controlling model, etc. Including these phenomena in the code would exceed the scope of the thesis, hence a simplified, yet realistic representation of wind forces is applied.

It is assumed based on the analyses performed in FLEX5 [33] that the turbulent wind can be represented in a simplified manner by using a linear combination of sinusoidal waves. For the present application five components are considered:

$$F_x(t) = c + \sum_{i=1}^5 A_i \sin(\omega_i t), \quad F_y(t) = 0.15F_x(t) \quad (7.1)$$

Wind consists of the quasi-static constant component  $c$  associated with the mean wind speed and the dynamic turbulent fluctuation with amplitudes  $A_i$  and frequency  $\omega_i$ . The main wind direction coincides with the jacket  $x$  axis, however due to wind turbulence also the perpendicular  $y$  direction is included as 15% of the main direction. Exemplary wind forces that are generated by the model according to Eq. 7.1 and presented in Fig. 7.5.

In order to keep the wind excitation as representative as possible, some analyses in FLEX have been conducted and based on them the wind parameters ( $c$   $A_i$   $\omega_i$ ) were found. The model that was used in order to find the excitation was the NREL 5MW and a reference 8MW wind turbine with a linearized jacket *superelement*, corresponding to  $SE_{LIN}$  model, and turbulent wind with speed  $u = 15 \frac{m}{s}$  and  $u = 25 \frac{m}{s}$ .

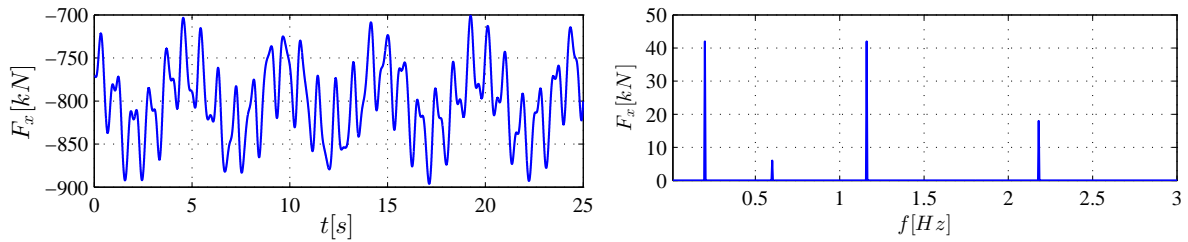


Figure 7.5: Wind forces. a) time and b) frequency spectrum

Wind forces have been applied to the turbine at the hub height in  $x$  direction as seen in Fig. 7.6. That corresponds to the case, where two of the jacket legs are in tension and one in compression.

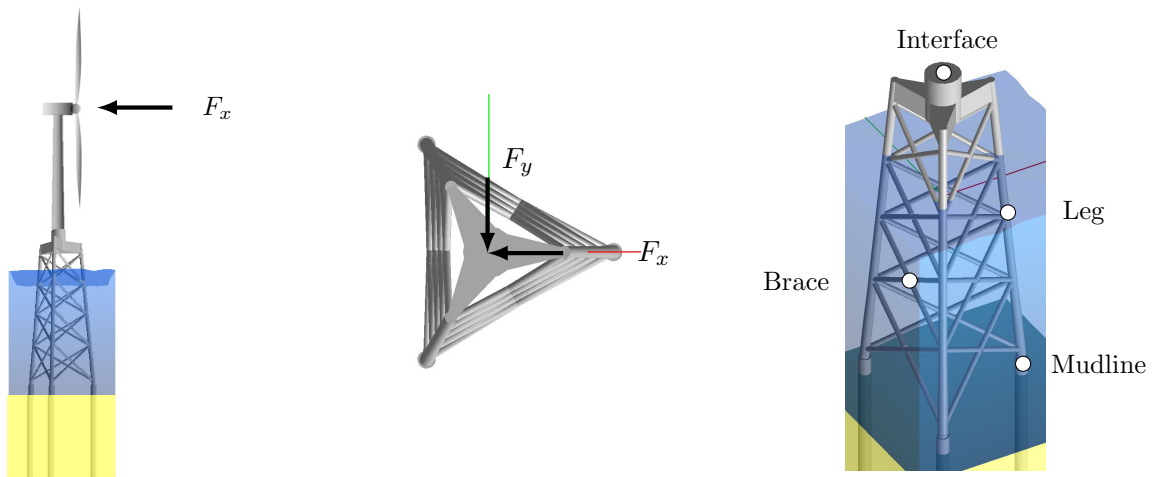


Figure 7.6: Wind loads and node naming for the results.

In order to demonstrate the importance of the non-linear soil model, three load cases were defined which are representing different load levels that are applied to the structure. The load case definition can be seen in Tab. 7.1.

**Table 7.1:** Load cases definition.

Load case	Wind speed	Turbine model
Low	rated 15m/s	NREL 5MW
Medium	cut-out 25m/s	NREL 5MW
High	cut-out 25m/s	Reference 8MW

The jacket foundation used in the study is intended for 7-8 MW turbine, therefore the low and medium load case should not result in a significant displacement level, while the high load level is expected to introduce displacements, where non-linearities might be relevant.

### 7.3 Results

In the following section, the results for the wind turbine with the linear and non-linear pile models are presented. The results are divided into two parts, qualitative comparison, where the timeseries of  $t = 25$  s of displacements are discussed and general observations are given in terms of differences in displacements patterns. Afterwards, a quantitative comparison of the differences is given and the general conclusions about the importance of soil models drawn.

The results are given for three load cases as described in Tab. 7.1. For each load case the results for different jacket levels are provided. Four specific nodes are chosen to provide a general overview of the sensitivity of the soil modelling on the jacket response. The selected nodes are: interface, leg at the mid jacket height, cross brace and the mudline. The figure 7.6c presents locations of the nodes. Each of the points is represented by two plots: the first column shows displacements in the wind direction which corresponds to the  $x$  model axis, where the second column provides more details regarding the vertical  $z$  direction.

## Low Level

Based on Fig. 7.7 the general conclusion for the low load case is that the results for both the linear and the non-linear soil models are indistinguishable.

Due to the fact, that the linear and non-linear models predict the same results, not only for the peaks, but also for the intermediate cases, it can be assumed that the load level does not introduce a non-linear soil behaviour.

All presented jacket locations in both horizontal and vertical direction give the same results. The maximum pile head displacement at the mudline (fourth row of the plots) are -4.2 and 2.5 mm for the lateral and axial direction. This in fact corresponds to the initial pile stiffness, therefore linear and non-linear models have the same soil stiffness, which explain the coinciding results.

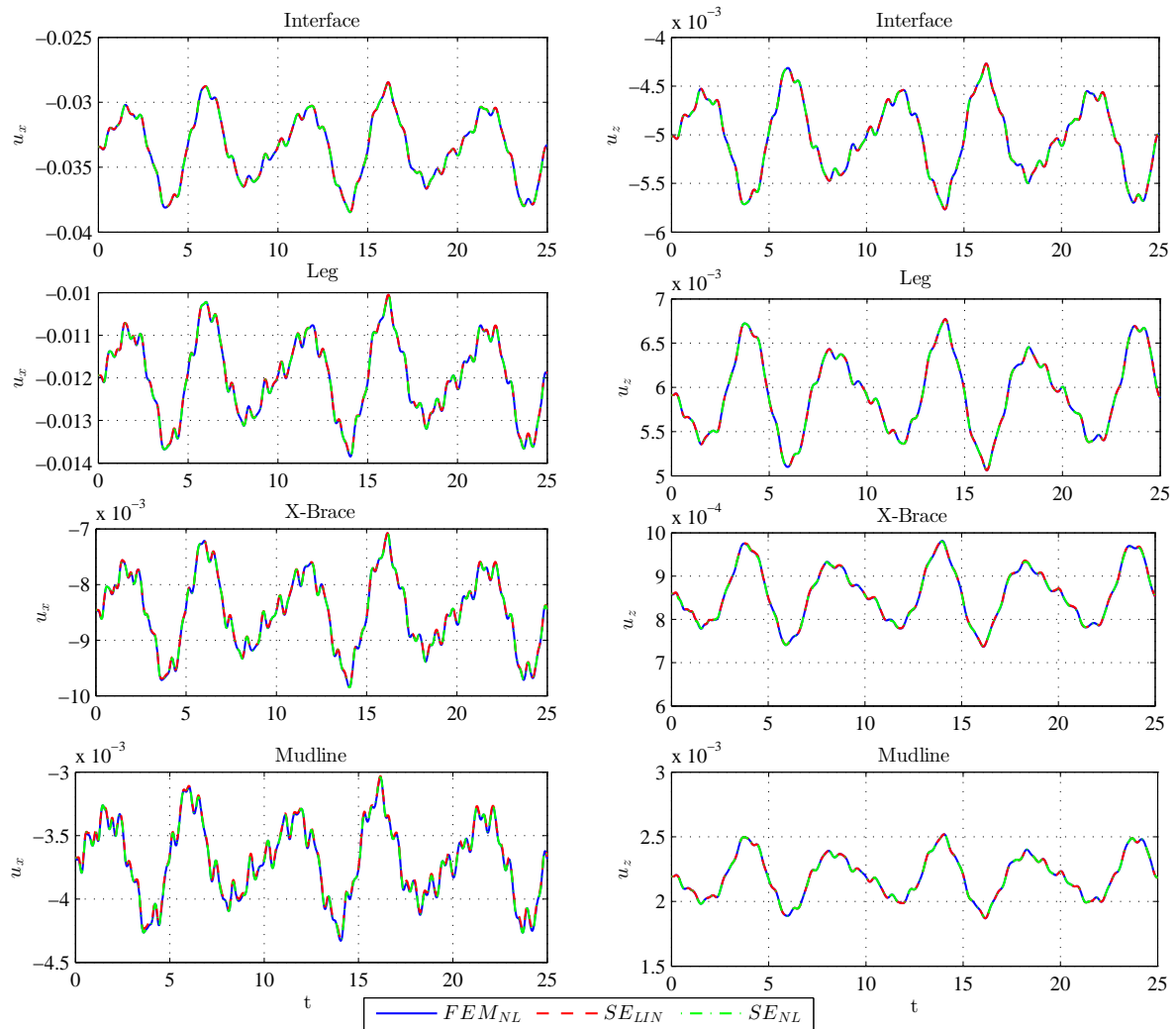


**Figure 7.7:** A comparison of the integrated wind turbine model with the linear and the non-linear soil model at different levels according for the low load case.

## Medium Level

The results for the medium load case introduce a noticeable difference especially in the vertical direction between the linear and the non-linear soil models, see Fig. 7.8.

Even though the significant difference in the displacements at the interface node cannot be seen, the closer to the mudline, the more significant differences become. From an engineering

point of view, leg displacements can be regarded as comparable. However, the brace and the mudline level are significantly different, especially with regard to the vertical direction.

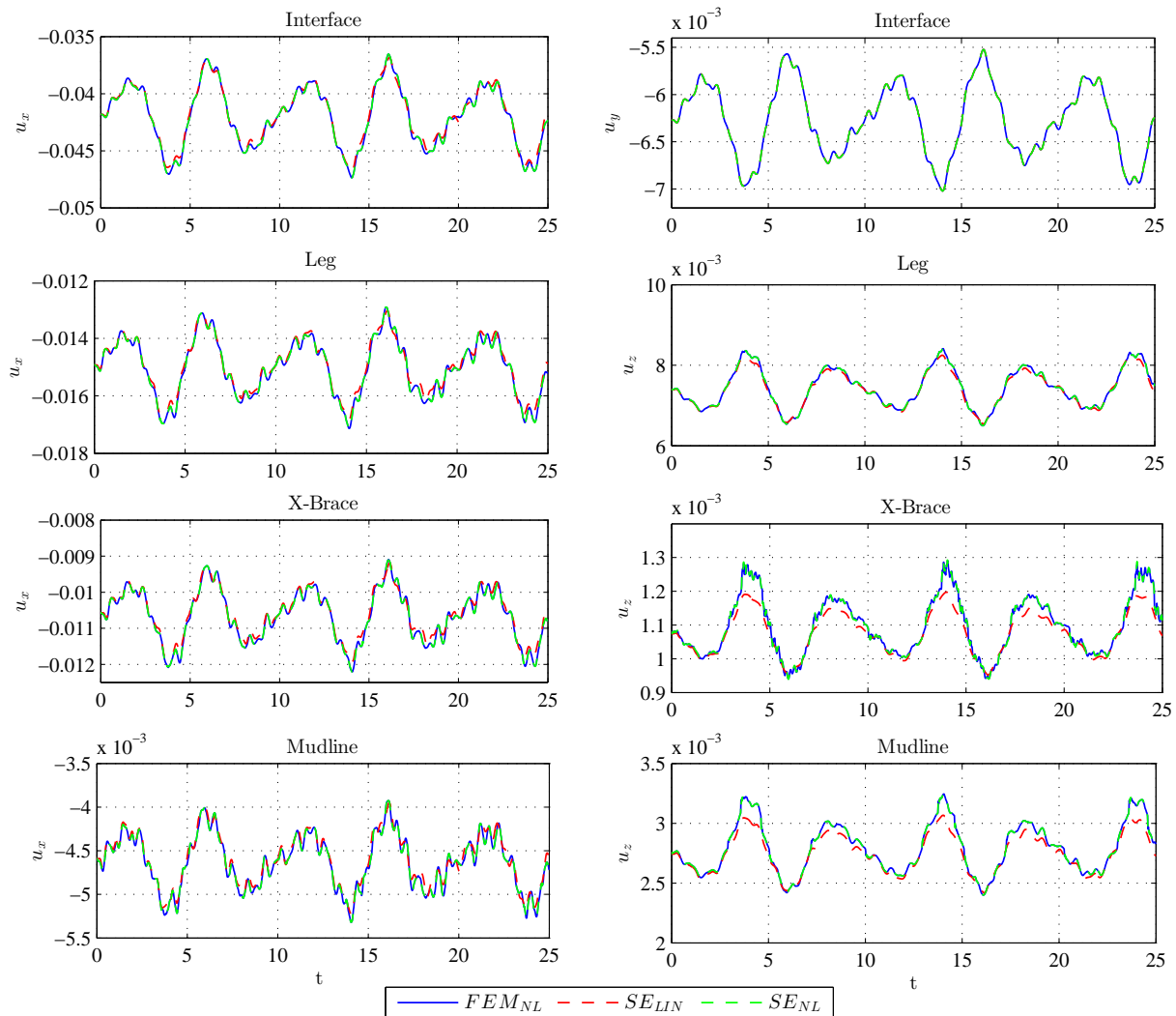


**Figure 7.8:** A comparison of the integrated wind turbine model with the linear and the non-linear soil model for the medium load case.

Maximum differences occur at the peak values in the pile axial direction. The displacement magnitude varies from 2.5 to 3.1 mm, which corresponds to the critical  $tz$  curve point, where the soil stiffness dramatically changes from initial stiffness to zero. This is explicitly reflected in the results both for the mudline and the brace. It can be noticed that when the displacements are around 2.5 mm, linear and non-linear models have the same axial stiffness, therefore the results are almost the same. However, once the critical level of 2.54 mm (0.1 inch) is exceeded, the results start to differ.

One should also notice that while the vertical direction, which is governed by  $tz$  curves, is significantly different, the results for the horizontal direction are still comparable. This is due to the fact, that the lateral  $py$  curves combined with the displacement level in that direction still correspond to the initial stiffness.

## High Level

The results for the high loadcase differ significantly over the all jacket levels, as depicted in Fig. 7.9. By starting from the interface level, the differences between the linear and the non-linear soil model can be clearly spotted. This relates to the fact that the soil influences not only the lower part of the jacket locally, but it becomes so important, that the soil can be considered as the factor governing the global jacket dynamics.

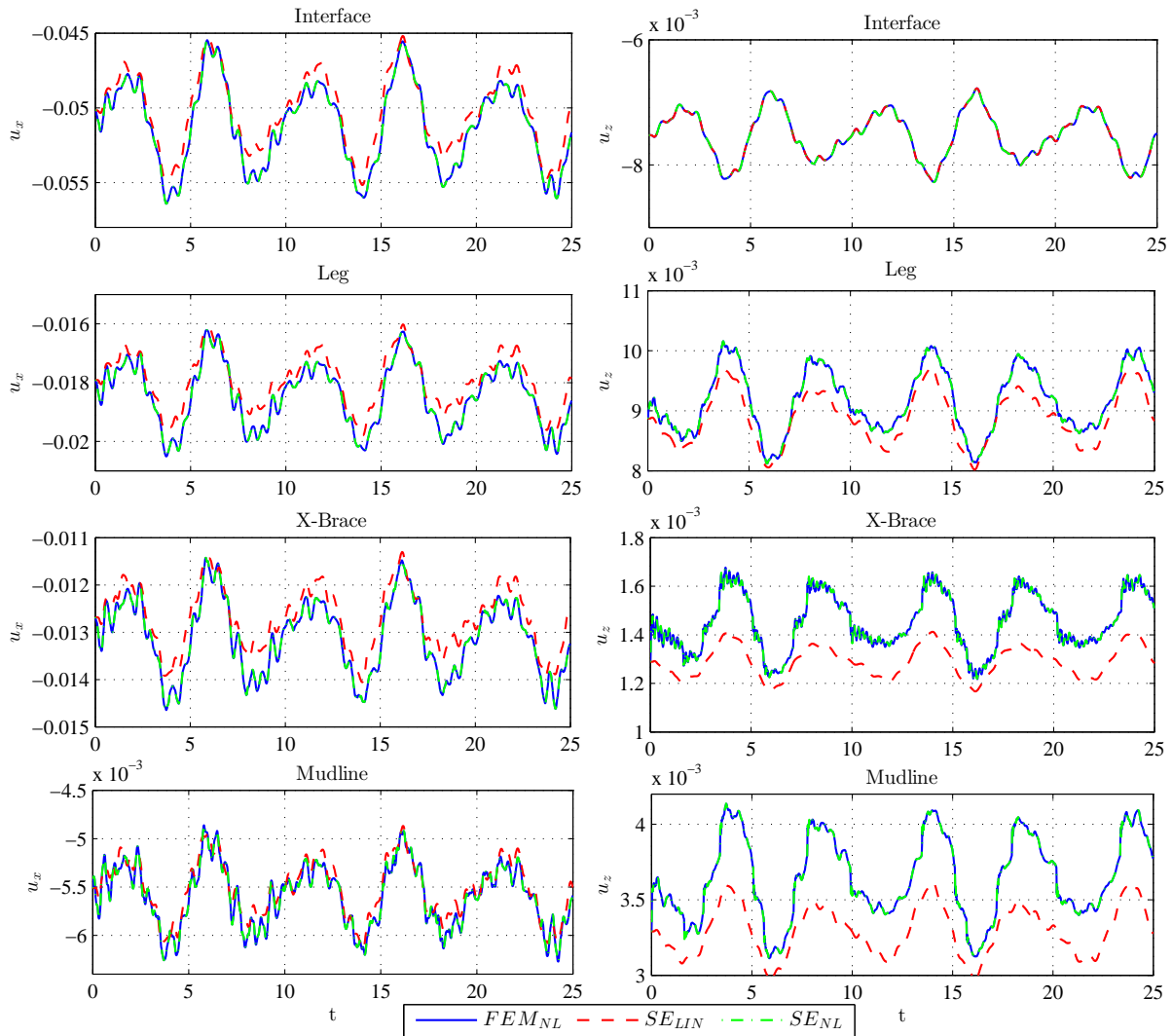


**Figure 7.9:** A comparison of the integrated wind turbine model with the linear and the non-linear soil model for the high load case.

When considering the middle part of the jacket, the significant differences are introduced for both vertical and horizontal displacements. Especially the horizontal direction is affected, not only in the amplitudes of oscillation, but also in the quasi-static *offset* component. That corresponds to the significant level of differences in the solution, because first only the error in the peaks will be introduced as in the medium load case, afterwards the differences are so significant that the solutions will diverge for the averaged value as well.

The reason for such a significant difference lays in the displacement level for the  $tz$  curve, corresponding to the axial pile stiffness. The linear solution is provide with the initial soil stiffness while the non-linear solution has a zero skin friction stiffness since the displacements are constantly above 2.5 mm. It can be noticed that even though the lateral displacements are close to the initial stiffness, some differences can be seen between the solutions. It results

from the influence of the axial and lateral stiffness, where displacements coupling lead to the combination of axial and lateral displacements. So the differences in the lateral solutions are caused by the axial one, even though the isolated lateral displacements should not introduce a significant difference.

For such extreme cases, where the axial stiffness of the pile is lost, the mechanism of the load transfer is significantly modified and the pile starts to act as if it was a so-called *short pile*. That means that the equilibrium between the external force and the soil will be established using the lateral soil capacity instead of the axial. In the case when the axial capacity is lost, the importance of the non-linear lateral *py* curves becomes crucial.

### Quantitative comparison

The following section outlines the quantitative comparison of the results from the three integrated turbine models, using both linear and non-linear soil models. The results from the linear model and the reduced non-linear model are compared by referring to the, non-reduced turbine model, according to Eq. 7.2.

$$\text{normalization : } \frac{\mathbf{SE}_{\text{NL}}}{\mathbf{FEM}_{\text{NL}}} , \frac{\mathbf{SE}_{\text{LIN}}}{\mathbf{FEM}_{\text{NL}}} \quad (7.2)$$

**Table 7.2:** A comparison of linear and non-linear soil models implemented into the integrated wind turbine model.

Load level	Displacement		$\mathbf{SE}_{\text{NL}}$	$\mathbf{SE}_{\text{LIN}}$	
Low	Interface	$u_x$	1.00	1.00	
		$u_z$	1.00	1.00	
	Leg	$u_x$	1.00	0.99	
		$u_z$	1.00	1.00	
	X-Brace	$u_x$	1.00	1.00	
		$u_z$	1.00	1.00	
	Mudline	$u_x$	1.00	0.99	
		$u_z$	1.00	1.00	
	Middle	Interface	$u_x$	1.00	0.99
			$u_z$	1.00	1.00
Leg		$u_x$	1.00	0.97	
		$u_z$	1.00	0.97	
X-Brace		$u_x$	1.00	0.97	
		$u_z$	1.00	0.93	
Mudline		$u_x$	1.00	0.98	
		$u_z$	1.00	0.95	
High		Interface	$u_x$	1.00	0.96
			$u_z$	1.00	1.00
	Leg	$u_x$	1.00	0.95	
		$u_z$	1.00	0.95	
	X-Brace	$u_x$	1.00	0.93	
		$u_z$	1.00	0.81	
	Mudline	$u_x$	1.00	0.96	
		$u_z$	1.00	0.85	

Table 7.2 combines the results from the previous section, where the plots were presented. It provides the maximum difference between the referenced and the analyzed models. The time step, where the difference between the solutions were at their maximum is considered and normalized in respect to the reference solution which corresponds to the same time step. The ratio of the solution is presented for both the linear and the non-linear reduced models.

The perfect match is obtained when the ratio between the solutions is 1.00. The more the ratio deviates from that value, the less accurate the model becomes.

Based on Tab. 7.2 a number of conclusions can be drawn with respect to the soil modelling approaches:

- The reduced, non-linear  $\mathbf{SE}_{NL}$  model shows a great accuracy compared to the linear  $\mathbf{SE}_{LIN}$  model. Practically, the suggested  $\mathbf{SE}_{NL}$  model has the same accuracy level as the referenced model.
- The low load level introduces no significant differences between the linear and non-linear solution. The medium load level introduces a maximum 7 % difference for the linear model. The high load level introduces a maximum error of 19% for the linear model.
- For each point the greatest differences were always found for the vertical direction.
- The greatest differences were found in the cross-brace and at the mudline. As long as the mudline differences are easy to expect, the brace differences are interesting to notice and also important to be aware of.
- The maximum differences for the interface level is 4%, however further down it corresponds to 19 % in the brace. Therefore, no conclusions that are only based on the interface comparison should be made.

## 7.4 User-definer linearization

As outlined in the previous section the assumption of a linear soil model is significantly violated while the displacement level is high. Therefore, there is a clear need for improving the currently used linear model.

As mentioned before, the linear model is created by using the initial soil stiffness, therefore no significant difference is introduced when displacement level is small. However, while greater load is applied the displacement level increase and the soil *soften*, which result in diverging the non-linear solution from the initial stiffness. That case is of great importance when the *Ultimate Limit State* load cases are analyzed and the ultimate bearing of the piles are evaluated.

The most robust method to reduce the error is to introduce the non-linear pile model into the aero-elastic code, which would correspond to the suggested  $\mathbf{SE}_{NL}$  model. However, that solution is demanding in terms of the implementation effort and would require a Wind Turbine Manufacturer to include it in their code. Therefore, as a mitigation, temporarily solution a linearization by using the modified soil stiffness could be suggested.

The idea is outlined in Fig 7.10a. As a starting point the expected displacement level should be estimated based on the engineering judgement, or a simple analyses. Based on that results the ultimate soil stiffness  $E_{1.0}$  should be estimated. The ultimate stiffness might correspond to the maximum displacement level over the analyses time, or the most *representative*  $E_{rep}$  soil stiffness.

The choice of the linearization point has a significant influence on the results. To illustrate that, a sensitivity analysis is presented in Fig. 7.10b. A series of analyses have been performed, where the soil stiffness has been linearized corresponding to the initial stiffness  $E_0$ , the ultimate stiffness  $E_{1.0}$  and a number of intermediate points  $[0, \dots, 1.0]$ . The corresponding error in respect to the non-linear solution is presented by mean of the normalized *Root Mean Square* error. The error for several points has been measured:  $P_x$ - lateral pile head direction,  $P_z$ - axial pile head direction,  $I_x$ - lateral direction for the interface point,  $T_x$ - lateral direction for the tower top node.

The soil modification mostly influences the axial pile displacement, due to the fact that this component behaves mostly in a non-linear manner. The initial 10% error for the initial soil

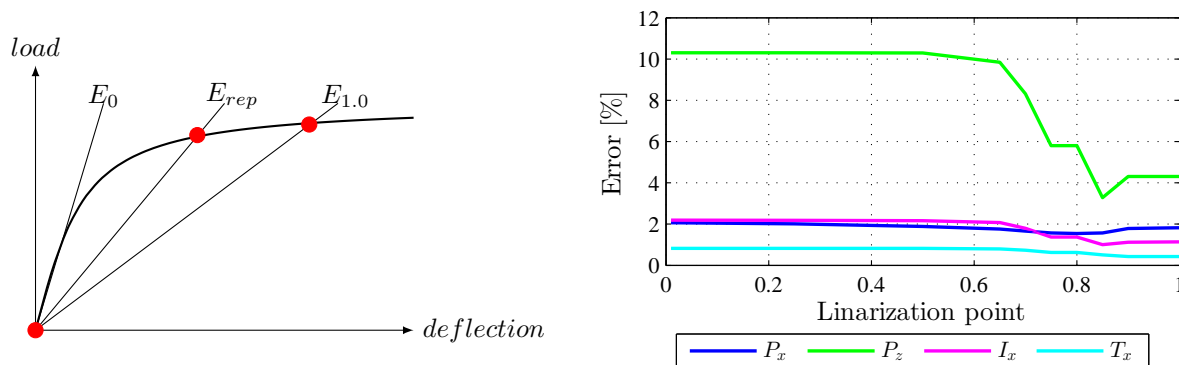


**Figure 7.10:** The idea of choosing the linearization point. Sensitivity study on the error in respect to the linearization point.

stiffness can be reduced to 3.5% where a representative stiffness is chosen and to 4% for the ultimate soil stiffness. Moreover, the lateral pile direction, as well as the tower and interface node are rather insensitive to the soil stiffness modifications.

From the practical point of view, the designer are especially interested in the design load cases. While for the FLS case, the displacement are rather small, therefore, it correspond to the case where the soil stiffness can successfully be approximated by using the initial soil stiffness. However, for the ULS load cases the maximum displacement might introduce some non-linear effects, therefore a *user-defined* linearization might improve the results compared to the initial stiffness case.

To investigate the potential of that method the analysis has been performed, where the soil has been linearized based on the maximal displacement level from the non-linear case. The results are presented in Fig. 7.11.

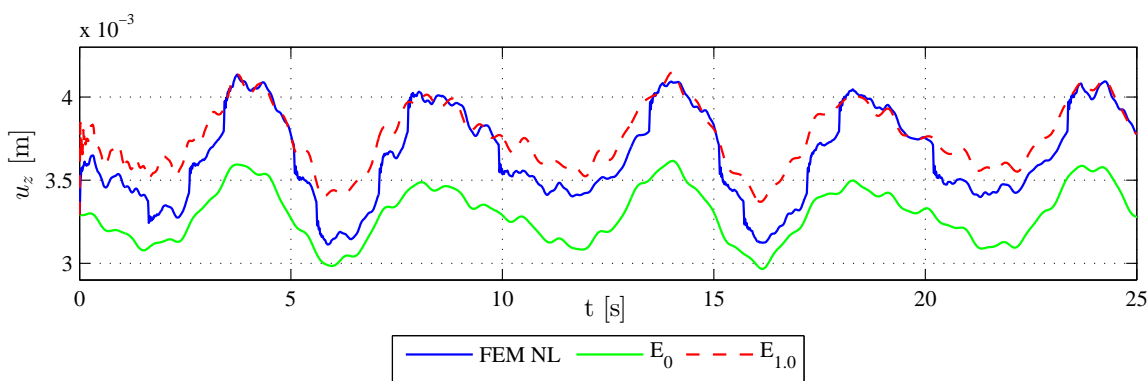


**Figure 7.11:** User-defined soil linearization for the ULS load cases.

The axial pile head displacements are compared for three cases:  $FEM_{NL}$ - non-linear reference case,  $E_0$ - initial stiffness linear case,  $E_{1.0}$ - ultimate soil stiffness linear case. The initial stiffness result introduces significant error compared to the reference solution. The suggested *user-defined* linear case delivers significantly better results, especially for the *peak* displacements, while in the intermediate states the error is increased. As long as the results are used to design pile for the ULS case, one is mostly interested in the most extreme case (*peaks*), therefore, the *user-defined* solution is significantly superior to the linear case based on the initial stiffness.

## 7.5 Discussion

When combining the time-series plots and the tabular results the general conclusions of the investigation for the importance of the non-linear soil model in the integrated wind turbine analysis can be derived.

- The difference between linear and non-linear solutions depends on the load level. The higher the load level applied (higher soil displacement), the greater are the differences between the models. Therefore, even though the linear solution for the low load level might deliver acceptable results, the difference might become significant, when a higher load level is applied.
- The linearized  $\mathbf{SE}_{LIN}$  model cannot properly describe the integrated wind turbine model when significant non-linear soil effects are introduced.
- The suggested reduced, non-linear  $\mathbf{SE}_{NL}$  model can successfully model non-linear soil effects in the integrated wind turbine model.

The above mentioned general findings are important in order to confirm that the soil-structure interaction might not be sufficiently well described by using currently implemented, linearized soil models in the industrial analyses. As long as the linear and non-linear estimation of the soil stiffness is comparable, the linear solution can deliver correct results. However, when a higher load level is applied, the differences might be significant.

To illustrate the importance of the non-linear part of the soil one can try to mark the displacement level calculated according to the linear theory on the non-linear soil curves. Afterwards by comparing the initial, linear soil stiffness with either tangential or secant stiffness corresponding to the specific displacement level it can be assessed how significant the non-linear influence can be. To visualize that method the displacements from the above presented load cases are plotted in Fig. 7.12. It should be noted that this approach can serve only as a rough idea of the non-linearities since it is based on the uni-axial displacement curves.

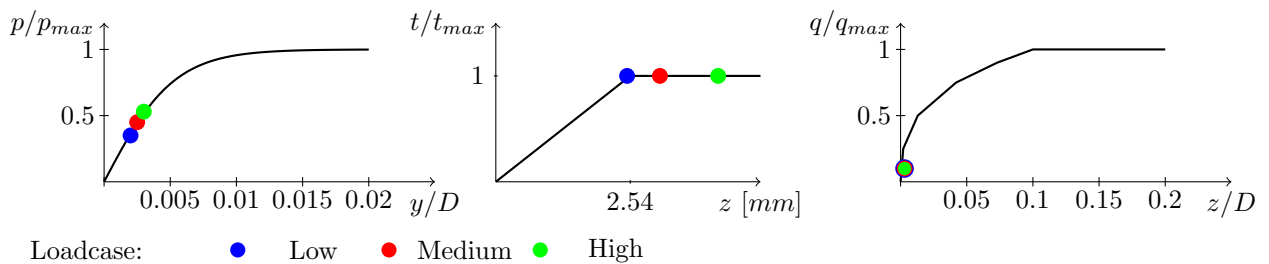


**Figure 7.12:** Estimation of the non-linear soil importance based on the specific displacement level compared with the soil curves. a) lateral soil resistance, b) skin friction resistance, c) tip end resistance

From the plots one can easily understand how the specific components affects the solution. The first plot presents  $py$  curve and for the analyzed cases it can be seen that the displacement level corresponds to the linear part, therefore no difference should be spotted here. The second plot presents the  $tz$  curve and more extreme cases can be found. The low load case has the exact same stiffness as the linear case, therefore as shown in the result comparison, they are indistinguishable. Where the medium and the high load case corresponds to zero tangential stiffness which is the reason for such a difference in the solutions. The last plot presents the  $qz$  tip resistance curve and for all cases is the same as the initial stiffness. To sum up, it is a handy tool to a priori estimate if the model requires linear or the non-linear soil description.

It should also be remembered that the modern structures are designed in order to increase the economical efficiency, which corresponds to a higher structural utilization and displacement level. The closer engineers get to the limit of the method, the more refined and advanced the modelling approach should be used. The question is whether it is the moment to include more refined soil modelling in the design procedures. The results of the presented study based on the realistic input data might indicate that more attention should be brought to the soil modelling within the offshore wind industry in order to efficiently and accurately describe physical phenomena of the complex real structure.

The  $\mathbf{SE}_{NL}$  model is the most robust and efficient from the presented, therefore it should be used. However, the implementation effort is significant and it lays within an Wind Turbine Manufacturer. If that will not implemented a Foundation Designer could introduce a mitigation approach, where the soil would be linearized according to a *user-defined* point, corresponding to the *ultimate* soil stiffness. As presented herein that approach can precisely predict the pile displacements in the most extreme *peaks*, which serves as a basis for the ULS case, where the currently used method fails. However, the *ultimate* soil stiffness cannot be determined, since the non-linear solution is not known a priori. Therefore, the engineering judgement should be used possible based on a limited number of the most representative ULS load cases, which would be solved internally by a Foundation Designer in a non-linear manner.



## Part III

# CLOSING REMARKS



# Roadmap

The following part of the thesis is intended to give the synthesis of the presented work, as depicted in Fig. 7.13. The main findings are summarized in relation to the thesis goal and research scopes. The practical implications of the findings are stated. Finally, the further research directions based on the work presented herein, are outlined.

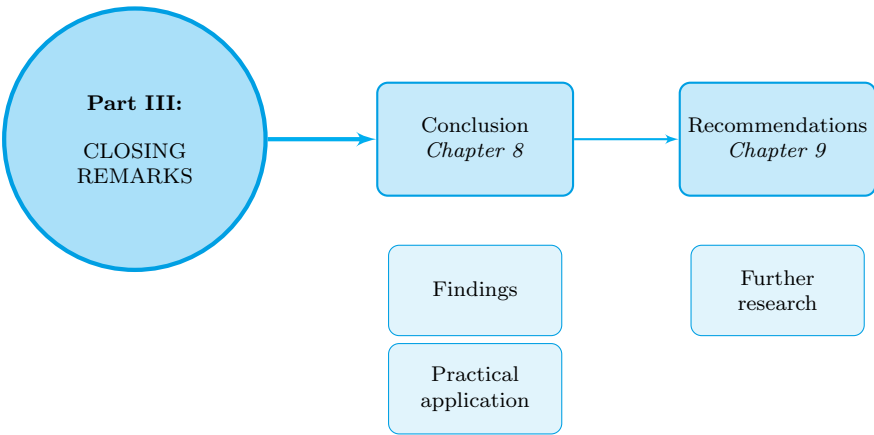


**Figure 7.13:** Outline of Part III of the thesis.



# Chapter 8

## Conclusion

The offshore wind industry is rapidly developing, therefore precise and robust methods to design great and sustainable turbines are required. To obtain the most precise dynamic response of the structure, which serves as a basis for the design, the fully coupled equation is the most appropriate approach to use.

However, due to non-engineering reasons e.g. legal and confidential, the industry adopted the so-called *Sequential Integrated* approach. It was developed in order to allow parties to analyze the model in their in-house software. The approach is equivalent to the coupled one, assuming the foundation is modelled as a non-reduced one with a non-linear soil model. That is not the case when using the state-of-the-art methods, because a foundation model is reduced and linearized, therefore the solution is not exact, but merely an approximation.

As for the simple foundations, i.e. monopiles, the current method is mature and delivers satisfactory results, whilst for the more complex and dynamically sensitive foundations, i.e. jackets, the same approach cannot be used. Based on the aforementioned reasoning, the clear need for more refined methods has been acknowledged. In order to close that gap and contribute to the industrial development, the following thesis goal was defined in the Introduction.

*Increasing efficiency and accuracy of reduced models used in load calculations for an offshore wind turbine design.*

By the virtue of the work presented, numerous findings were established in the thesis and implementing these improvements leads to a significant increase of both, the quality of the results and the efficiency of the methods. The findings can be synthesized in three main groups, coinciding with the research scopes defined in the introductory chapter:

- **Improve spectral and spatial convergence of a reduced foundation model by implementing the appropriate theory**

The three reduction methods have been investigated (Guyan, Craig-Bampton, Augmented Craig-Bampton) and as identified, the Augmented Craig-Bampton delivers the results on the same level of accuracy as the non-reduced foundation. Therefore, this method is recommended to be used for in the analyses of the jacket foundation. Disregarding the internal dynamic, using the Guyan method leads to an artificial resonance, which results in 10 times higher out-of-plane brace displacements. This significantly reduces the fatigue life and results in an increase of the steel usage. The inefficiency of the Craig-Bampton method in capturing the internal wave loading results in the requirement of approximately 200 modes for the analyzed case to properly describe the brace vibration, while the Augmented Craig Bampton method delivers the same results by just including 50 modes. The reason for that is the introduction of additional load dependent vectors in the Augmented Craig-Bampton method, which are specifically suited for describing the internal load.

- **Assess the accuracy of the modal tower representation in aero-elastic calculations.**

The modal tower representation has been investigated based on the FLEX5 code, which is used in the industry. What has been found is that the approach used in the code (2 tower bending modes per direction) does not deliver accurate results. Based on the sensitivity study, it has been demonstrated that the required number of the tower modes should be increased to 10 per direction instead of the currently used 2 modes.

- **Investigate the importance of the non-linear soil modelling on the coupled wind turbine dynamic response.**

The assumption of the linearized soil used in the state-of-the-art method, has been significantly violated in the analysis presented in the thesis. It was demonstrated that especially for the high displacement level, corresponding to the *Ultimate Limit State* load case the linear assumption introduces a significant difference compared to the reference non-linear soil model (up to 20%). Based on these results, the user-defined linearization approach was suggested, which can be used in the ULS cases in order to minimize the error. However, this approach is only the mitigation of the linear soil model used in the method. The currently used soil modelling approach is rather simplistic, therefore the soil parameters are estimated based on a conservative assumptions in order to account for the method uncertainties. When the more realistic non-linear approach is implemented, the level of conservatism hopefully can be reduced, which finally leads to a more accurate design.

Due to the fact that the thesis was conducted in collaboration with Rambøll, the practicality of the analyses and investigations was given a high priority. As a result, a number of practical improvements have been delivered as described above.

Based on the number of practical applications to the offshore wind industry, which arise from the findings identified herein, it can be concluded that the thesis goal was reached. As usual, after an in-depth investigation of a specific scientific and engineering field, some interesting ideas arise that could not be investigated due the time limitation. Therefore, the next chapter briefly summarizes the points that could possibly be beneficial for further research in order to push the boundary of the state-of-the-art methods even further.

## Chapter 9

# Recommendation for Further Research

- **Include a Rotor Nacelle Assembly reduced model in a Foundation Designer software**– in the design process for a wind turbine, one of the first stages is to come up with the initial reduced jacket model and a reduced wave loading. A Foundation Designer performs these calculations based on the detailed jacket and tower model, while the RNA is simplified as a point mass. Based on that model, the reduced wave forces are calculated, which afterwards are given to a Wind Turbine Manufacturer. The reduced model of the RNA is extremely simple and might not represent the physical properties, therefore it introduces some differences in the dynamic of the structure excited with the load. If a more refined model, including blades dynamic, could be implemented, it might contribute to a better wave representation.
- **Investigate the free interface reduction methods**– the internal dynamic of the reduced foundation models both, for the Craig-Bampton and the Augmented Craig-Bampton, are based on the so-called fixed interface modes. These modes, as described in Ch. 2, are obtained by restraining the interface nodes and computing the internal dynamic modes of a modified structure. However, the physical foundation is not restrained at this point and the reason for doing so is solely theoretical to perform an assembly process. To model the structure more reasonably and possibly increase the efficiency, the reduction methods based on the so-called free interface modes [37, 38, 39] could be investigated. That concern has already been raised in [40], but no clear conclusion has been drawn.
- **Include more refined soil models**– the currently used soil model (*py* curves) were developed mostly for the oil and gas application, where the dynamic does not play an important role. Now it is adopted to the offshore wind industry, which is all but a static case. Especially damping, included in the *py* method, is modelled rather simplistic. Recently, the more realistic dynamic version of the *py* curve has been suggested in [19]. The method has also been briefly summarized herein in Ch. 3. The implementation of that method could potentially improve the *Fatigue Limit State* calculations, by introducing more refined damping models.
- **Investigate the possibility of including the non-linear reduced model**– the currently used reduced models are linear and the implementation approach does not allow for the non-linear models. Therefore, in order to include the non-linear soil models, piles have to be extracted and included in the non-reduced manner. This certainly introduces additional computational effort due to the detailed pile representation. In order to increase efficiency in that field, the non-linear reduced soil-pile elements could be used instead of the non-reduced one. There exist some theoretical studies, where the non-linear reduced

models have been addressed [41, 42], however no offshore applications for foundations exist. Therefore, it would be interesting and potentially beneficial to investigate the implementation effort along with the accuracy of that method in the offshore implementation.

- **Fully coupled approach**– as a starting point in the thesis, it was assumed that the *Sequential integrated* approach is the one to use in the design process. Even though that approach might not be the most efficient one, nor straight-forward, it is the one currently used by the industry to design turbines supported by the monopiles and jackets. There exist some publications [43, 44] where the coupled method was used and compared with the integrated method. The results indicate that for both, monopiles and jackets, a more optimized structure could be obtained by using the coupled method. Even though it might be true, it is almost not likely that this approach will be implemented in the industry, however in terms of the floating structures, it actually could be possible. The floating wind turbines are significantly more complicated in the design process compared to the fixed-bottom turbines and the *Sequential integrated* approach in the current form cannot be applied. Therefore, the coupled approach is the one to use as for now. That opens new research and practical possibilities, where the reduced models can be implemented as well.

# Bibliography

- [1] 2012 annual report. Technical report, International Energy Agency, July, 2013.
- [2] Offshore wind in europe. Technical report, The European Wind Energy Association, March, 2015.
- [3] Michael Drunsić. Lcoe reduction for offshore wind. *U.S. Offshore Wind Market and Supply Chain Workshop*, March, 2014.
- [4] P. Passon and K. Branner. Load calculation methods for offshore wind turbine foundations. *Ships and Offshore Structures*, **9**:433–449, 2013.
- [5] W. Popko, F. Vorpahl, and P. Antonakas. Investigation of local vibration phenomena of a jacket sub-structure caused by coupling with other components of an offshore wind turbine. *Journal of Ocean and Wind Energy*, **1**:111–118, 2014.
- [6] S.N. Voormeeren, P.L.C van der Valk, B.P. Nortier, D-P Molenaar, and D.J. Rixen. Accurate and efficient modeling of complex offshore wind turbine support structures using augmented superelements. *WIND ENERGY*, **17**:1035–1054, 2014.
- [7] N. Janbu. Soil models in offshore engineering. *Geotechnique*, **35**(3):241–281, 1985.
- [8] A. Verruijt. *Offshore Soil Mechanics*. Delft University of Technology, 2 edition, 2006.
- [9] D. De Klerk, D.J. Rixen, and S.N. Voormeeren. General framework for dynamic substructuring: History, review and classification of techniques. *AIAA Journal*, **46**:1169–1181, 2008.
- [10] D.J. Rixen. *Substructuring and Dual Methods in Structural Analysis*. PhD thesis, Universite de Liege, Faculte des Sciences Appliquees, 1997.
- [11] R. Guyan. Reduction of stiffness and mass matrices. *AIAA Journal*, **3**:380, 1965.
- [12] R. Craig and M. Bampton. Coupling of substructures for dynamic analysis. *AIAA Journal*, **6**:1313–1319, 1968.
- [13] D. J. Rixen. Generalized mode acceleration methods and modal truncation augmentation. *AIAA Journal* 2001–1300, 2001,.
- [14] J.M. Dickens, J.M. Nakagawa, and M.J. Wittbrodt. A critique of mode acceleration and modal truncation augmentation methods for modal response analysis. *Computers and Structures*, **62**(6):985 – 998, 1997.
- [15] G. Kerschen and J.C. Golinval. Physical interpretation of the proper orthogonal modes using the singular value decomposition. *Journal of Sound and Vibration*, **249**:849–865, 2002.
- [16] P.L.C. van der Valk. *Coupled Simulations of Wind Turbines and Offshore Support Structures*. PhD thesis, Technische Universiteit Delft, 2014.

- [17] DNV-OS-J101. Design of offshore wind turbine structures. Standard, Det Norske Veritas, DNV, 2014.
- [18] Api recommended practice 2a-wsd. recommended practice for planning, designing and constructing fixed offshore platforms– working stress design. Technical report, American Petroleum Institute, 2014.
- [19] E. Van Buren and M. Muskulus. Improving pile foundation models for use in bottom-fixed offshore wind turbine applications. *Energy Procedia*, **24**:363–370, 2012.
- [20] E. Winkler. Die lehre von der elastizitt und festigkeit (the theory of elasticity and stiffness) Prague, 1867.
- [21] W R. Cox, L. C. Reese, and B. R. Grubbs. Field testing of laterally loaded piles in sand. *Offshore Technology Conference*, 1974.
- [22] T. W. O’Neil. M. W, Dunnivant. A study of effect of scale, velocity, and cyclic degradability on laterally loaded single piles in overconsolidated clay. *University of Houston, Texas*, 1984.
- [23] K. T. Brodbaek, M. Moller, S. P. H. Sorensen, and A. H. Augustesen. Review of  $p$ - $y$  relationship in cohesionless soil. Technical report, Aalborg University, 2009.
- [24] P. L. Pasternak. On a new method of analysis of an elastic foundation by means of two foundation constants. *Gosudarstvennoe Izdatelstvo Literaturi po Stroitelstvu I Arkhitekture* 355–421, 1954.
- [25] S. Belkhir, S. Mezazigh, and D. Levacher. Non-linear behaviour of lateral-loaded pile taking into account the shear stress at the sand. *Geotechnical Testing Journal*, **22**:308–316, 1999.
- [26] M. Ashour, G. Norris, and P. Pilling. Lateral loading of a pile in layered soil using the strain wedge model. *Computer Methods in Applied Mechanics and Engineering*, **124**:303–315, 1998.
- [27] C. C. Fan and J. H. Long. Assessment of existing methods for predicting soil response of laterally loaded piles in sand. *Computers and Geotechnics*, **32**:274–289, 2005.
- [28] S.H.J.A. Fransen. A comparison of recovery methods for reduced dynamic substructure models with internal loads. In *44th AIAA/ASME/ASCE/AHS Structures, Structural Dynamics, and Materials Conference* 1–11, Norfolk, Virginia, USA, April 2003.
- [29] P.L.C. van der Valk and S. Voormeeren. An overview of modelling approaches for complex offshore wind turbine support structures. In *PROCEEDINGS OF ISMA2012-USD2012*, Leuven, Belgium, 2012.
- [30] P.C. van der Valk, S.N. Voormeeren, P.C. de Valk, and Rixen D.J. Dynamic models for load calculation procedures of offshore wind turbine support structures: Overview, assessment, and outlook. *Journal of Computational and Nonlinear Dynamics*, **10**:041013–041013–15, 2014.
- [31] S.H.J.A. Fransen. Data recovery methodologies for reduced dynamic substructure models with internal loads. *AIAA Journal*, **42**:2130–2142, 2004.
- [32] M. B. Nielsen, J. F Jensen, D. Augustyn, and R. R Pedersen. Efficient response recovery procedures for detailed design of jacket foundations. *SEMC 2016: The 6th International Conference on Structural Engineering, Mechanics and Computation*, Cape Town, South Africa, 2016.

- [33] LACFlex. Aero-elastic simulation software. Technical report, Ramboll, 2013.
- [34] J. M. Jonkman, S. Butterfield, W. Musical, and G. Scott. Definition of a 5-MW reference wind turbine for offshore system development. Technical report, National Renewables Energy Laboratory, Colorado, USA, 2009.
- [35] J. Chung and G. M. Hulbert. A time integration algorithm for structural dynamics with improved numerical dissipation: The generalized-alpha method. *Journal of Applied Mechanics*, **60**:371–375, 1993.
- [36] Robert D. Cook, David S. Malkus, Michael E. Plesha, and Robert J. Witt. *Concepts and Applications of Finite Element Analysis*. Wiley, 4th edition, 2001.
- [37] S. Rubin. an improved component-mode representation. *AIAA Journal*, **13**:995–1006, 1975.
- [38] R. H. MacNeal. A hybrid method of component mode synthesis. *Journal of Computers and Structures*, **1**:581–601, 1971.
- [39] A. Majed and E. E. Henkel. A residual flexibility mixed-boundary method in component-mode synthesis. *JPL Conference*, 2002.
- [40] S.N. Voormeeren. *Dynamic Substructuring Methodologies for Integrated Dynamic Analysis of Wind Turbines*. PhD thesis, Technische Universiteit Delft, 2012.
- [41] G. Kerschen and J.C. Golinval. Nonlinear normalmodes, part i: A useful framework for the structural dynamicist. *Mechanical Systems and Signal Processing 23rd* 170–194, 2009.
- [42] S. Idelsohn and A. Cardona. A reduction method for nonlinear structural dynamic analysis. *Computer Methods in Applied Mechanics and Engineering*, **49**:253–279, 1985.
- [43] R. Haghi, T. Ashuri, van der Valk P. L. C., and Molenaar D. P. Integrated multidisciplinary constrained optimization of offshore support structures. *Proceedings of the Science of Making Torque from Wind (TORQUE)* 133–143, 2012.
- [44] King J., Cordle A., McCann G., and et al. Cost reductions in offshore wind turbine jacket design using integrated analysis methods and advanced control. *International Society of Offshore and Polar Engineers*, 2013.



Part IV

**APPENDICES**



## Appendix A

# Boolean matrices

The following appendix provides more details on how to construct the Boolean matrix  $\mathbf{B}$  and the localized matrix  $\mathbf{L}$ . These matrices are crucial in the assembly process, therefore they are described herein.

The assembly procedure provides the compatibility and the equilibrium between two (or more) assembled structure, which mathematically is given in terms of  $\mathbf{B}$  matrix for the compatibility and  $\mathbf{L}$  for the equilibrium equation.

$$\begin{aligned} \mathbf{B}\mathbf{u} &= \mathbf{0}, \\ \mathbf{L}^T\mathbf{g} &= \mathbf{0}, \end{aligned} \tag{A.1}$$

where  $\mathbf{u}$  is the displacement vector and  $\mathbf{g}$  is the interface forces.

To give an example on constructing of these matrices a general structure is considered as depicted in Fig. A.1.

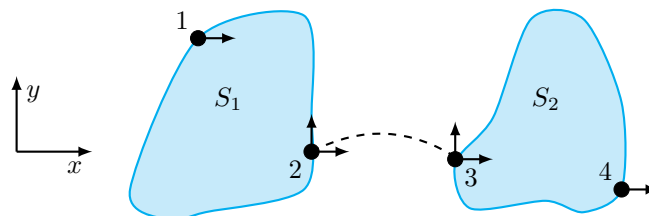


**Figure A.1:** Coupling of two structures.

The system consists of two independent structures  $S_1$  and  $S_2$ , which have to be coupled via an interface nodes 2 and 3. The total system consists of 4 nodes. Note that nodes can have different number of DoFs (node 1 and 4 has only one DoF). This might be useful for e.g. assembling shells and beams or solids.

The coupling on this example is fulfilled via nodes 2 and 3, therefore displacements of that nodes has to be equal:

$$\begin{cases} u_{2x} = u_{3x} \\ u_{2y} = u_{3y} \end{cases} . \tag{A.2}$$

That creates two coupling equations. The equations can also be presented in a matrix form, which introduces a Boolean matrix  $\mathbf{B}$ :

$$\mathbf{B}\mathbf{u} = \mathbf{0}. \tag{A.3}$$

Equation is in fact the compatibility equation, which is used in the assembly procedure. The equation couple the displacements of the interface nodes, where the system DoFs are assembled into:

$$\mathbf{u} = [u_{1x} \quad u_{2x} \quad u_{2y} \quad u_{3x} \quad u_{3y} \quad u_{4x}]^T. \tag{A.4}$$

Rewriting the Eq. A.2 in a matrix form (A.3), by using the set of displacement  $\mathbf{u}$  yields:

$$\mathbf{B} = \begin{bmatrix} 0 & 1 & 0 & -1 & 0 & 0 \\ 0 & 0 & 1 & 0 & -1 & 0 \end{bmatrix}, \quad (\text{A.5})$$

which is the sought  $\mathbf{B}$  Boolean matrix. Note that the size of the matrix is always  $n \times m$ , where  $n$  is the number of constraints that are applied and  $m$  is the original number of DoFs for the full system. In this case only one node was the interface, which has 2 DoFs, that corresponds to  $n = 2$ , where the total number of DoFs is  $m = 6$ . Therefore, the size of the  $\mathbf{B}$  matrix is  $2 \times 6$ .

When it comes down to the localized matrix  $\mathbf{L}$  it can be mathematically calculated as a null space of  $\mathbf{B}$ :

$$\mathbf{B}\mathbf{L} = \mathbf{0}. \quad (\text{A.6})$$

The physical interpretation of the localized matrix  $\mathbf{L}$  is to combine the full set of DoFs  $\mathbf{u}$  into a unique set of  $\mathbf{q}$ :

$$\mathbf{u} = \mathbf{L}\mathbf{q}. \quad (\text{A.7})$$

In the process it has to be decided which node will be retained as a *master* and which will be *slave*:

$$\mathbf{u} = \mathbf{L}\mathbf{q} = \begin{bmatrix} u_{1x} \\ u_{2x} \\ u_{2y} \\ u_{3x} = u_{2x} \\ u_{3y} = u_{2y} \\ u_{4x} \end{bmatrix} = \begin{bmatrix} 1 & 0 & 0 & 0 \\ 0 & 1 & 0 & 0 \\ 0 & 0 & 1 & 0 \\ 0 & 1 & 0 & 0 \\ 0 & 0 & 1 & 0 \\ 0 & 0 & 0 & 1 \end{bmatrix} \begin{bmatrix} u_{1x} \\ u_{2x} \\ u_{2y} \\ u_{4x} \end{bmatrix}. \quad (\text{A.8})$$

It is solely the theoretical operation, without any physical meaning. In this case the node 2 is the *master*. Therefore we can see, that the DoFs associated with node 3 depends on node 2. Again, the matrix formulation is used and by applying it, the localized matrix  $\mathbf{L}$  can be created, with a physical interpretation.

The localized matrix in the assembly process is used to fulfil the equilibrium equation in terms of the interface forces  $\mathbf{g}$ . The forces at the interface from one structure has to be equal with the opposite sign. In the matrix form that corresponds to:

$$\mathbf{L}^T \mathbf{g} = \begin{bmatrix} 1 & 0 & 0 & 0 & 0 & 0 \\ 0 & 1 & 0 & 1 & 0 & 0 \\ 0 & 0 & 1 & 0 & 1 & 0 \\ 0 & 0 & 0 & 0 & 0 & 1 \end{bmatrix} \begin{bmatrix} 0 \\ g_{2x} \\ g_{2y} \\ g_{3x} \\ g_{3y} \\ 0 \end{bmatrix} = \begin{bmatrix} 0 \\ g_{2x} + g_{3x} \\ g_{2y} + g_{3y} \\ 0 \end{bmatrix} = \mathbf{0}. \quad (\text{A.9})$$

## Appendix B

# Derivation of Augmented Craig-Bampton reduction method

As a starting point to derive the Augmented Craig-Bampton reduction method the relation between internal  $\mathbf{u}_i$  and boundary  $\mathbf{u}_b$  DoFs is recalled in B.1

$$\mathbf{M}_{ii}\ddot{\mathbf{u}}_i + \mathbf{K}_{ii}\mathbf{u}_i = \mathbf{f}_i - \mathbf{M}_{ib}\ddot{\mathbf{u}}_b - \mathbf{K}_{ib}\mathbf{u}_b. \quad (\text{B.1})$$

The solution for the internal DoFs displacement can be split into a static and a dynamic part as in B.2

$$\mathbf{u}_i = \mathbf{u}_{i,stat} + \mathbf{u}_{i,dyn}. \quad (\text{B.2})$$

The static response can be found from B.1 when the inertia part is neglected ( $\ddot{\mathbf{u}}_i$  and  $\ddot{\mathbf{u}}_b$  are zero)

$$\mathbf{u}_{i,stat} = \Psi_C \mathbf{u}_b + \mathbf{K}_{ii}^{-1} \mathbf{f}_i. \quad (\text{B.3})$$

In the classic Craig-Bampton the first term on the right-hand side is the static constraint modes and the second term (excitation on the internal DoFs  $\mathbf{f}_i$ ) is assumed to be zero. However, now the second term is taken into account to be the key to the MTA augmentation.

The equation of motion taking the internal excitation into account can be introduced

$$\mathbf{M}_{ii}\ddot{\mathbf{u}}_{i,dyn} + \mathbf{K}_{ii}\mathbf{u}_{i,dyn} = -\mathbf{M}_{ii}\mathbf{K}_{ii}^{-1}\ddot{\mathbf{f}}_i - (\mathbf{M}_{ii}\Psi_C - \mathbf{M}_{ib})\ddot{\mathbf{u}}_b. \quad (\text{B.4})$$

The first right-hand side of the B.4 is associated with the internal excitation and the second term can be interpreted as load vector associated with acceleration of the interface.

Based on that equation it can be seen, that the augmentation contributes to the precision of the solution twofold. First, accounting for internal forces, but also including additional acceleration from adjacent substructures via the interface nodes.

For the convenience B.4 can be rewritten into B.5

$$\mathbf{M}_{ii}\ddot{\mathbf{u}}_{i,dyn} + \mathbf{K}_{ii}\mathbf{u}_{i,dyn} = -\mathbf{M}_{ii}\mathbf{K}_{ii}^{-1} \left( \ddot{\mathbf{f}}_i - \mathbf{Y}\ddot{\mathbf{u}}_b \right), \quad (\text{B.5})$$

using

$$\mathbf{Y} = \mathbf{K}_{ib} - \mathbf{K}_{ii}\mathbf{M}_{ii}^{-1}\mathbf{M}_{ib}. \quad (\text{B.6})$$

The bracket of the B.5 shows even more clearly dual improvement in the dynamic part of the solution.

The dynamic part of the solution can be split into series of the quasi-static solution represented by the series of MTA vectors organized into  $\Phi_{MTA}$  matrix and residual dynamic part approximated by the fixed interface vibration modes  $\Phi_i$  from the classic Craig-Bampton reduction.

The MTA matrix can be calculated by introducing quasi-static solution to B.5

$$\tilde{\Phi}_{MTA,j} = \mathbf{P} (\mathbf{K}_{ii}^{-1} \mathbf{M}_{ii})^j \mathbf{K}_{ii}^{-1} [\mathbf{Y} \quad \mathbf{F}_i] \quad j = 0, \dots, k-1. \quad (\text{B.7})$$

The MTA vectors are forming the *Krylov sequence*, where the precision of the solution increase with the higher order of the sequence  $j$ . However, the first order is suffice for the offshore application.

To avoid *information overlap* between MTA modes and fixed vibration modes ( $\Phi_i$ ) the orthogonal projector  $\mathbf{P}$  is introduced

$$\mathbf{P} = \mathbf{I} - \Phi_i \Phi_i^T \mathbf{M}_{ii}. \quad (\text{B.8})$$

It accounts for the fact, that both vibration modes  $\Phi_i$  and MTA vectors are used to capture the response of the system to the external loading. In extreme cases these could lead to the linear dependency decreasing numerical stability. To account for the overlapping the contribution from the vibration modes should be subtracted (B.8).

Finally, the different orders of MTA vectors can be gathered into the MTA matrix as in B.9

$$\tilde{\Phi}_{MTA} = [\tilde{\Phi}_{MTA,1} \quad \dots \quad \tilde{\Phi}_{MTA,j} \quad \dots \quad \tilde{\Phi}_{MTA,k}]. \quad (\text{B.9})$$

To preserve sparsity and improve numerical robustness the MTA matrix will be orthonormalized by solving the *interaction problem*

$$\left( \tilde{\Phi}_{MTA}^T \mathbf{K} \tilde{\Phi}_{MTA} \right) \mathbf{y} = \sigma^2 \left( \tilde{\Phi}_{MTA}^T \mathbf{M} \tilde{\Phi}_{MTA} \right) \mathbf{y}. \quad (\text{B.10})$$

The orthonormalized MTA are found by expansion of the reduced eigenmodes in the MTA space

$$\Phi_{MTA} = \tilde{\Phi}_{MTA} \mathbf{y}. \quad (\text{B.11})$$

As the last step the matrix  $\Phi_{MTA}$  is mass normalized.

The reduced system matrices using the Augmented Craig-Bampton method can be found in the similar way as in the classic Craig-Bampton way, expanding the reduction basis for MTA vectors

$$\tilde{\mathbf{M}} = \mathbf{T}_{ACB}^T \mathbf{M} \mathbf{R}_{ACB} \quad , \quad \tilde{\mathbf{K}} = \mathbf{T}_{ACB}^T \mathbf{K} \mathbf{R}_{ACB} \quad , \quad \tilde{\mathbf{C}} = \mathbf{T}_{ACB}^T \mathbf{C} \mathbf{R}_{ACB} \quad , \quad (\text{B.12})$$

the same for the condensed force vector

$$\tilde{\mathbf{f}} = \mathbf{R}_{ACB}^T \mathbf{f}. \quad (\text{B.13})$$

## Appendix C

# Proper Orthogonal Decomposition

The Proper Orthogonal Decomposition is a mathematical method for handling large amount of data. The method can efficiently reduce the complex space of  $n$  correlated variables into a significantly lower in size space of uncorrelated variables. The data that can be analyzed by the method can be e.g., the wave forces on the offshore structure. By applying the complex, time-dependent wave force vector  $\mathbf{f}$  one can decompose it into a set of uncorrelated orthogonal modes, which in sense of the energy will capture most of the complex wave excitation [41].

Therefore, the Proper Orthogonal Decomposition is the method used to create a modes representing the internal wave excitation. These modes are incorporated into the Augmented Craig-Bampton combining the structure and the internal excitation. The brief explanation of most basic equation for the method is given below.

Assume that the force vector is given in the format as in C.1

$$\mathbf{f} = \begin{bmatrix} f_1 & \dots & f_i & \dots & f_m \end{bmatrix} = \begin{matrix} \text{time} \rightarrow \\ \begin{bmatrix} f_{11} & \dots & f_{i1} & \dots & f_{m1} \\ \vdots \\ f_{1j} & & \ddots & & \\ \vdots \\ f_{1n} & & & & f_{mn} \end{bmatrix} \cdot \text{DoF} \end{matrix} \quad (\text{C.1})$$

where the force vector for  $n$  DoFs is represented by  $m$  time steps and  $f_i$  is a force vector for all DoFs for  $i^{\text{th}}$  time-step.

For a convenient definition of the covariance matrix zero mean of each time-step is introduced

$$\mathbf{x}_i = \mathbf{f}_i - \mu, \quad (\text{C.2})$$

where  $\mu$  is the mean of the time step.

With the modified force vector the covariance matrix can be formulated

$$\mathbf{C} = \frac{1}{m} \sum_{i=1}^N \mathbf{x}_i \mathbf{x}_i^T = \frac{1}{m} \mathbf{X} \mathbf{X}^T. \quad (\text{C.3})$$

The physical interpretation of the covariance matrix is the correlation of the specific DoF in terms of the wave forces.

By solving the eigenvalue problem of the covariance matrix one obtain the  $j = 1 \dots n$  uncorrelated eigenmodes and corresponding eigenvalues

$$\mathbf{C} \phi_j = \lambda_j \phi_j. \quad (\text{C.4})$$

The eigenvectors  $\phi_j$  are used in the Augmented Craig-Bampton method to decompose the internal wave loading. The corresponding eigenvalues  $\lambda_j$  describes the relative energy associated

with the corresponding mode. Therefore, by using that information one could decide how many modes should be included to properly describe the internal wave loading.

# Appendix D

## Jacket geometry

The following appendix provides additional information on the jacket and soil model used in the analyses. If no specific information is provided about the parameters along the thesis it should be assumed that the parameters from this appendix are used.

The appendix contains three figures:

- Node coordinates of the jacket– Fig. (D.1). The information given in the figure should suffice to recreate the jacket geometry. Each of the standard element in the figure was additionally augmented with 3 sub-elements in the code. That should increase accuracy of the wave loading and fulfil proper jacket internal deformation. The transition piece is modelled as a concrete beam elements, the rest of the jacket elements are steel *S355*.
- Cross sectional properties of the jacket elements’– Fig. (D.2). The figure presents the cross sectional parameters of the jacket pipe elements in the plane of the legs. The jacket is identical in two another planes, therefore only one plot was included. The cross sectional properties are given in the specific format:  $Pdddxtt$   
...

where *P* means that pipe element was used, sometimes is can also be *C* which stands for cone. *ddd* is the diameter in millimeters, *x* is a separation between diameter and *tt* which stands for thickness in millimeters. The element can be subdivided into a number of elements with different cross sectional properties. The description corresponds to the further sub-elements in the direction which is drawn in the element. The regions where articular cross section properties is valid is symbolized by the perpendicular line on the element.

- Soil parameters and pile specification– Fig. (D.3). The soil parameters including e.g. soil type, friction angle, submerged unit weight, etc. is given in the tabular format, along the pile length. The piles are perfectly vertical. The pile starts in three points, which specifies the mudline: *00A0C0*, *00B0A0*, *00C0B0* according to Fig. D.1. The pile length is 48 m, diameter 2134 mm and the thickness is 50 mm.

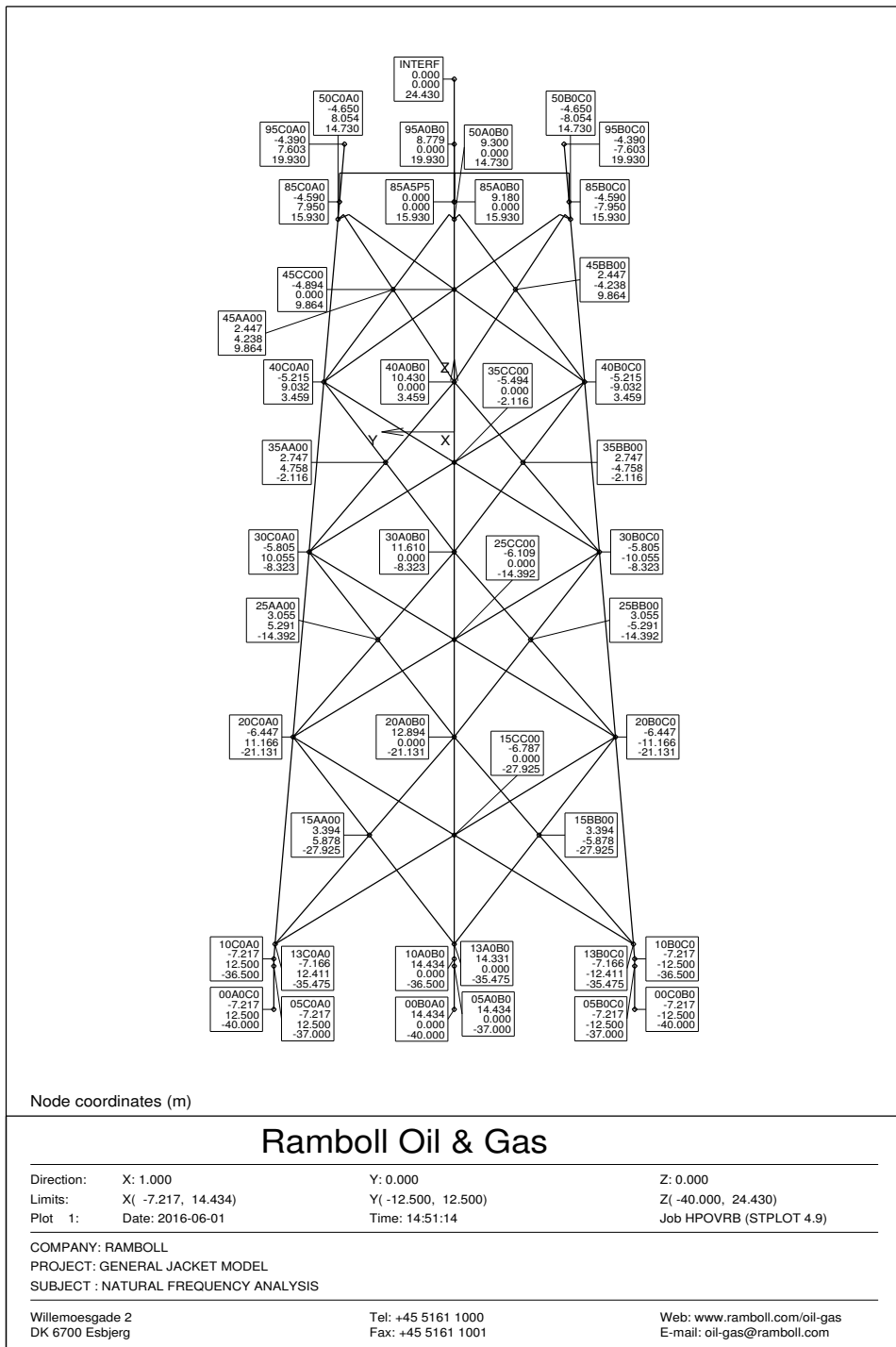


Figure D.1: Node coordinates of the jacket.

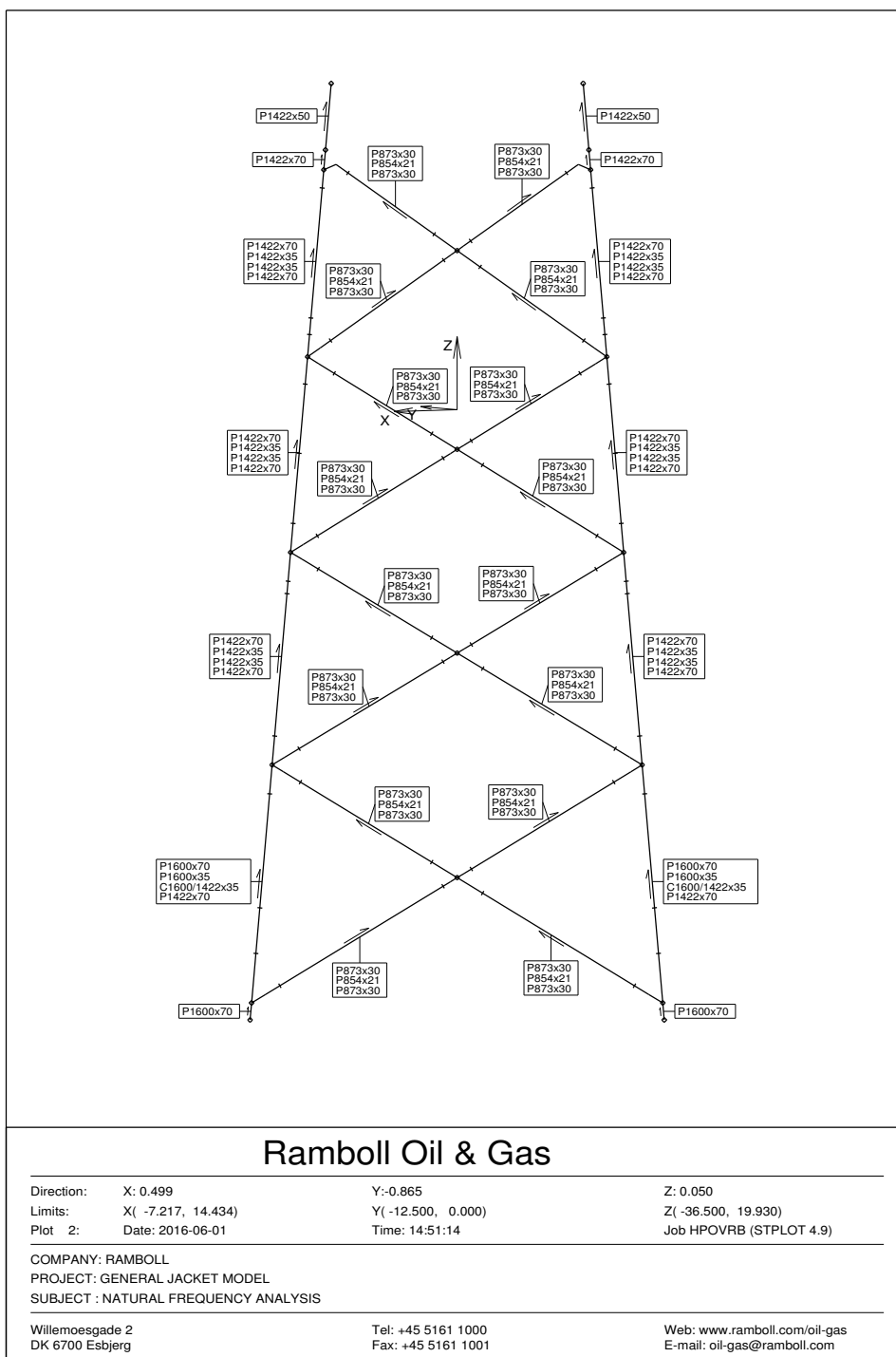


Figure D.2: Outer diameter and thickness of the jacket

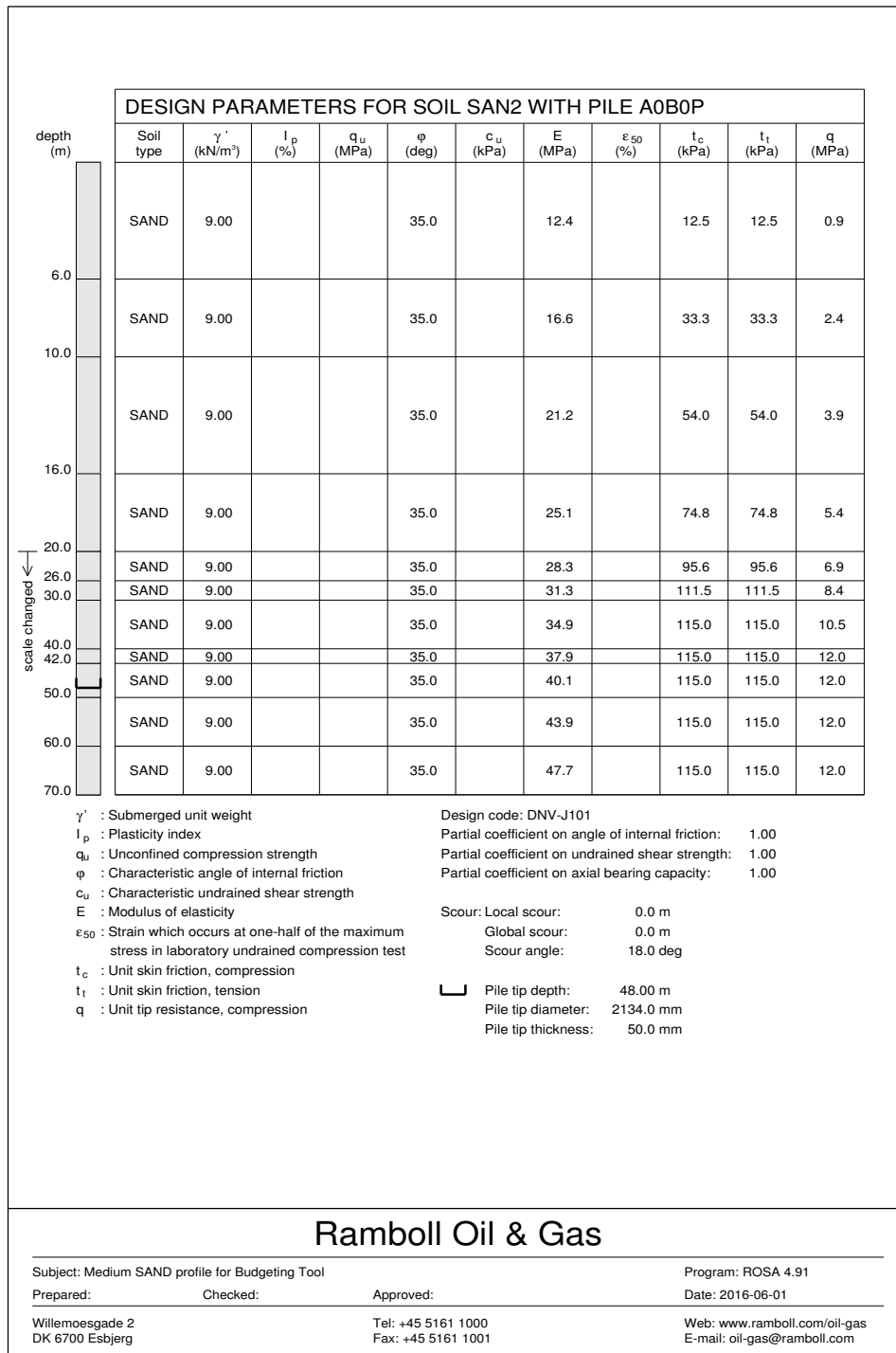


Figure D.3: Pile and soil properties.



